Quarkonium as a probe of hot matter

with potential Nonrelativistic QCD and Open Quantum Systems

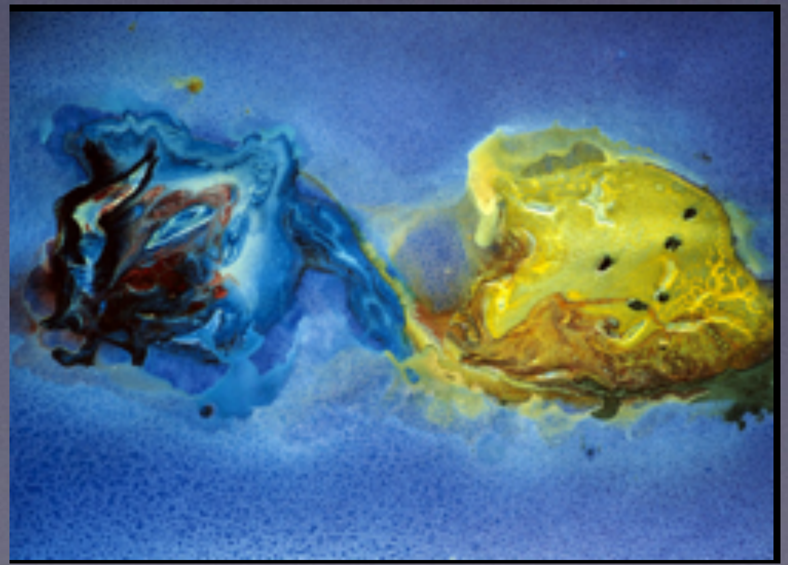

Physik Department TUM
T30f

Nora Brambilla

- Heavy Quarks are important probes of the QGP

- Heavy Quarks are important probes of the QGP
- Quarkonium suppression and R_AA has been identified as a probe of QGP by Matsui and Satz in 1986 in relation to screening

- Heavy Quarks are important probes of the QGP
- Quarkonium suppression and R_AA has been identified as a probe of QGP by Matsui and Satz in 1986 in relation to screening
- Quarkonium is indeed a golden probe of the QGP and the reason for this is that it is a multiscale system well understood at T=0 on the basis of effective field theories (EFTs), i.e. in QCD, and lattice

- Heavy Quarks are important probes of the QGP
- Quarkonium suppression and R_AA has been identified as a probe of QGP by Matsui and Satz in 1986 in relation to screening
- Quarkonium is indeed a golden probe of the QGP and the reason for this is that it is a multiscale system well understood at T=0 on the basis of effective field theories (EFTs), i.e. in QCD, and lattice
- Using EFTs to determine quarkonium interaction at finite T we get a change of paradigm: suppression not driven by screening but by the imaginary parts in the potentials which have a physical interpretation

- Heavy Quarks are important probes of the QGP
- Quarkonium suppression and R_AA has been identified as a probe of QGP by Matsui and Satz in 1986 in relation to screening
- Quarkonium is indeed a golden probe of the QGP and the reason for this is that it is a multiscale system well understood at T=0 on the basis of effective field theories (EFTs), i.e. in QCD, and lattice
- Using EFTs to determine quarkonium interaction at finite T we get a change of paradigm: suppression not driven by screening but by the imaginary parts in the potentials which have a physical interpretation
- Use quarkonia of small radius as a diagnostic tool of a strongly coupled QGP

- Heavy Quarks are important probes of the QGP
- Quarkonium suppression and R_AA has been identified as a probe of QGP by Matsui and Satz in 1986 in relation to screening
- Quarkonium is indeed a golden probe of the QGP and the reason for this is that it is a multiscale system well understood at T=0 on the basis of effective field theories (EFTs), i.e. in QCD, and lattice
- Using EFTs to determine quarkonium interaction at finite T we get a change of paradigm: suppression not driven by screening but by the imaginary parts in the potentials which have a physical interpretation
- Use quarkonia of small radius as a diagnostic tool of a strongly coupled QGP
- We can describe the nonequilibrium evolution of bottomonium in the fireball using EFT (pNRQCD) and open quantum systems-> fully quantum and nonabelian descriptio with dissociations and recombinations.

- Heavy Quarks are important probes of the QGP
- Quarkonium suppression and R_AA has been identified as a probe of QGP by Matsui and Satz in 1986 in relation to screening
- Quarkonium is indeed a golden probe of the QGP and the reason for this is that it is a multiscale system well understood at T=0 on the basis of effective field theories (EFTs), i.e. in QCD, and lattice
- Using EFTs to determine quarkonium interaction at finite T we get a change of paradigm: suppression not driven by screening but by the imaginary parts in the potentials which have a physical interpretation
- Use quarkonia of small radius as a diagnostic tool of a strongly coupled QGP
- We can describe the nonequilibrium evolution of bottomonium in the fireball using EFT (pNRQCD) and open quantum systems-> fully quantum and nonabelian descriptio with dissociations and recombinations.
- The QGP is characterized by two transport coefficients defined in terms of nonperturbative correlators calculated on the lattice->no free parameter

- Heavy Quarks are important probes of the QGP
- Quarkonium suppression and R_AA has been identified as a probe of QGP by Matsui and Satz in 1986 in relation to screening
- Quarkonium is indeed a golden probe of the QGP and the reason for this is that it is a multiscale system well understood at T=0 on the basis of effective field theories (EFTs), i.e. in QCD, and lattice
- Using EFTs to determine quarkonium interaction at finite T we get a change of paradigm: suppression not driven by screening but by the imaginary parts in the potentials which have a physical interpretation
- Use quarkonia of small radius as a diagnostic tool of a strongly coupled QGP
- We can describe the nonequilibrium evolution of bottomonium in the fireball using EFT (pNRQCD) and open quantum systems-> fully quantum and nonabelian descriptio with dissociations and recombinations.
- The QGP is characterized by two transport coefficients defined in terms of nonperturbative correlators calculated on the lattice->no free parameter
- To do involves extending the description to charmonium, B_c

NOTICE:

NOTICE:

- What I discuss can be applied to jets using SCET and open quantum systems

NOTICE:

- What I discuss can be applied to jets using SCET and open quantum systems

- What I discuss can be generalised to X Y Z using BOEFT (Born-Oppenheimer EFT that we developed) and open quantum systems

NOTICE:

- What I discuss can be applied to jets using SCET and open quantum systems

- What I discuss can be generalised to X Y Z using BOEFT (Born-Oppenheimer EFT that we developed) and open quantum systems

- What I discuss is not depending on the medium : it can be a hot medium or a dense medium, weakly or strongly coupled

in what I will present T may be substituted as the inverse of a correlation length characterising the system—> may be useful to treat processes at non vanishing chemical potential and at EIC

Material for discussion/references

N. Brambilla, M. A. Escobedo, J. Soto and A. Vairo, Phys. Rev. D **96** (2017) no.3, 034021 [arXiv:1612.07248 [hep-ph]].

N. Brambilla, M. A. Escobedo, J. Soto and A. Vairo, Phys. Rev. D **97** (2018) no.7, 074009 [arXiv:1711.04515 [hep-ph]].

N. Brambilla, M. A. Escobedo, A. Vairo and P. Vander Griend, Phys. Rev. D **100** (2019) no.5, 054025 [arXiv:1903.08063 [hep-ph]].

N. Brambilla, M. A. Escobedo, M. Strickland, A. Vairo, P. Vander Griend and J. H. Weber, [arXiv:2012.01240 [hep-ph]]. and arXiv: 2107 .06222

M. Escobedo *Phys.Rev.D* 103 (2021) 3, 034010 • e-Print: 2010.10424 [

Non-equilibrium evolution in QGP

#4

N. Brambilla,J. Ghiglieri, A. Vairo, Peter Petreczky
Phys.Rev.D 78 (2008) 014017 • e-Print: 0804.0993 [hep-ph]

N. Brambilla, M. Escobedo, J. Ghiglieri, A. Vairo
JHEP 05 (2013) 130 • e-Print: 1303.6097 [hep-ph]

N. Brambilla, M. Escobedo, J. Ghiglieri, A. Vairo
JHEP 12 (2011) 116 • e-Print: 1109.5826 [hep-ph]

N. Brambilla, M. Escobedo, J. Ghiglieri, J. Soto, A. Vairo
JHEP 09 (2010) 038 • e-Print: 1007.4156 [hep-ph]

Potential and energies in medium

N. Brambilla, V. Leino, Peter Petreczky, A. Vairo
Phys.Rev.D102 (220) 074503 • e-Print 2007.10078 [hep-ph]

Lattice calculation of the heavy quark transport coefficient

Heavy quarks are QGP probes

- heavy quark are produced at the beginning and remain up to the end

- The heavy-quark mass introduces one or more large scales, whose contributions may be factorized and computed in perturbation theory ($\alpha_{\mathrm{s}}(M) \ll 1$).

- Low-energy scales are sensitive to the temperature.
  Low-energy contributions may be accessible via lattice calculations.

Heavy quarks are QGP probes

- heavy quark are produced at the beginning and remain up to the end
- The heavy-quark mass introduces one or more large scales, whose contributions may be factorized and computed in perturbation theory ($\alpha_{\mathrm{s}}(M) \ll 1$).
- Low-energy scales are sensitive to the temperature.
  Low-energy contributions may be accessible via lattice calculations.

Quarkonia are better hard probes
because they are multi scale systems

Quarkonium scales

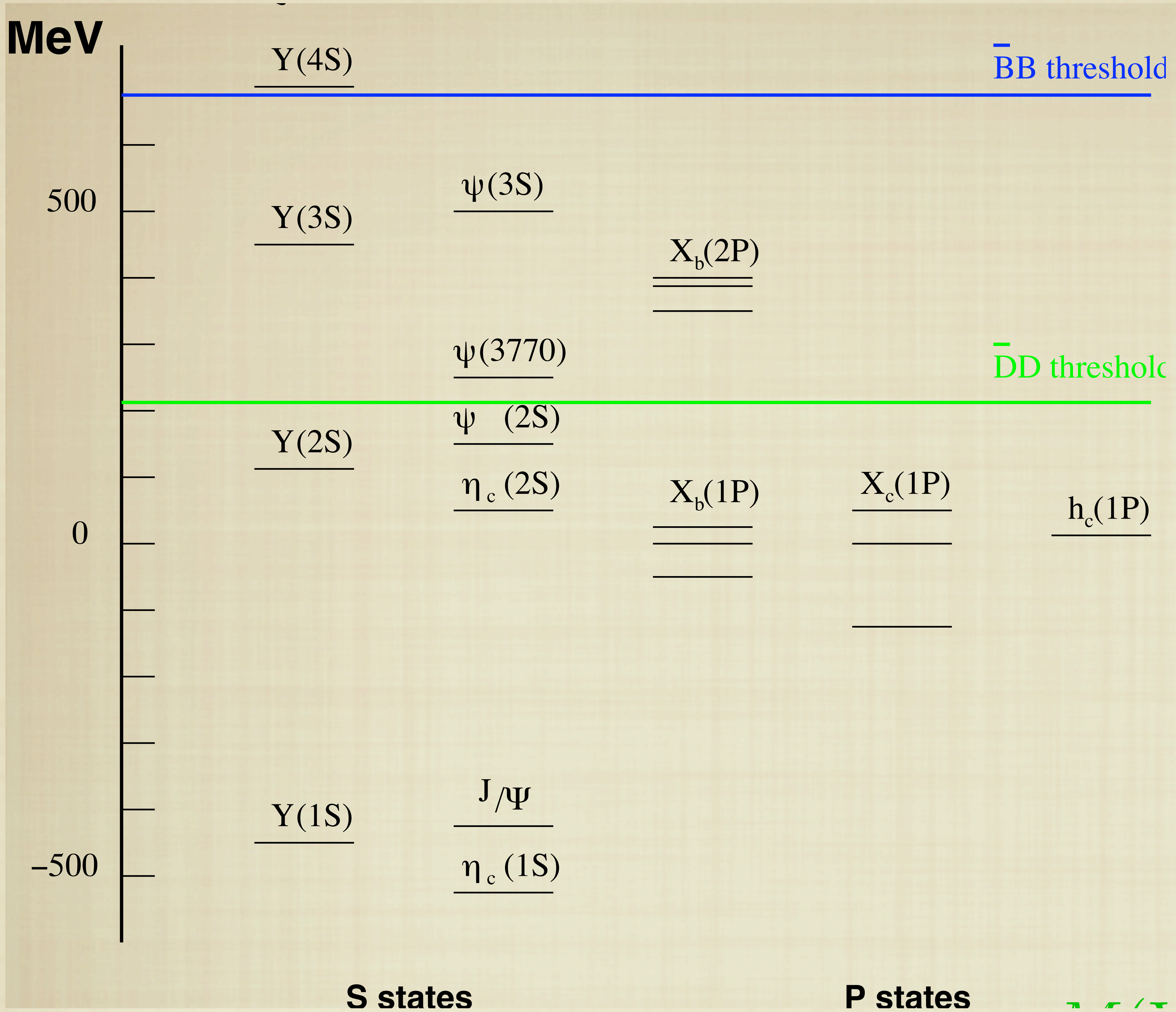

Normalized with respect to $\chi_b(1P)$ and $\chi_c(1P)$

$$^{2S+1}L_J$$

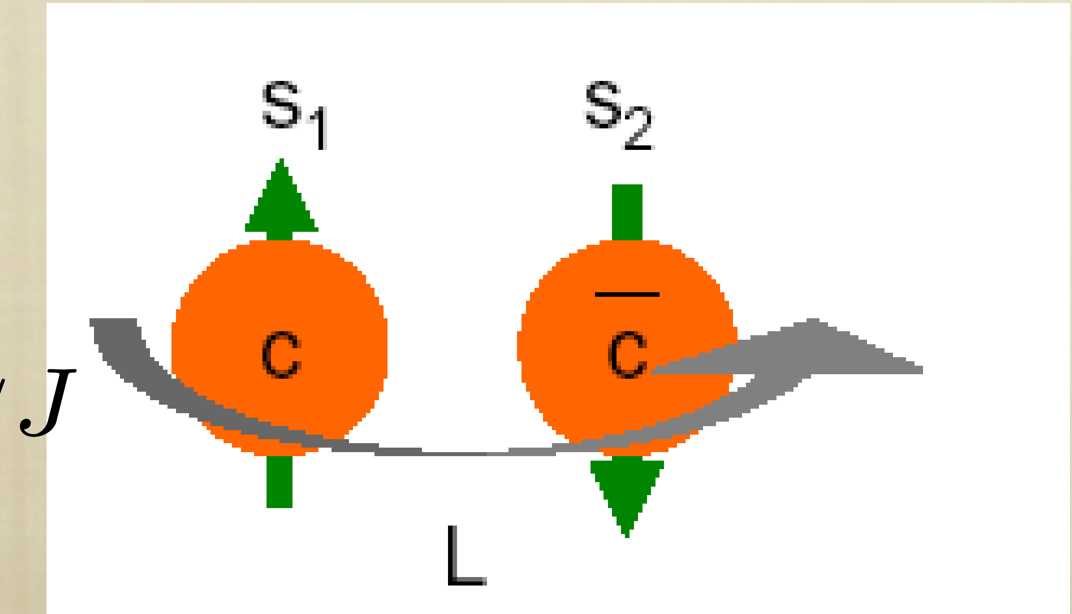

THE MASS SCALE IS PERTURBATIVE

$$m_Q \gg \Lambda_{\rm QCD}$$

$$m_b \simeq 5\,\text{GeV};\, m_c \simeq 1.5\,\text{GeV}$$

$$M(Y(1S)) = 9460\,\text{GeV}$$

$$M(J/\Psi) = 3097\,\text{GeV}$$

Quarkonium scales

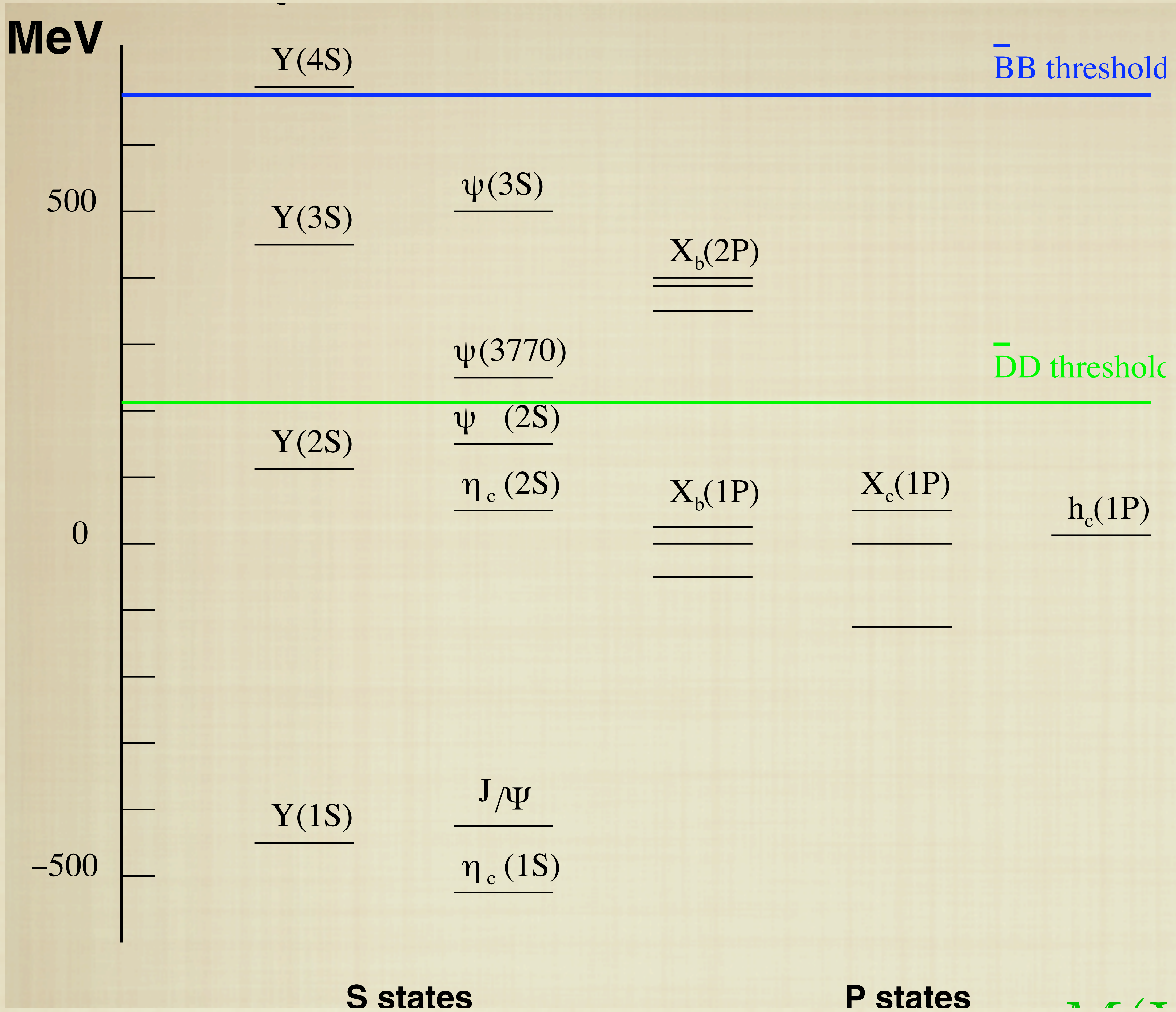

Normalized with respect to $\chi_b(1P)$ and $\chi_c(1P)$

$^{2S+1}L_J$

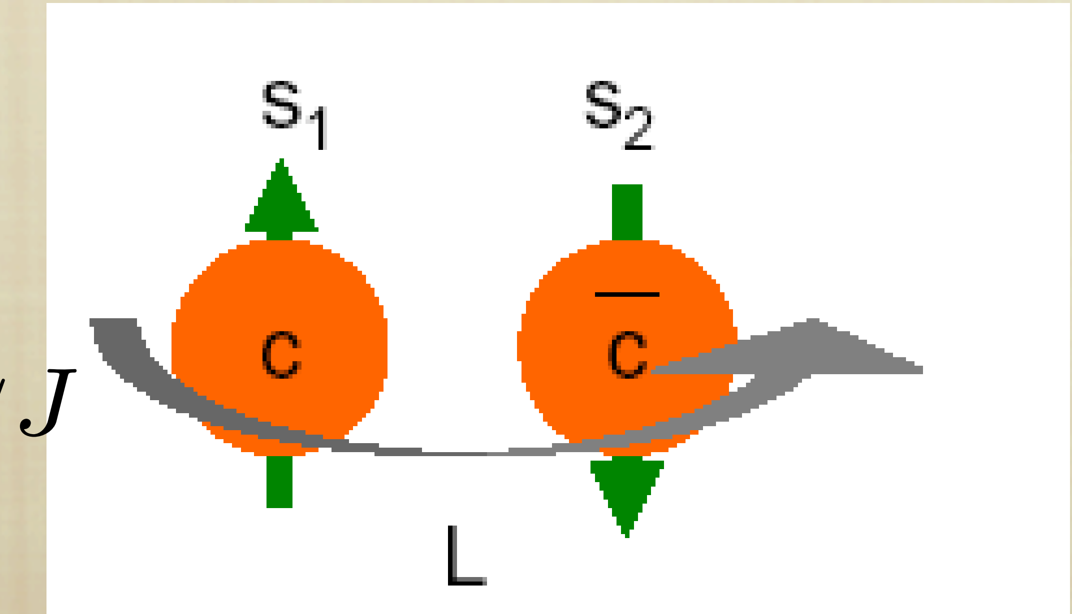

$$M(Y(1S)) = 9460\,\mathrm{GeV}$$
$$M(J/\Psi) = 3097\,\mathrm{GeV}$$

The system is nonrelativistic(NR)

$$\Delta E \sim mv^2, \Delta_{fs} E \sim mv^4$$

$$v_b^2 \sim 0.1, v_c^2 \sim 0.3$$

The mass scale is perturbative

$$m_Q \gg \Lambda_{\mathrm{QCD}}$$

$$m_b \simeq 5\,\mathrm{GeV}; m_c \simeq 1.5\,\mathrm{GeV}$$

Quarkonium scales

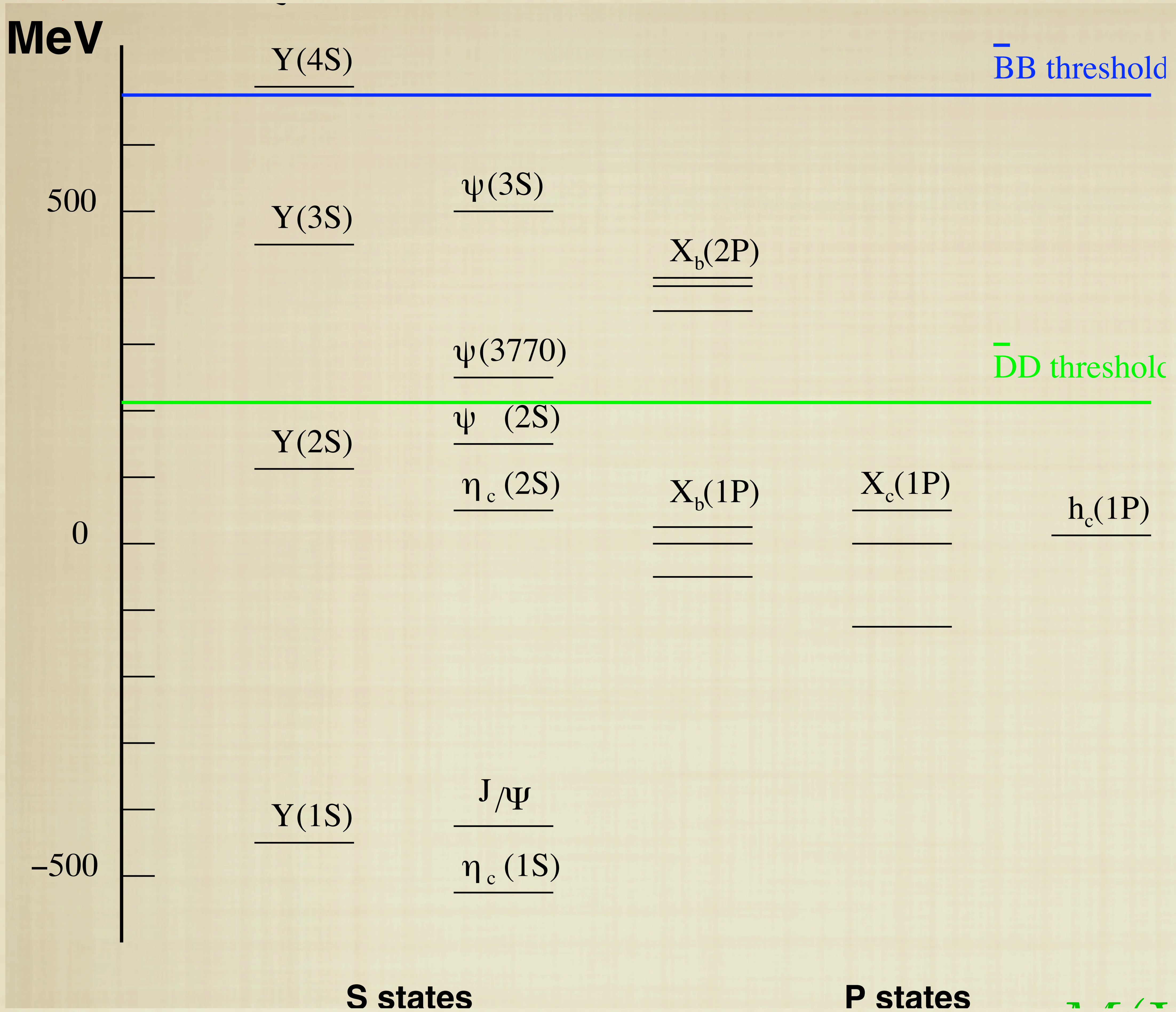

Normalized with respect to $\chi_b(1P)$ and $\chi_c(1P)$

$$^{2S+1}L_J$$

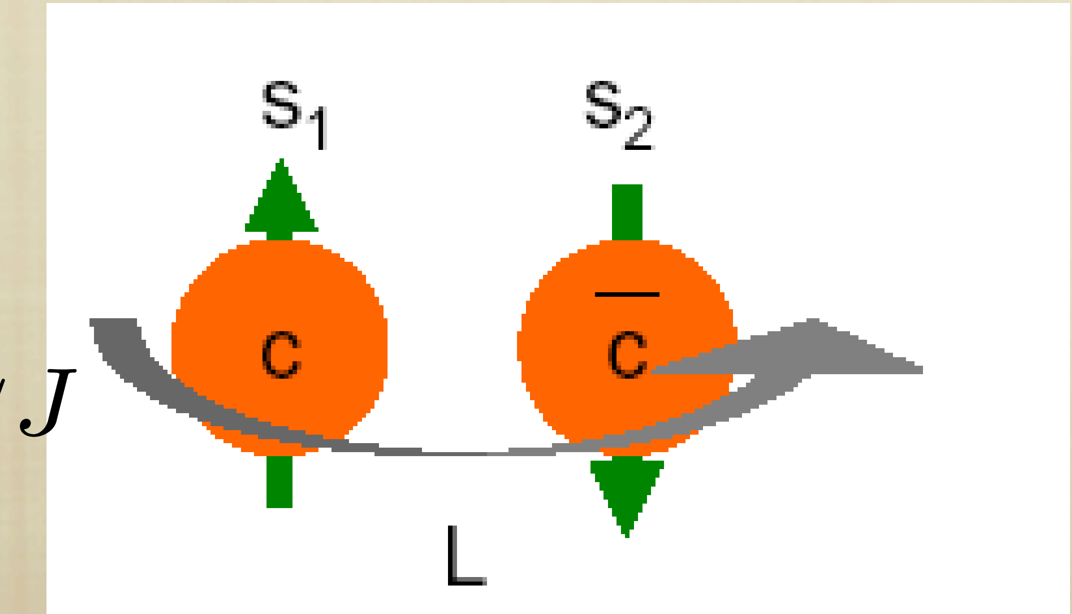

NR bound states have at least 3 scales

$$m \gg mv \gg mv^2 \qquad v \ll 1$$

The system is nonrelativistic(NR)

$$\Delta E \sim mv^2, \Delta_{fs} E \sim mv^4$$

$$v_b^2 \sim 0.1, v_c^2 \sim 0.3$$

The mass scale is perturbative

$$m_Q \gg \Lambda_{\text{QCD}}$$

$$m_b \simeq 5\,\text{GeV}; m_c \simeq 1.5\,\text{GeV}$$

$$M(Y(1S)) = 9460\,\text{GeV}$$

$$M(J/\Psi) = 3097\,\text{GeV}$$

Quarkonium scales

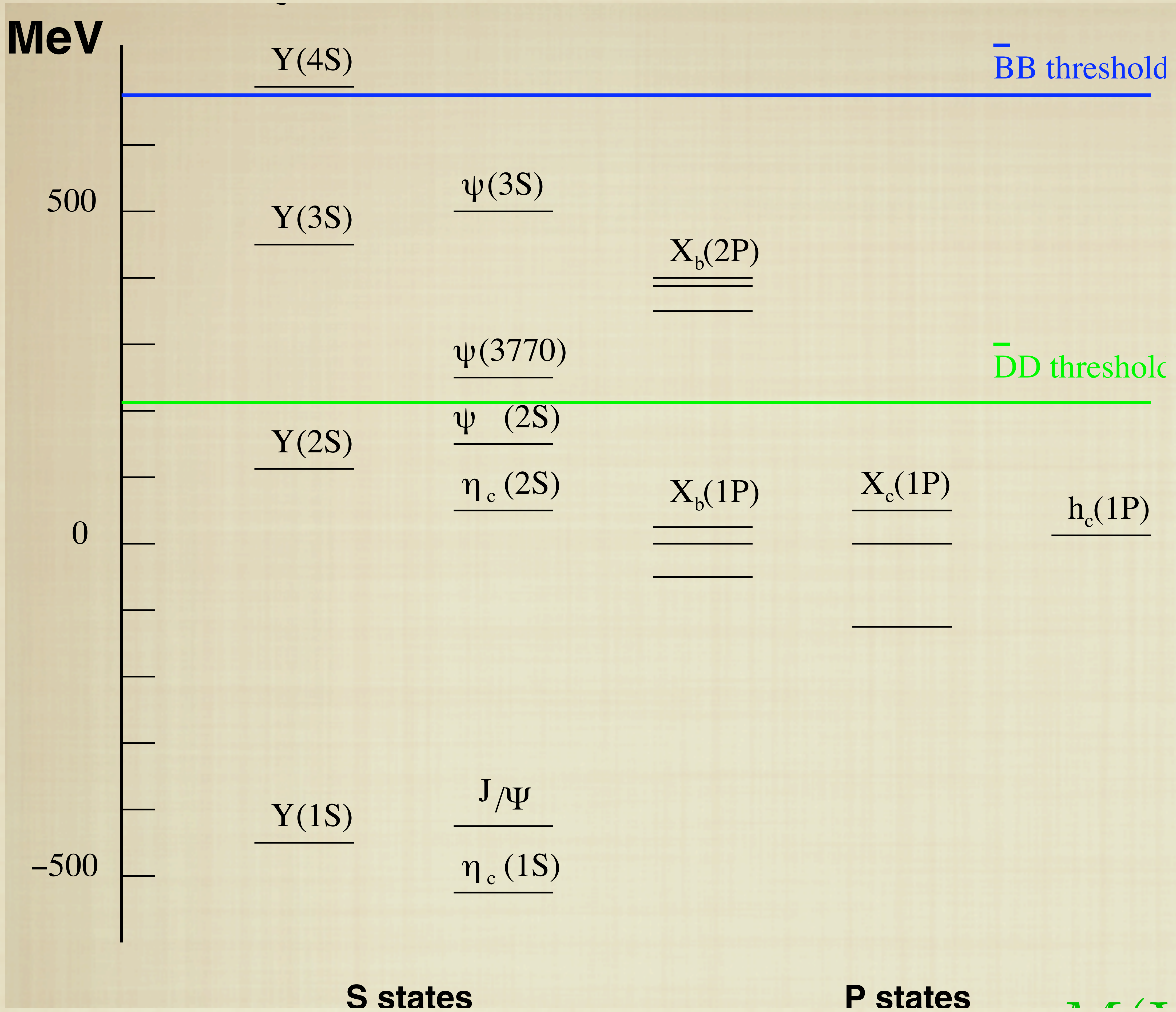

Normalized with respect to $\chi_b(1P)$ and $\chi_c(1P)$

$^{2S+1}L_J$

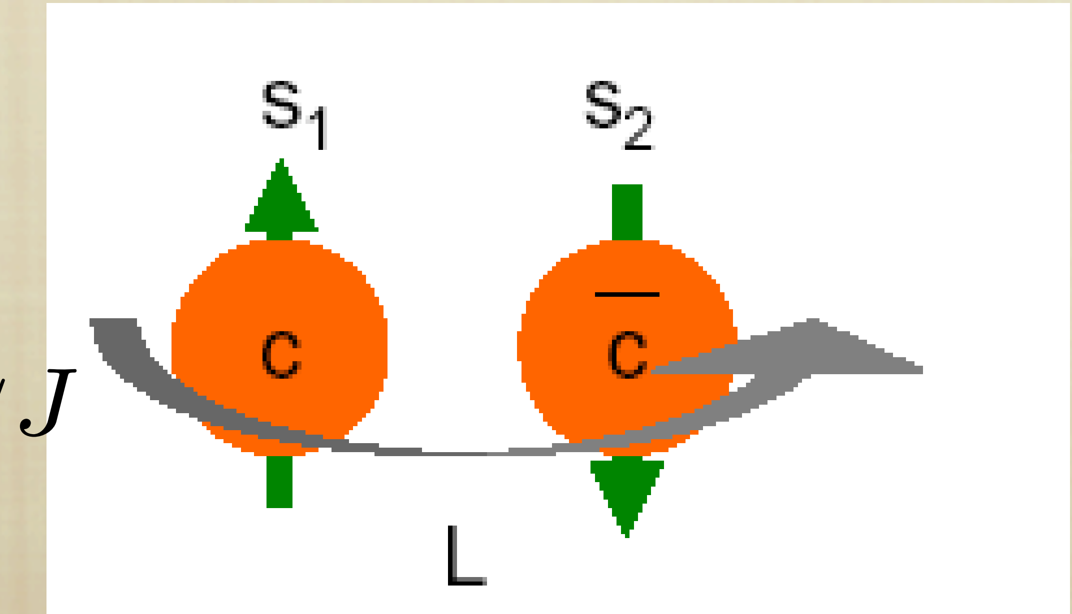

$$M(Y(1S)) = 9460\,\mathrm{GeV}$$
$$M(J/\Psi) = 3097\,\mathrm{GeV}$$

NR bound states have at least 3 scales

$$m \gg mv \gg mv^2 \qquad v \ll 1$$
$$mv \sim r^{-1}$$

The system is nonrelativistic(NR)

$$\Delta E \sim mv^2, \Delta_{fs} E \sim mv^4$$
$$v_b^2 \sim 0.1, v_c^2 \sim 0.3$$

The mass scale is perturbative

$$m_Q \gg \Lambda_{\mathrm{QCD}}$$
$$m_b \simeq 5\,\mathrm{GeV}; m_c \simeq 1.5\,\mathrm{GeV}$$

Quarkonium scales

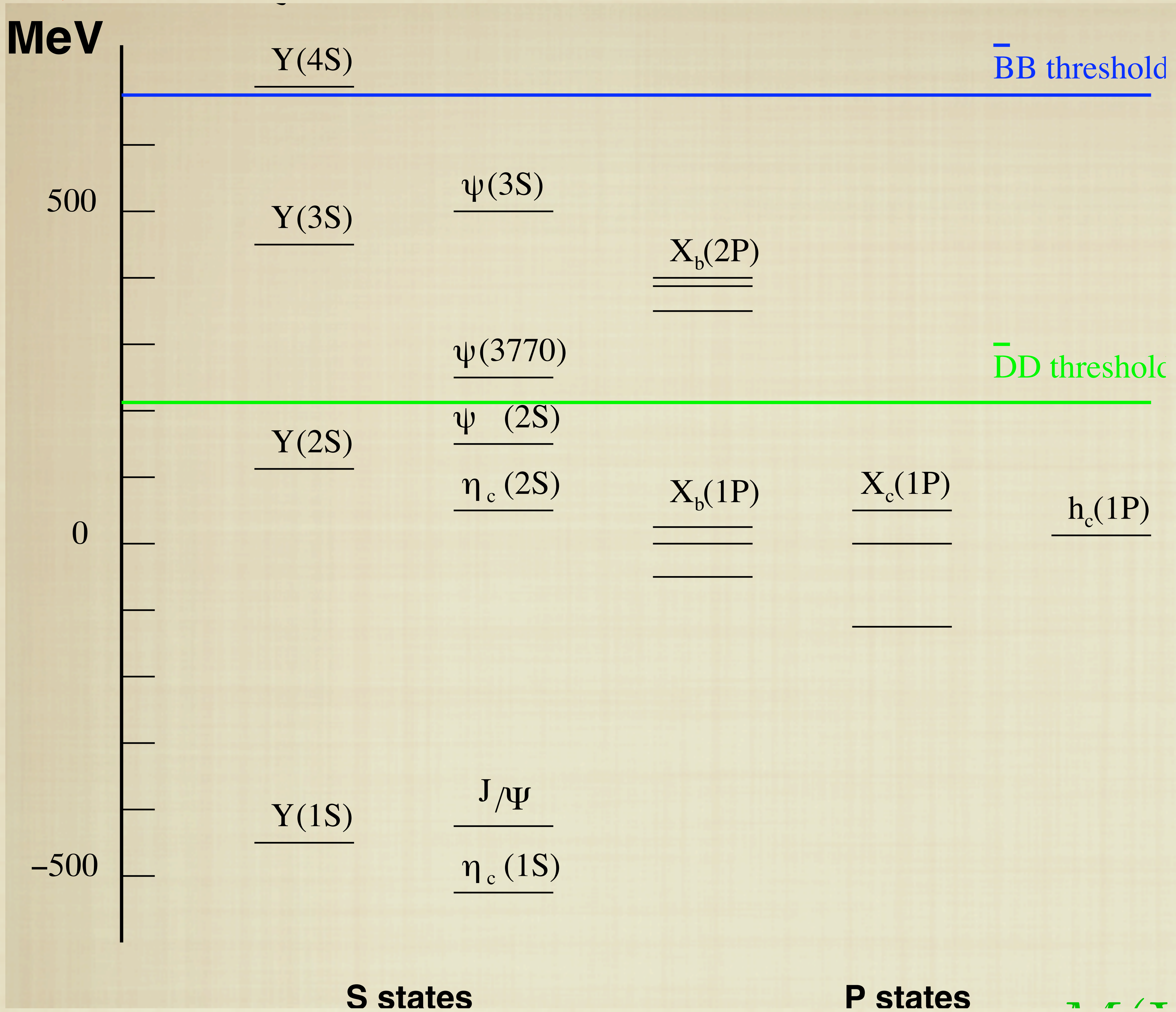

Normalized with respect to $\chi_b(1P)$ and $\chi_c(1P)$

$^{2S+1}L_J$

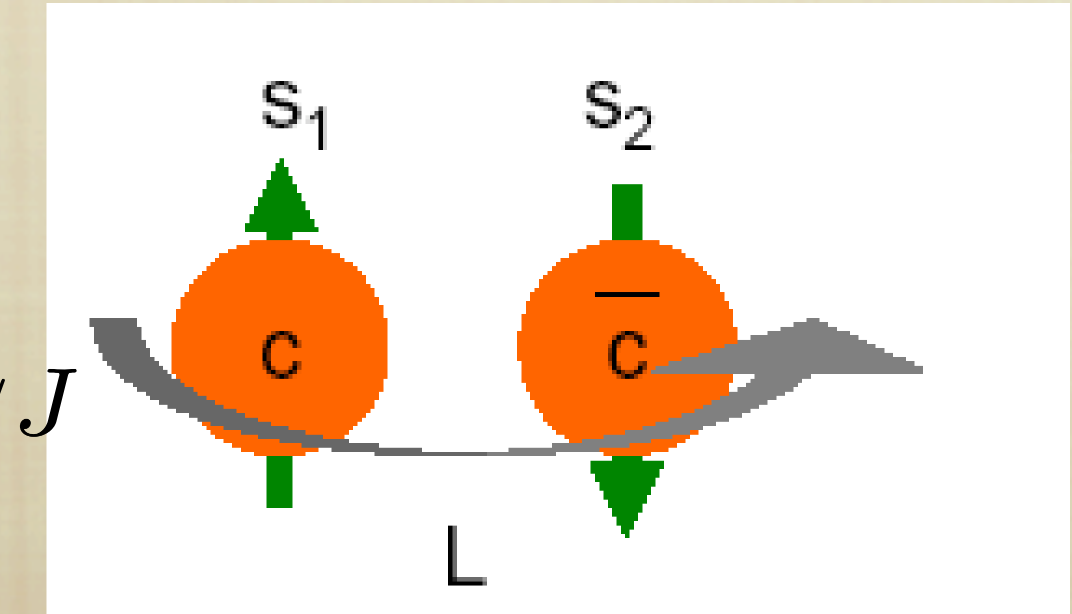

$M(Y(1S)) = 9460\,\mathrm{GeV}$

$M(J/\Psi) = 3097\,\mathrm{GeV}$

NR BOUND STATES HAVE AT LEAST 3 SCALES

$$m \gg mv \gg mv^2 \quad v \ll 1$$

$$mv \sim r^{-1}$$

and Λ_{QCD}

THE SYSTEM IS NONRELATIVISTIC(NR)

$$\Delta E \sim mv^2, \Delta_{fs} E \sim mv^4$$

$$v_b^2 \sim 0.1, v_c^2 \sim 0.3$$

THE MASS SCALE IS PERTURBATIVE

$$m_Q \gg \Lambda_{\mathrm{QCD}}$$

$$m_b \simeq 5\,\mathrm{GeV}; m_c \simeq 1.5\,\mathrm{GeV}$$

Quarkonium as a confinement probe

The rich structure of separated energy scales makes QQbar an ideal probe

At zero temperature

- The different quarkonium radii provide different measures of the transition from a Coulombic to a confined bound state.

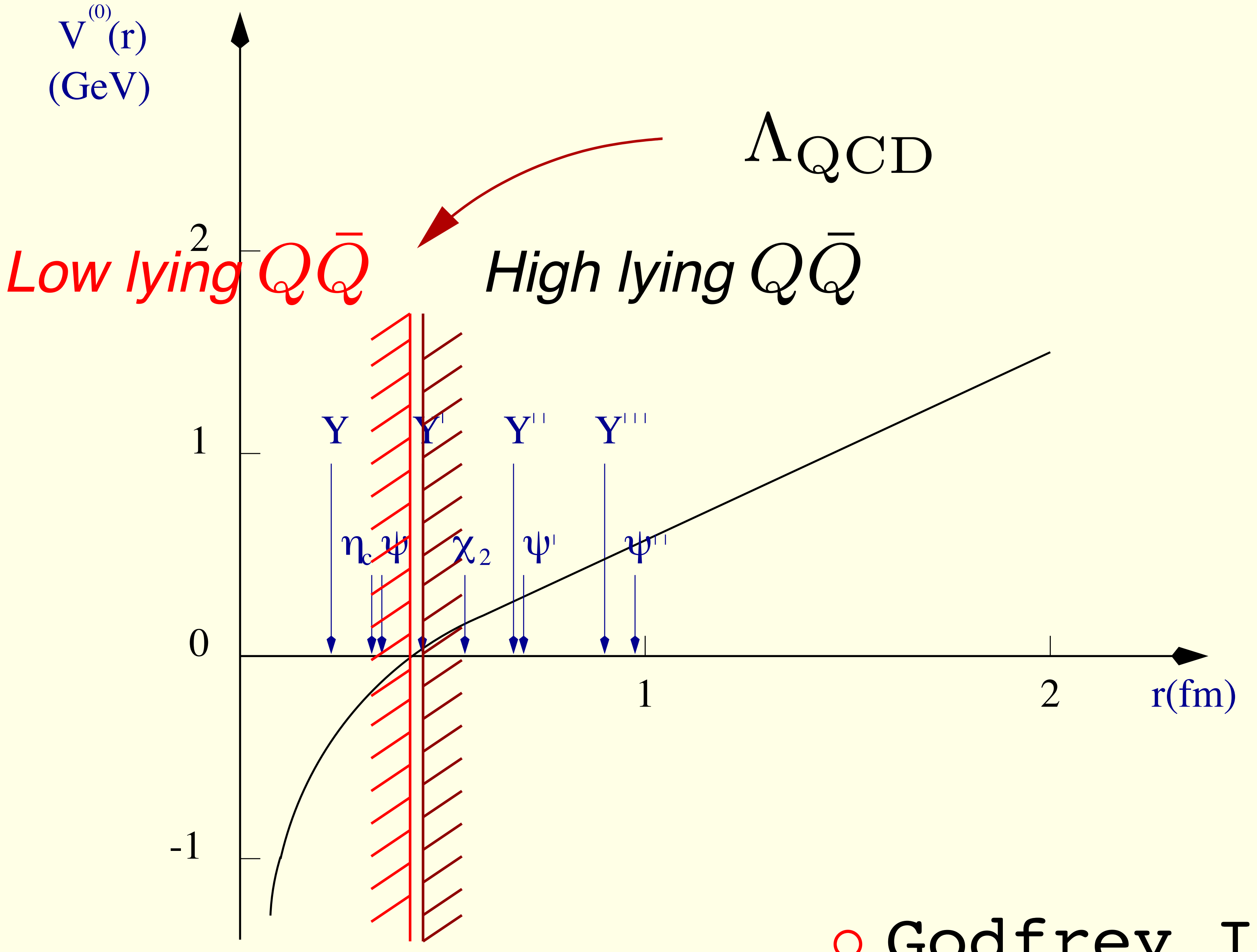

- Godfrey Isgur PRD 32(85)189

quarkonia probe the perturbative (high energy) and non perturbative region (low energy) as well as the transition region in dependence of their radius r

Quarkonium as a confinement probe

The rich structure of separated energy scales makes QQbar an ideal probe

At zero temperature

- The different quarkonium radii provide different measures of the transition from a Coulombic to a confined bound state.

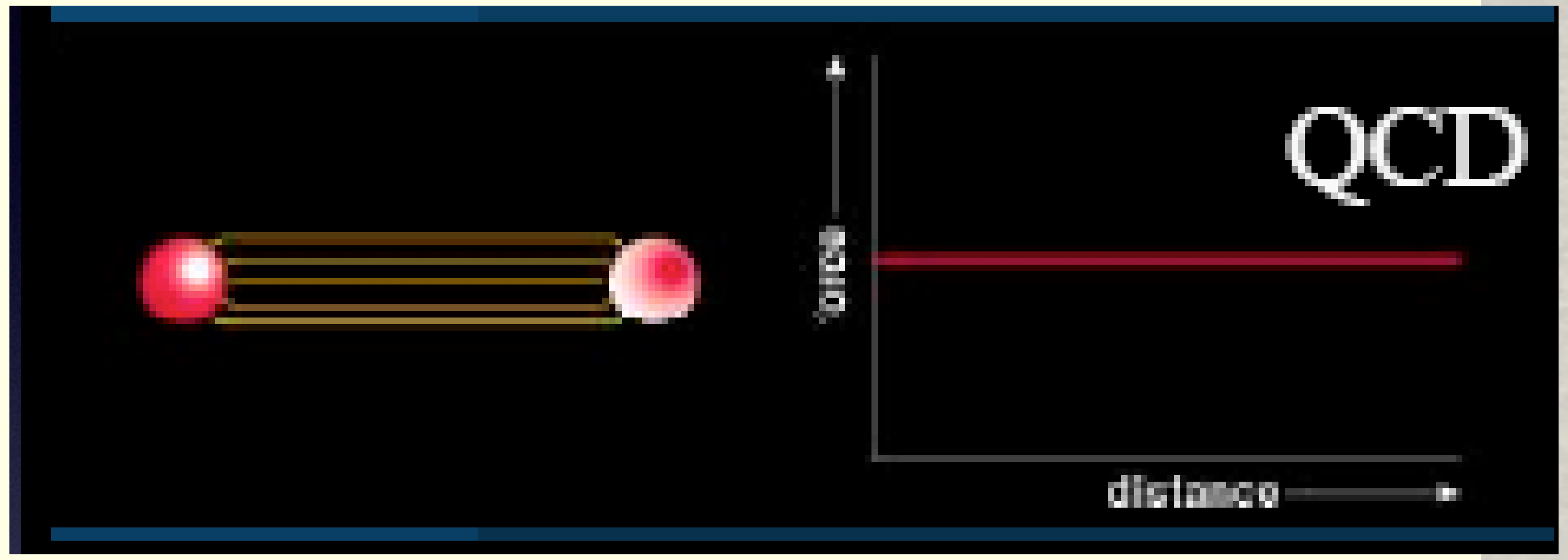

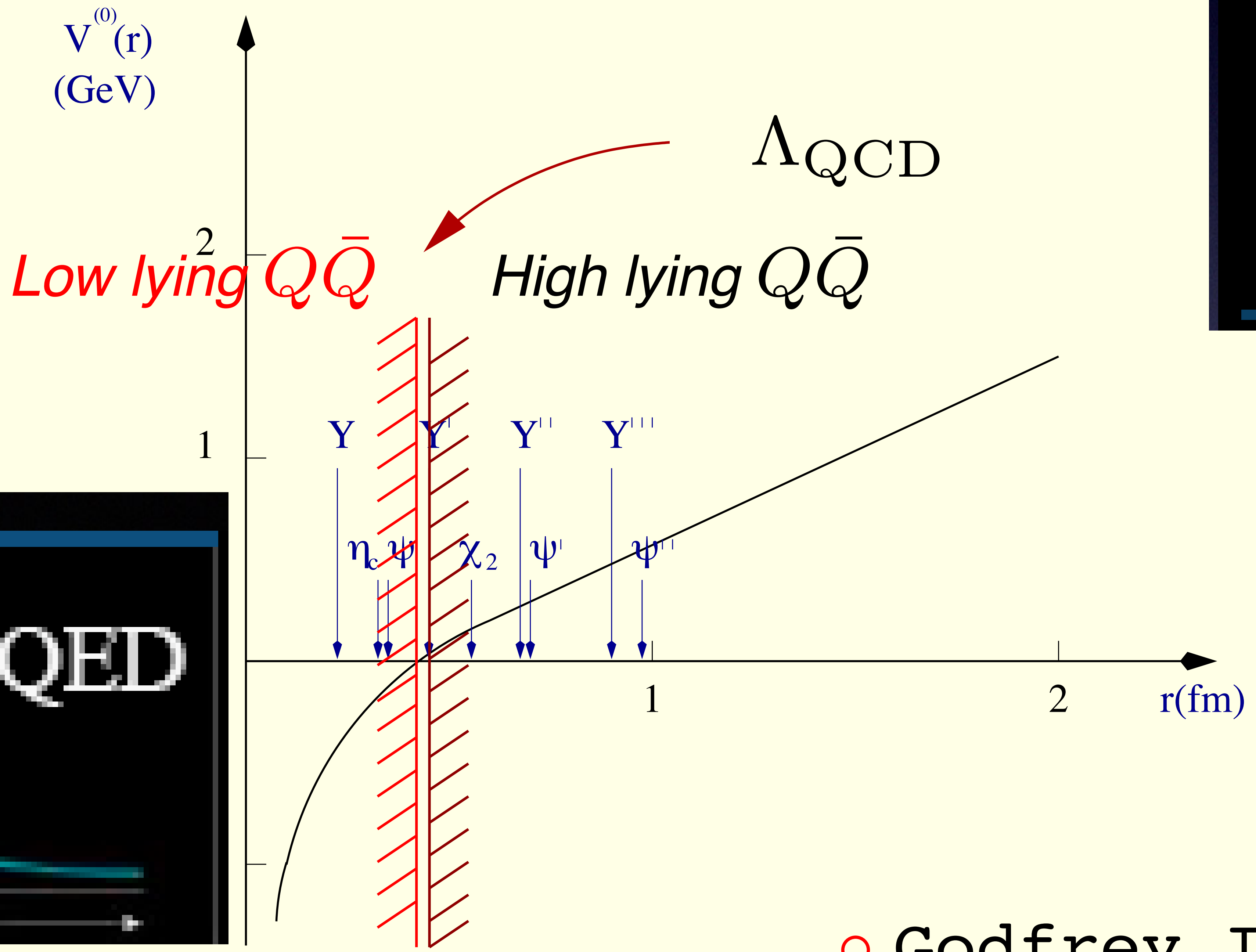

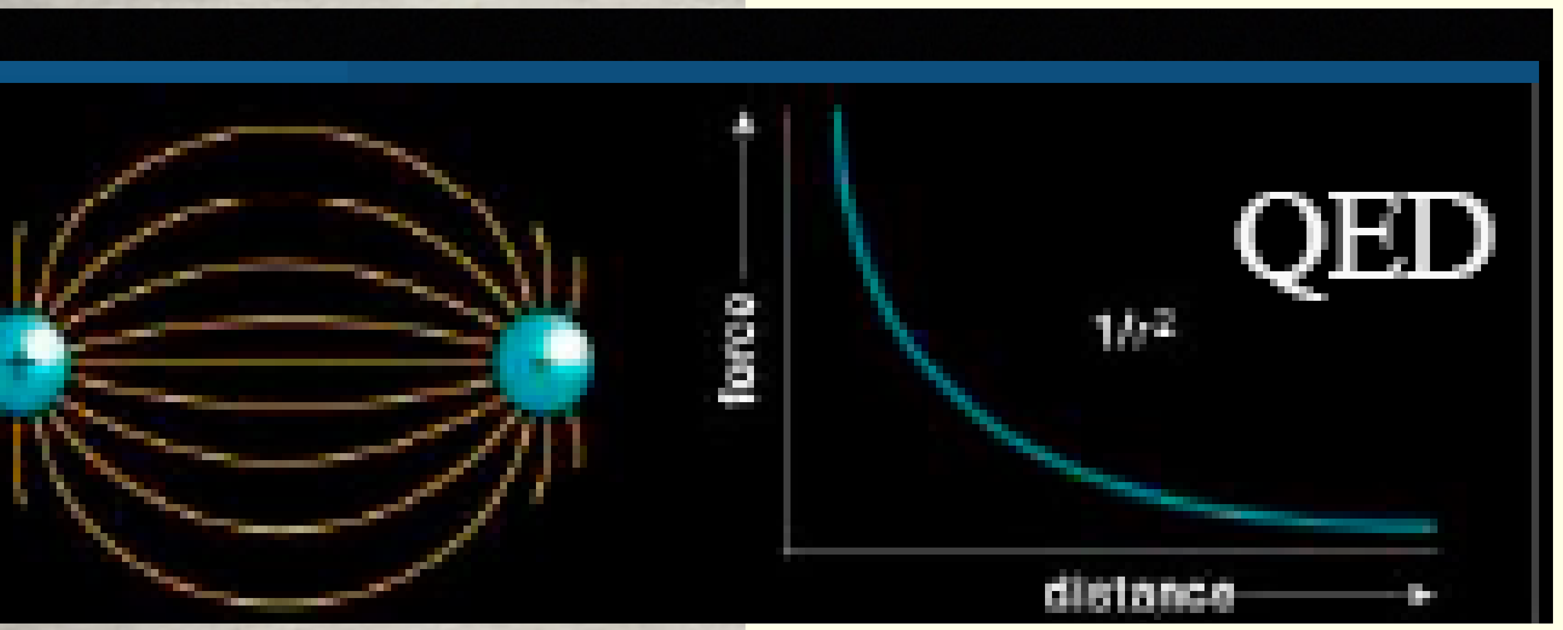

- Godfrey Isgur PRD 32(85)189

quarkonia probe the perturbative (high energy) and non perturbative region (low energy) as well as the transition region in dependence of their radius r

Quarkonium as a confinement and deconfinement probe

At finite temperature T they are sensitive to the formation of a quark gluon plasma via color screening

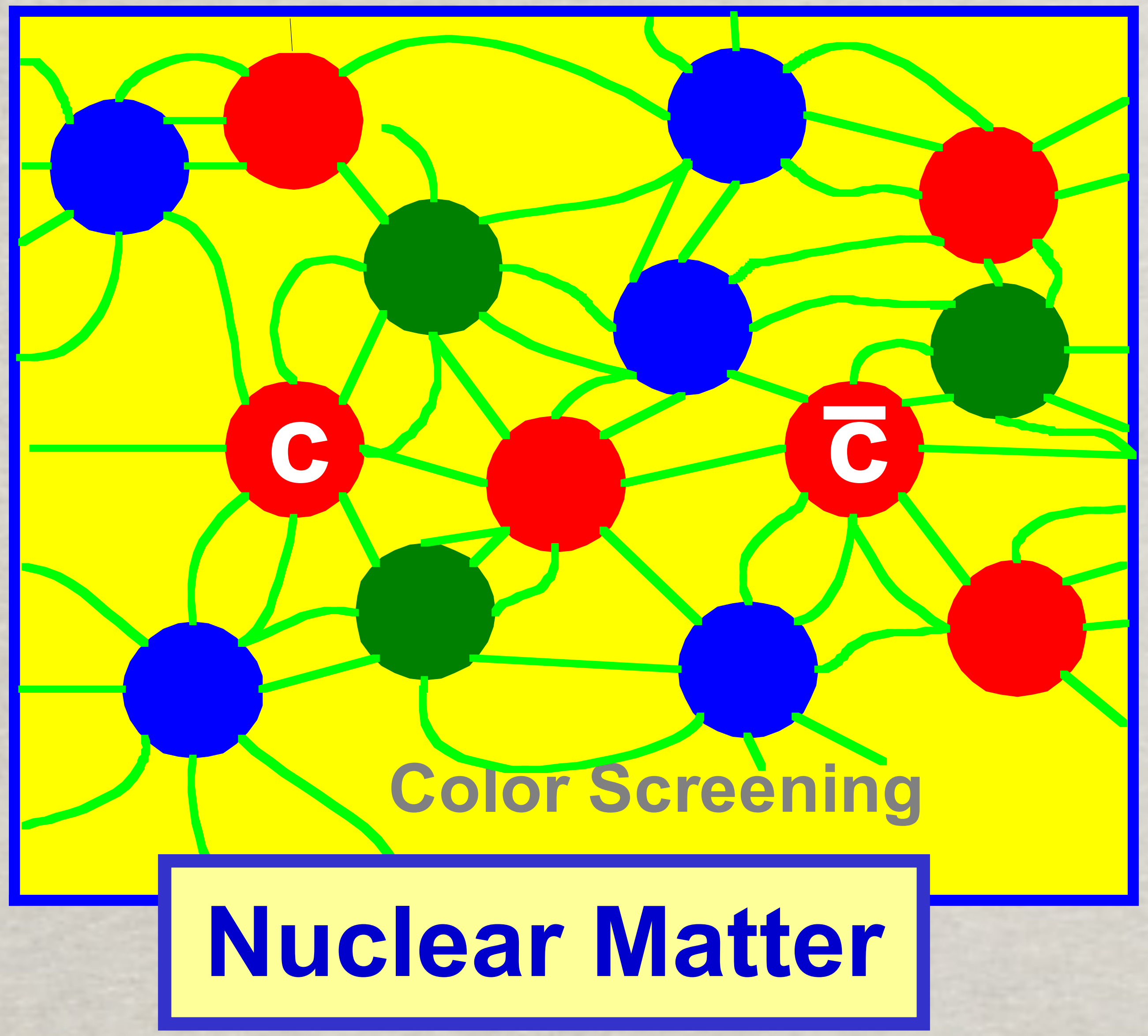

Debye charge screening $m_D \sim gT$

$$V(r) \sim -\alpha_s \frac{e^{-m_D r}}{r}$$

Matsui Satz 1986

A simulated collision of lead ions, courtesy the A
experiment at CERN

Quarkonium as a confinement and deconfinement probe

At finite temperature T they are sensitive to the formation of a quark gluon plasma via color screening

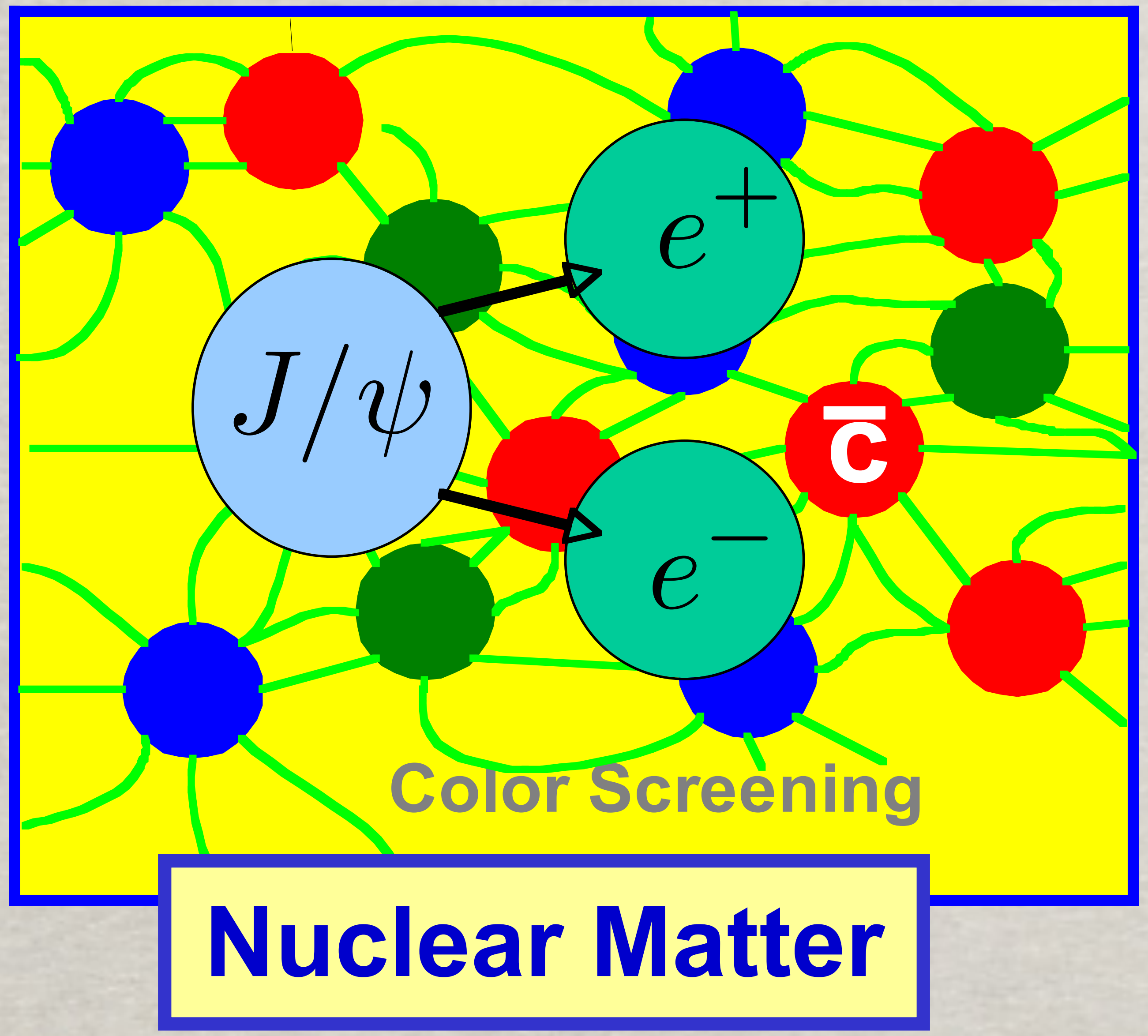

Debye charge screening $m_D \sim gT$

$$V(r) \sim -\alpha_s \frac{e^{-m_D r}}{r}$$

Matsui Satz 1986

A simulated collision of lead ions, courtesy the A
experiment at CERN

Quarkonium as a confinement and deconfinement probe

At finite temperature T they are sensitive to the formation of a quark gluon plasma via color screening

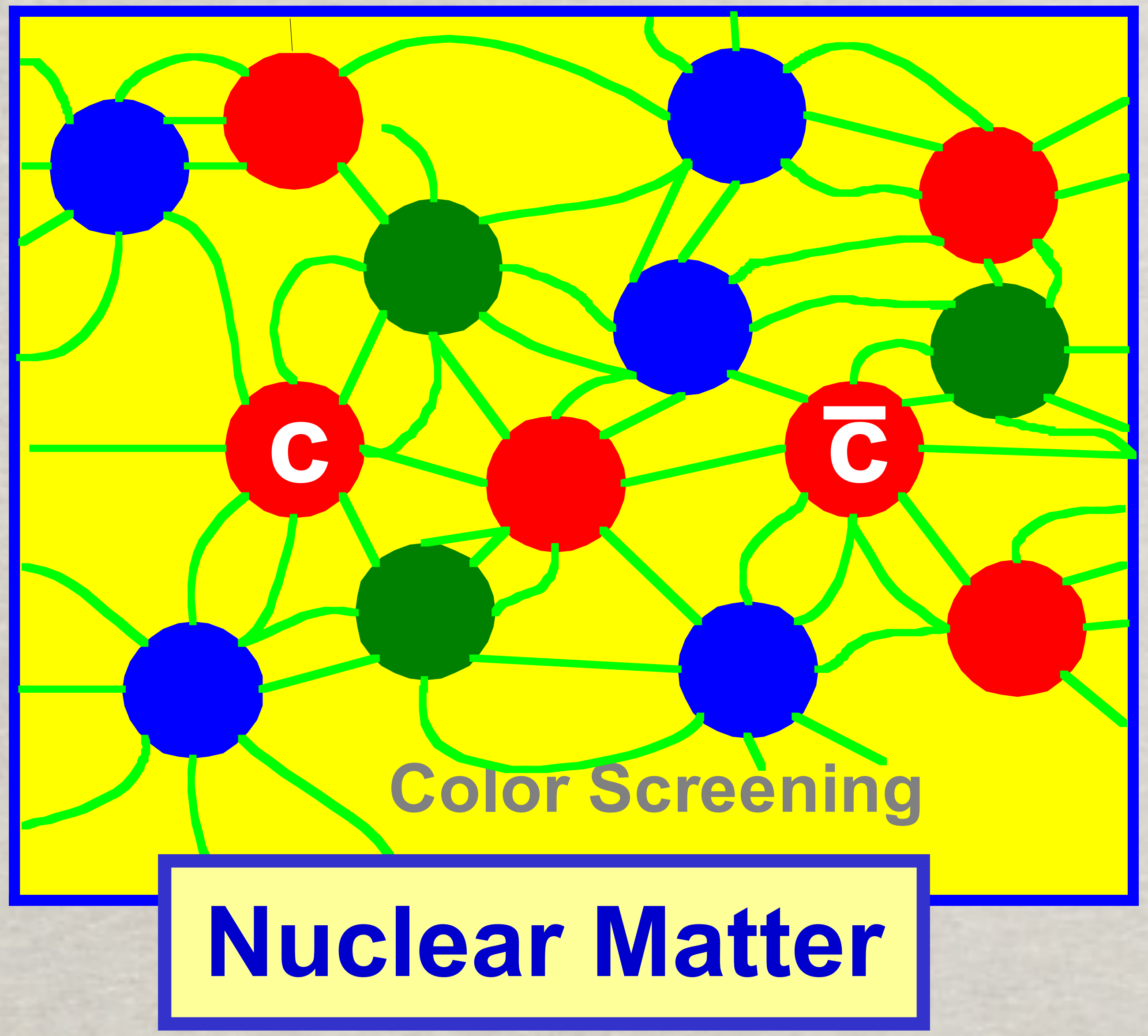

Debye charge screening $m_D \sim gT$

$$V(r) \sim -\alpha_s \frac{e^{-m_D r}}{r}$$

Matsui Satz 1986

A simulated collision of lead ions, courtesy the A
experiment at CERN

Quarkonium as a confinement and deconfinement probe

At finite temperature T they are sensitive to the formation of a quark gluon plasma via color screening

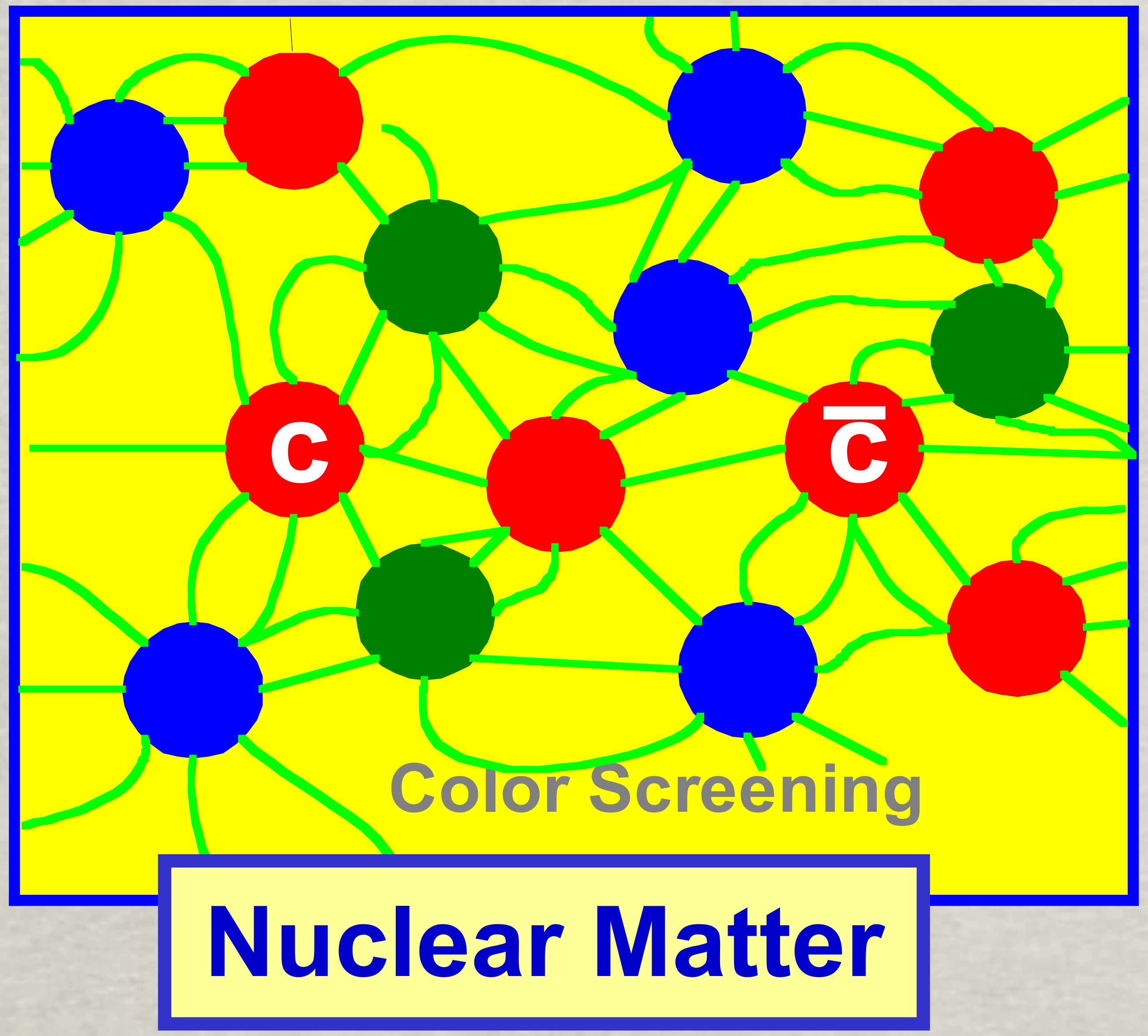

Debye charge screening $m_D \sim gT$

$$V(r) \sim -\alpha_s \frac{e^{-m_D r}}{r}$$

Matsui Satz 1986

$$r \sim \frac{1}{m_D} \longrightarrow$$ Bound state dissolves

A simulated collision of lead ions, courtesy the Al experiment at CERN

Quarkonium as a confinement and deconfinement probe

At finite temperature T they are sensitive to the formation of a quark gluon plasma via color screening

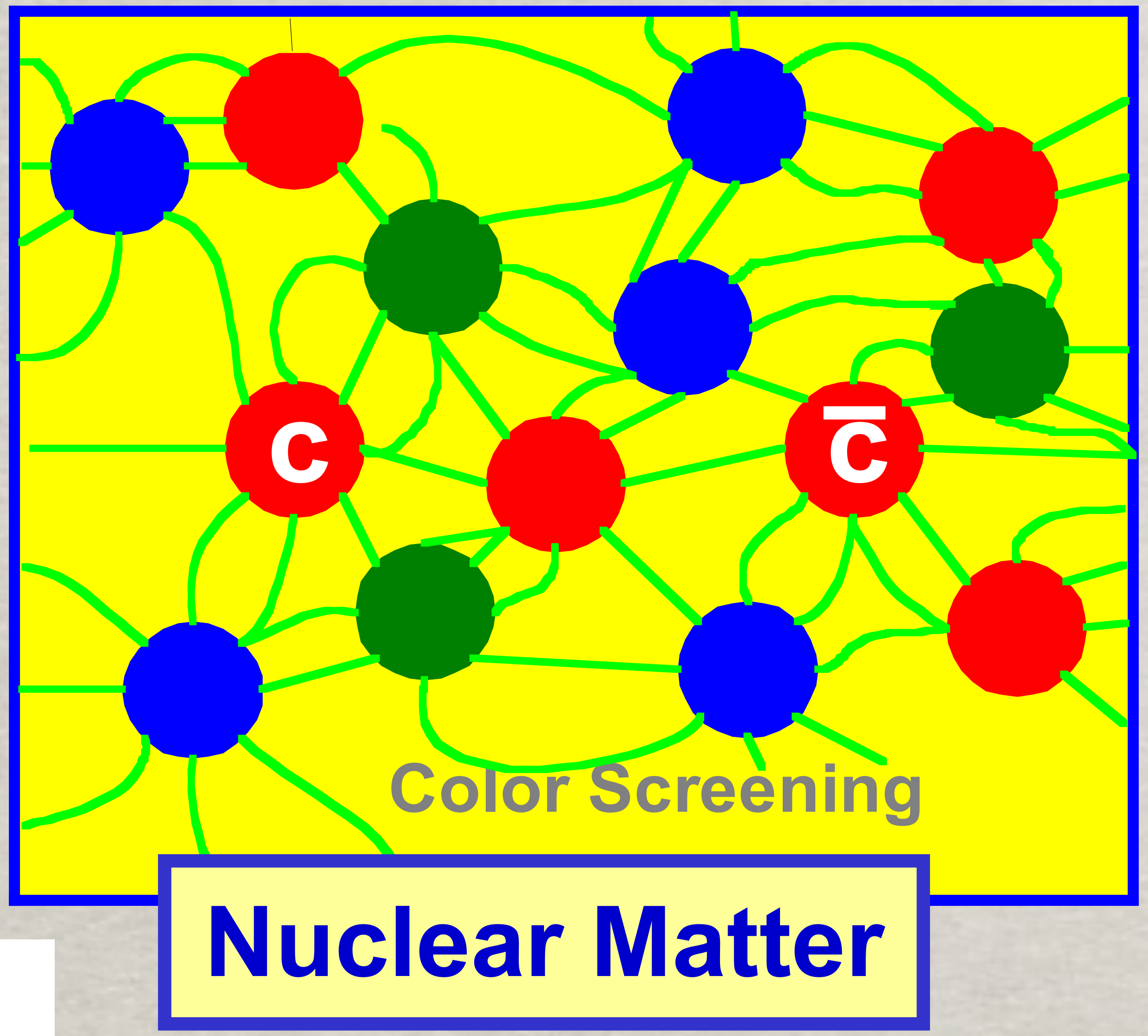

Debye charge screening $m_D \sim gT$

$$V(r) \sim -\alpha_s \frac{e^{-m_D r}}{r}$$

Matsui Satz 1986

$$r \sim \frac{1}{m_D} \longrightarrow$$ Bound state dissolves

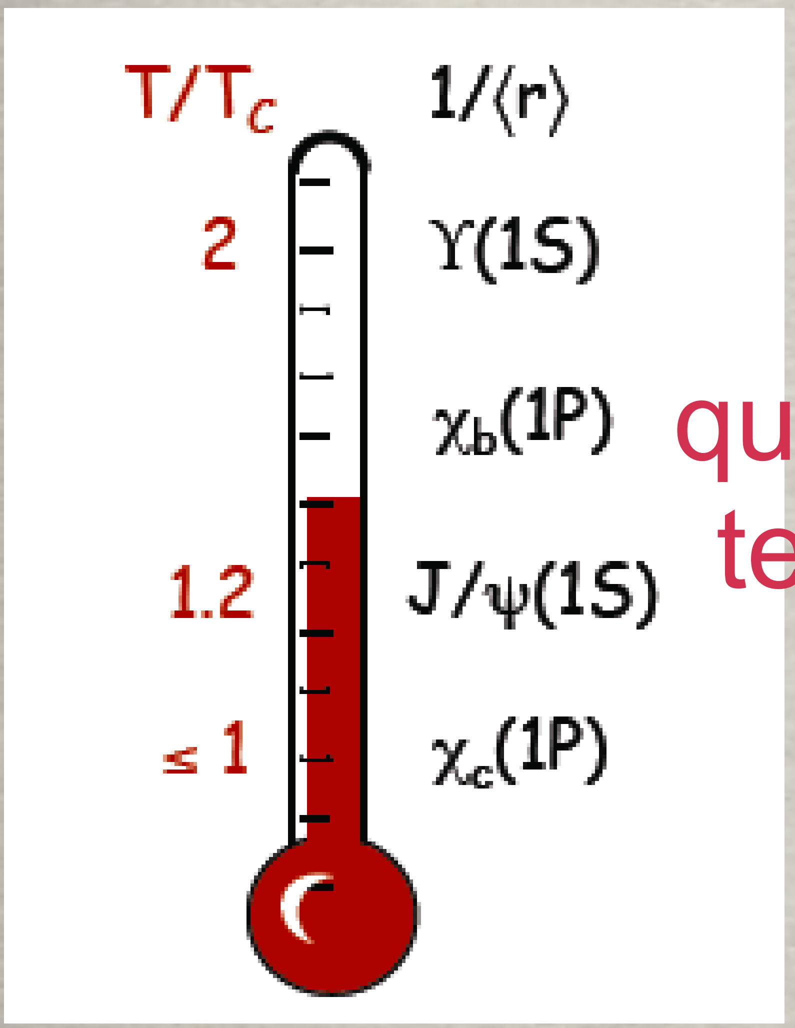

quarkonia dissociate at different temperature in dependence of their radius: they are a Quark Gluon Plasma thermometer

A simulated collision of lead ions, courtesy the A
experiment at CERN

Quarkonium as a confinement and deconfinement probe

At finite temperature T they are sensitive to the formation of a quark gluon plasma via color screening

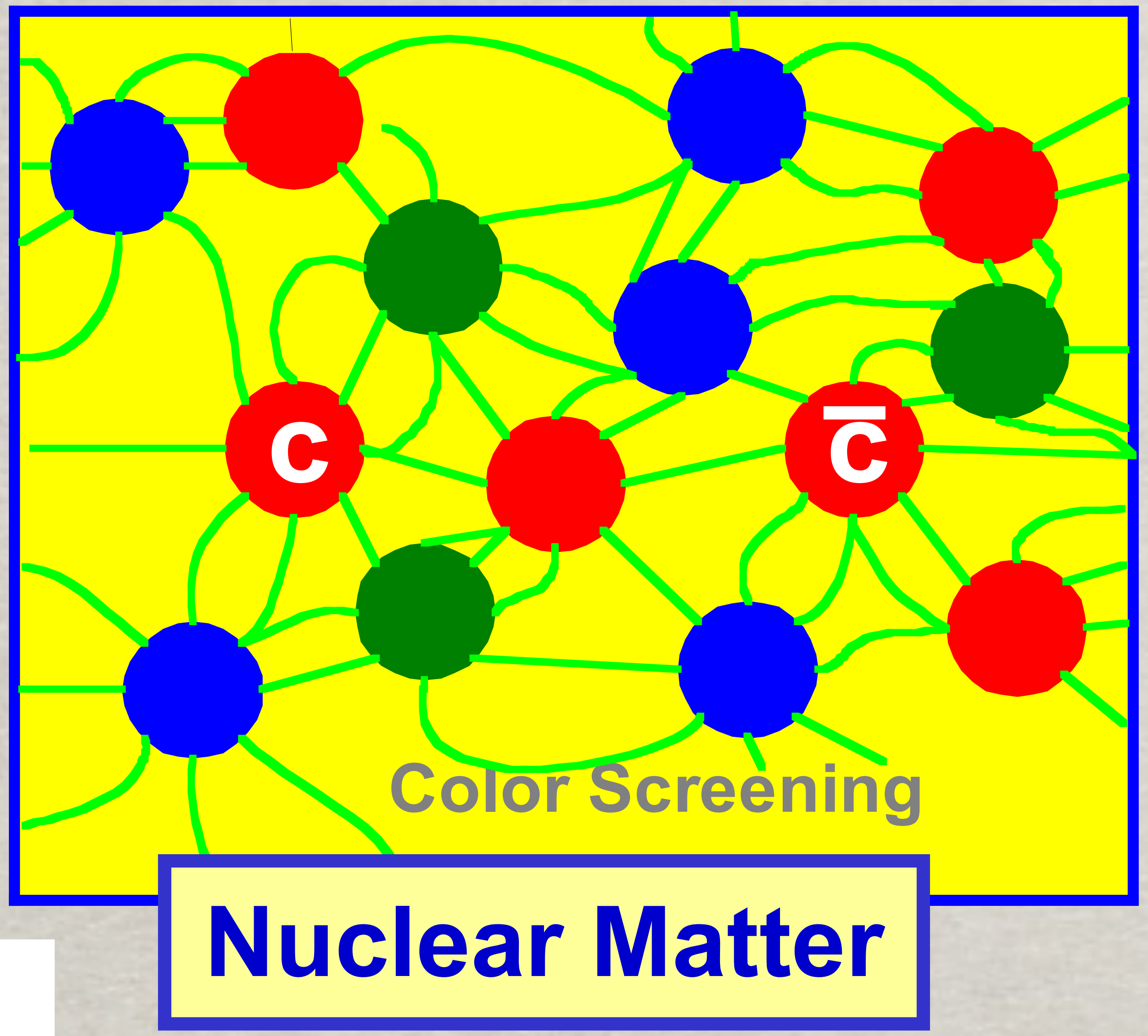

Debye charge screening $m_D \sim gT$

$$V(r) \sim -\alpha_s \frac{e^{-m_D r}}{r}$$

Matsui Satz 1986

$$r \sim \frac{1}{m_D} \longrightarrow$$ Bound state dissolves

nuclear modificatio

$$R_{AA} = \frac{Yield^{q\bar{q}}_{AA}}{\langle N_{coll} \rangle \times Yield^{q\bar{q}}_{pp}}$$

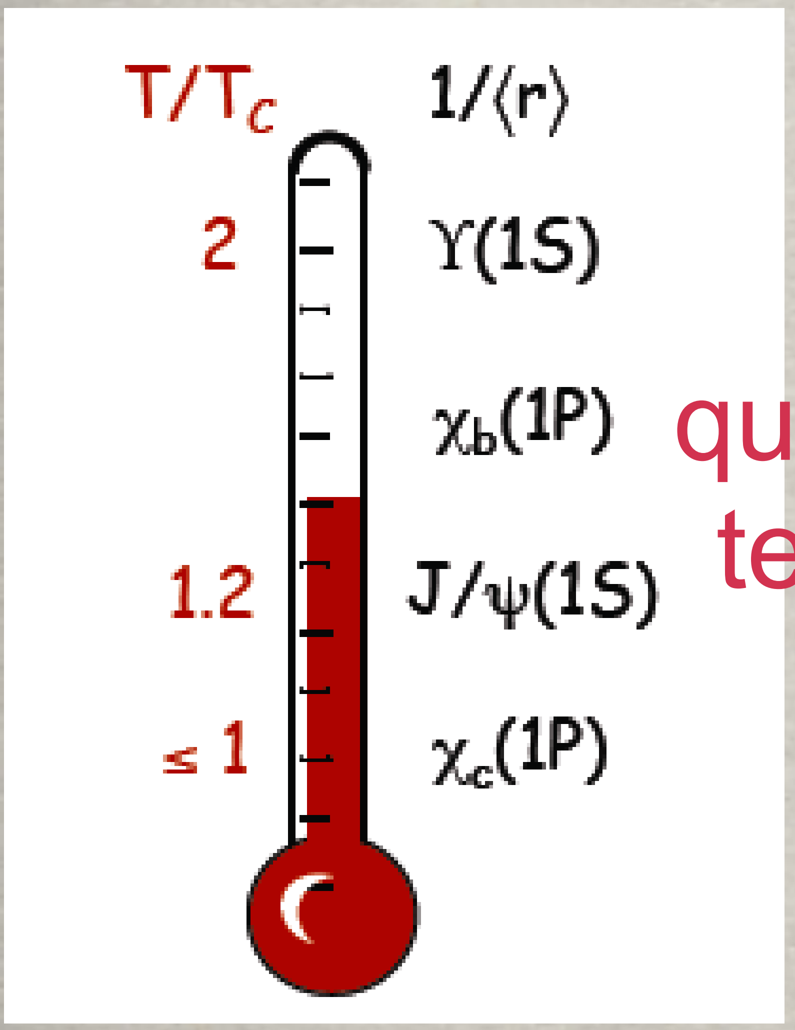

quarkonia dissociate at different temperature in dependence of their radius: they are a Quark Gluon Plasma thermometer

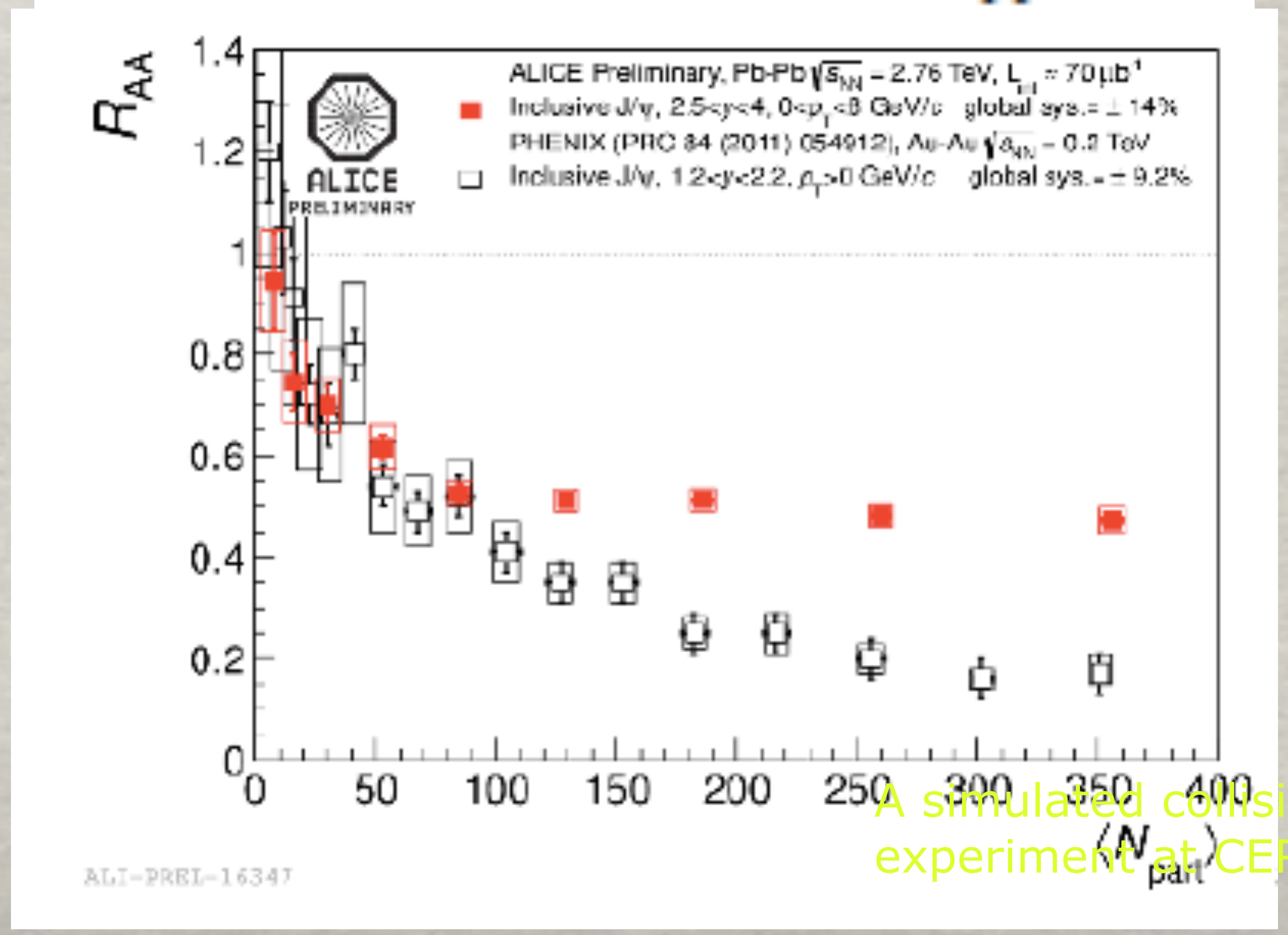

A simulated collision of lead ions, courtesy the A experiment at CERN nt and deconfinement probe

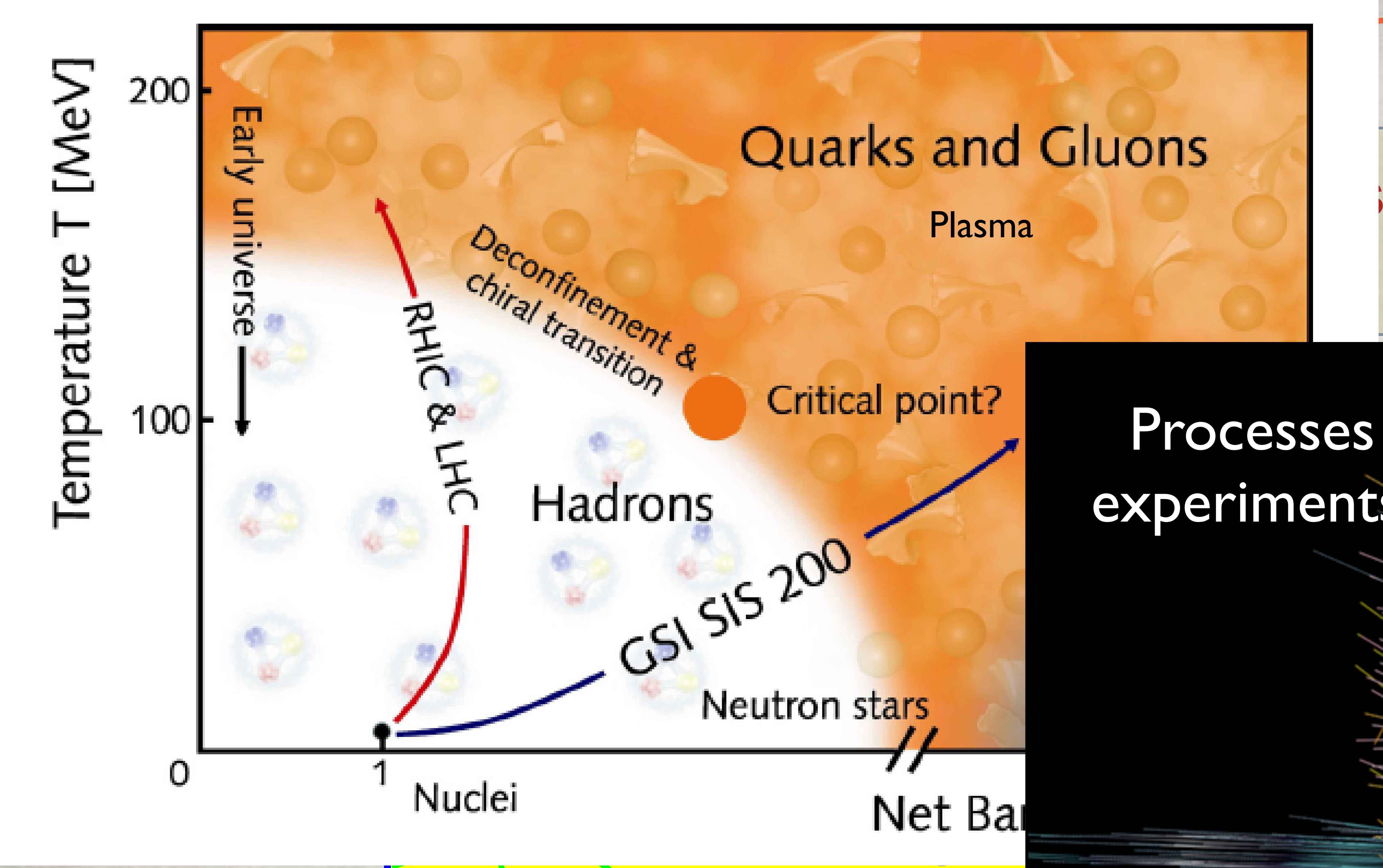

sitive to the formation of a quark gluon

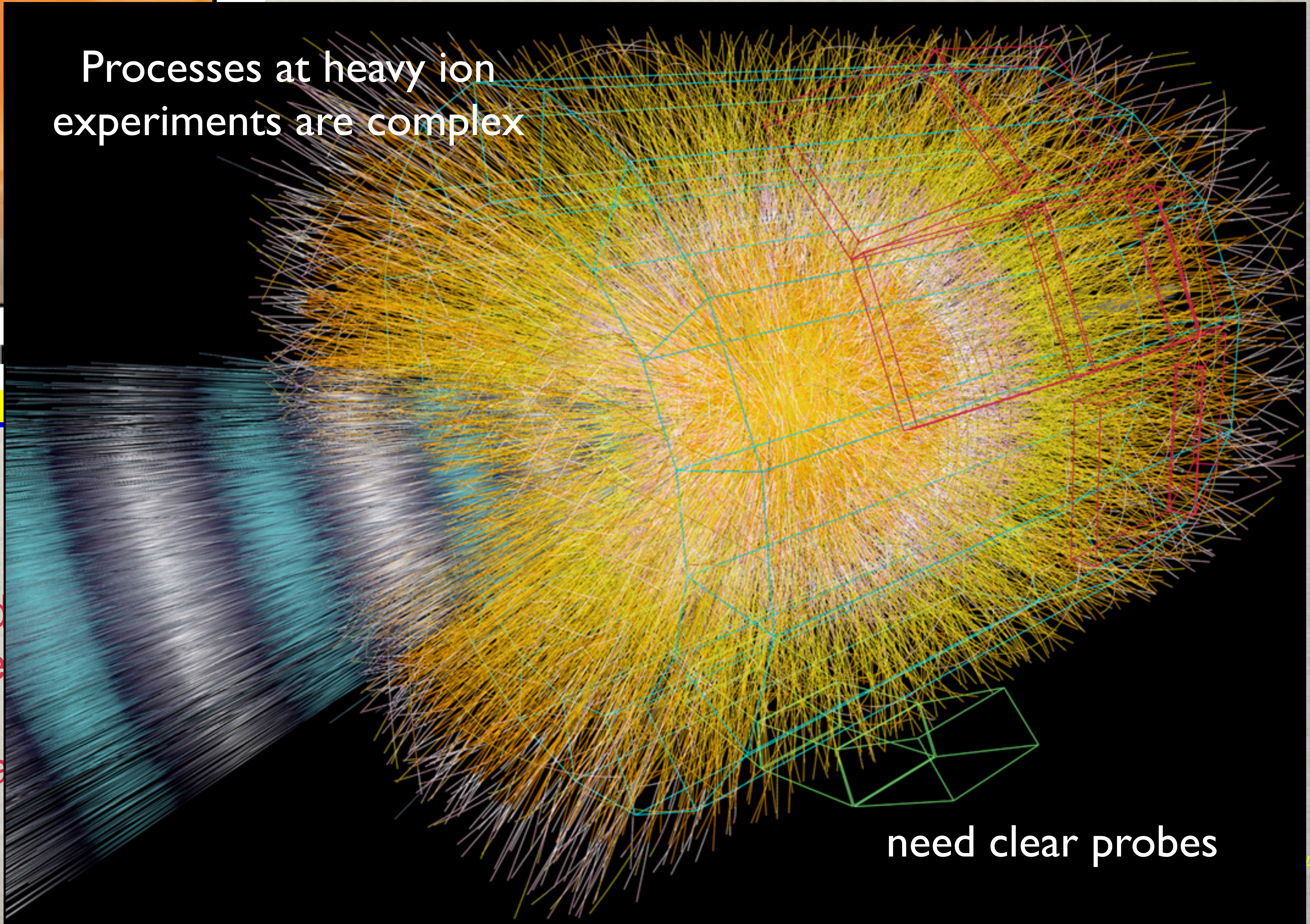

Nuclear Matter

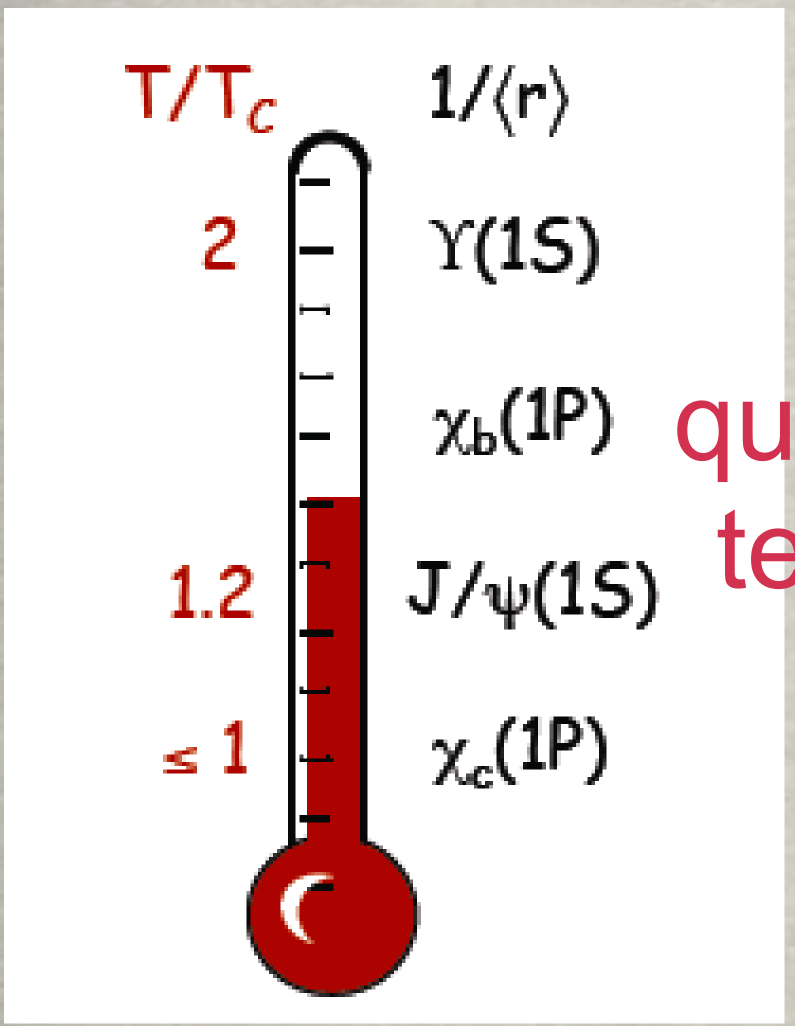

quarkonia dissociate at d
temperature in depende
their radius: they
are a Quark Gluon Pla
thermometer

but what is the QCD potential?
and what are the other nonpotential effects to the spectrum and decay
coming from QCD, i.e defined in QFT?

but what is the QCD potential?
and what are the other nonpotential effects to the spectrum and decay coming from QCD, i.e defined in QFT?

Nonrelativistic Effective Field Theories (NREFTs) can give an answer to this
in particular potential Nonrelativistic QCD (pNRQCD)

QCD theory of Quarkonium: a very hard problem even at T=0

QCD theory of Quarkonium: a very hard problem even at T=0

Close to the bound state $\alpha_s \sim v$

QCD theory of Quarkonium: a very hard problem even at T=0

Close to the bound state $\alpha_s \sim v$

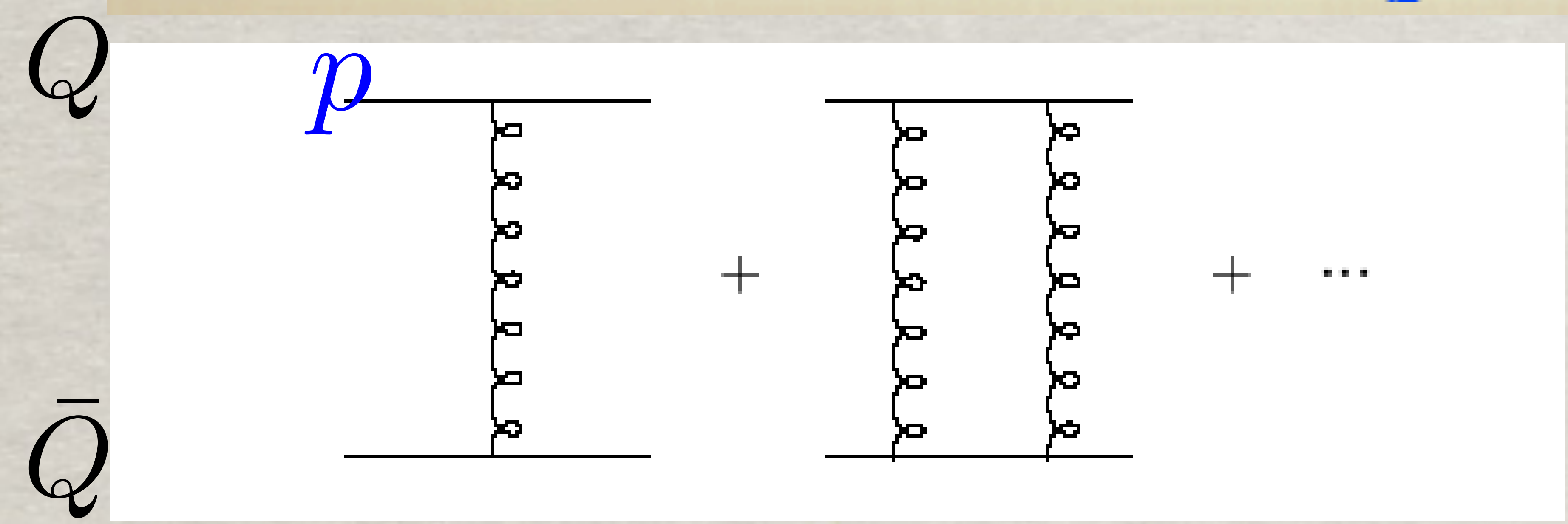

QCD theory of Quarkonium: a very hard problem even at T=0

Close to the bound state $\alpha_s \sim v$

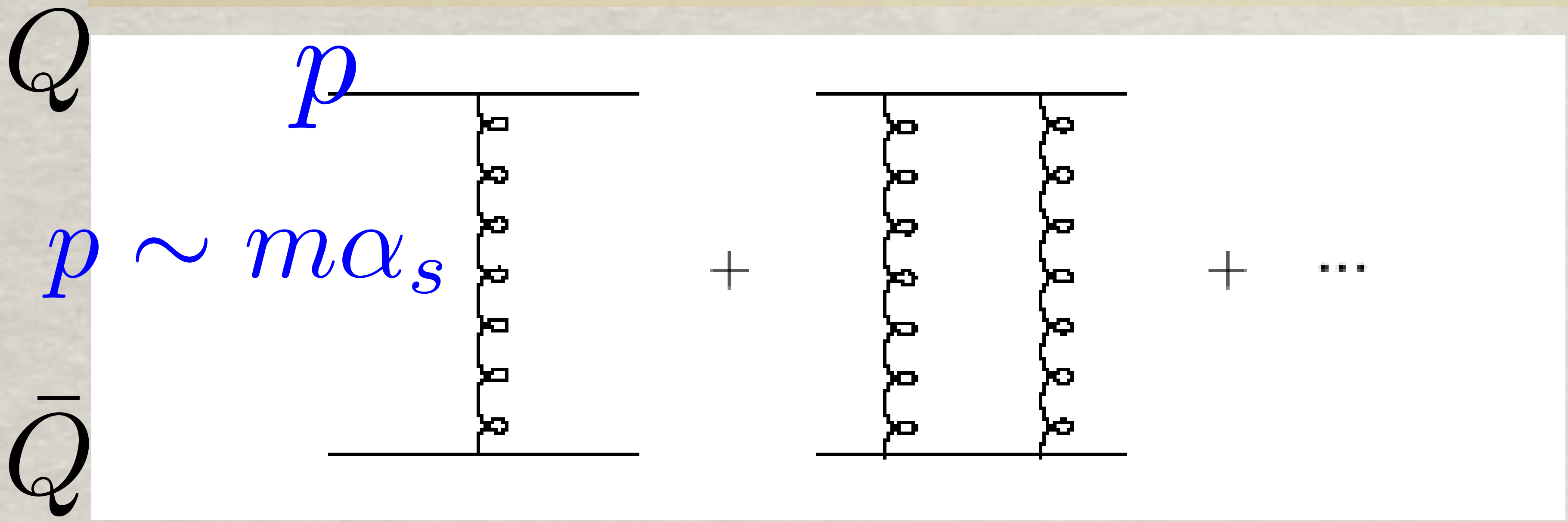

QCD theory of Quarkonium: a very hard problem even at T=0

Close to the bound state $\alpha_s \sim v$

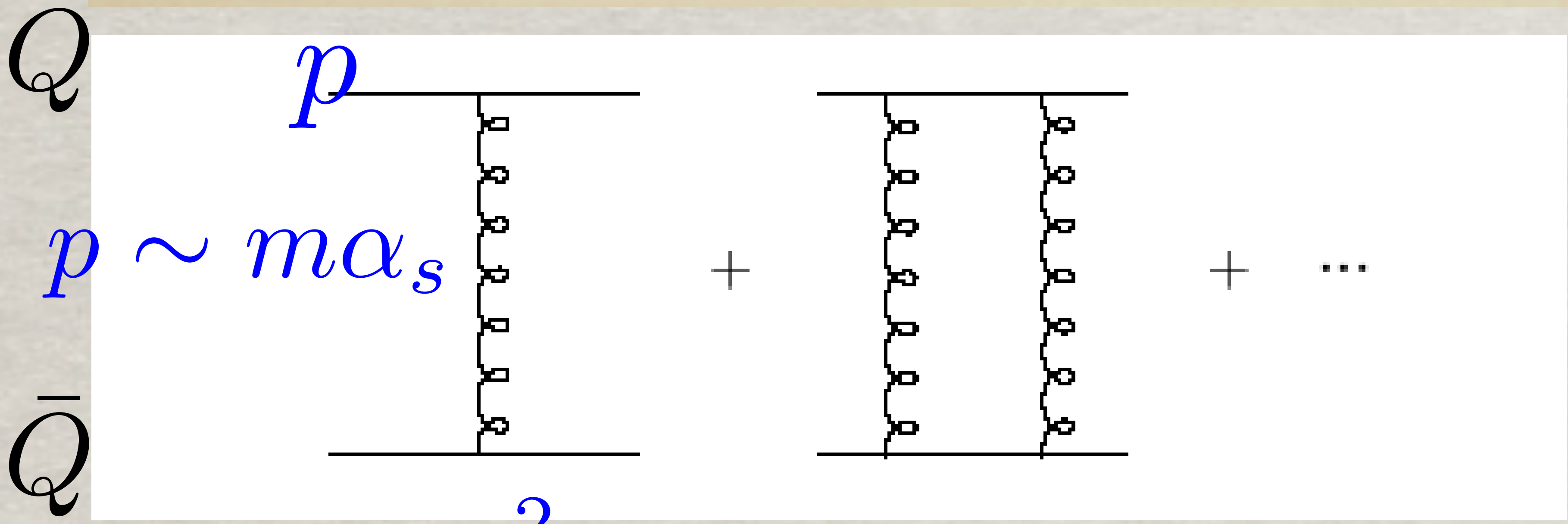

$$\frac{g^2}{p^2}\left(1 + \frac{m\alpha_s}{p}\right)$$

QCD theory of Quarkonium: a very hard problem even at T=0

Close to the bound state $\alpha_s \sim v$

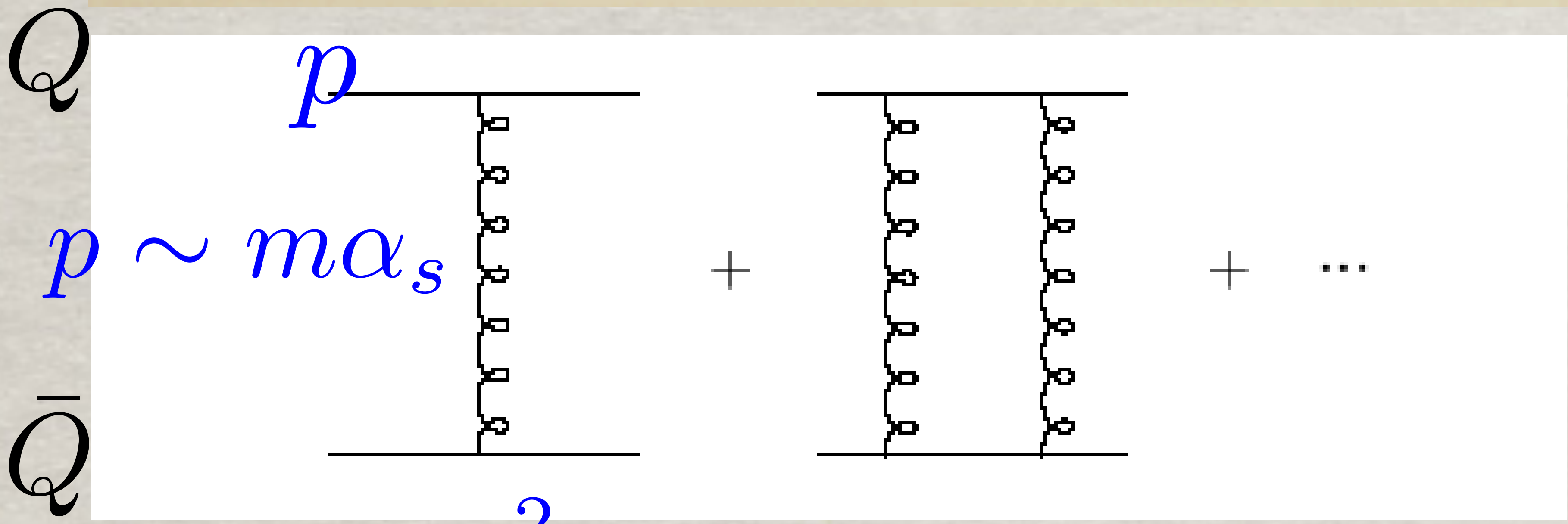

$$\frac{g^2}{p^2}\left(1 + \frac{m\alpha_s}{p}\right)$$

$$\sim \frac{1}{E - \left(\frac{p^2}{m} + V\right)}$$

QCD theory of Quarkonium: a very hard problem even at T=0

Close to the bound state $\alpha_s \sim v$

Q p

$p \sim m\alpha_s$

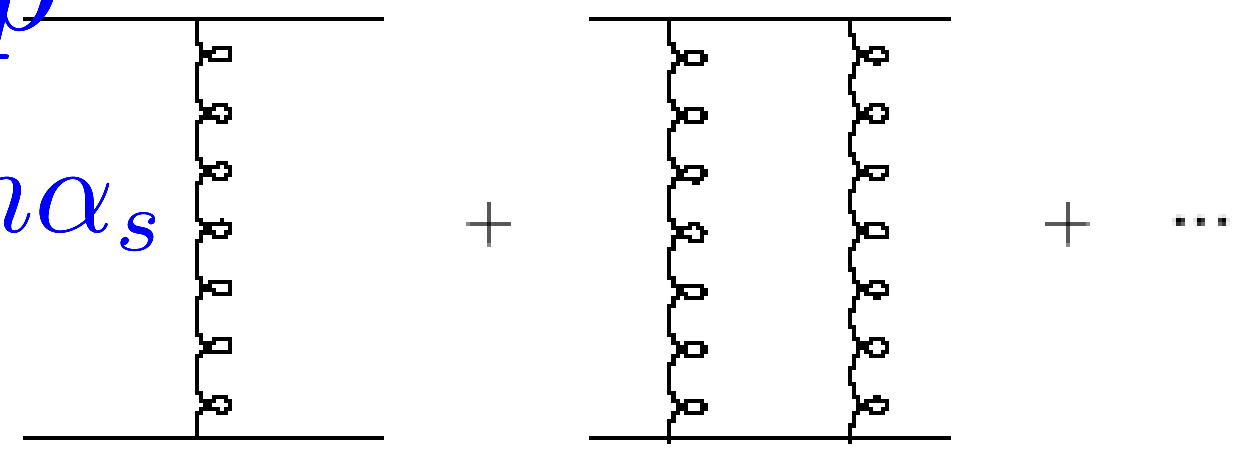

$\bar{Q}$

$$\frac{g^2}{p^2}\left(1+\frac{m\alpha_s}{p}\right)$$

$$\sim \frac{1}{E-\left(\frac{p^2}{m}+V\right)}$$

- From $(\frac{p^2}{m}+V)\phi = E\phi \to p \sim mv$ and $E = \frac{p^2}{m} + V \sim mv^2$.

QCD theory of Quarkonium: a very hard problem even at T=0

Close to the bound state $\alpha_s \sim v$

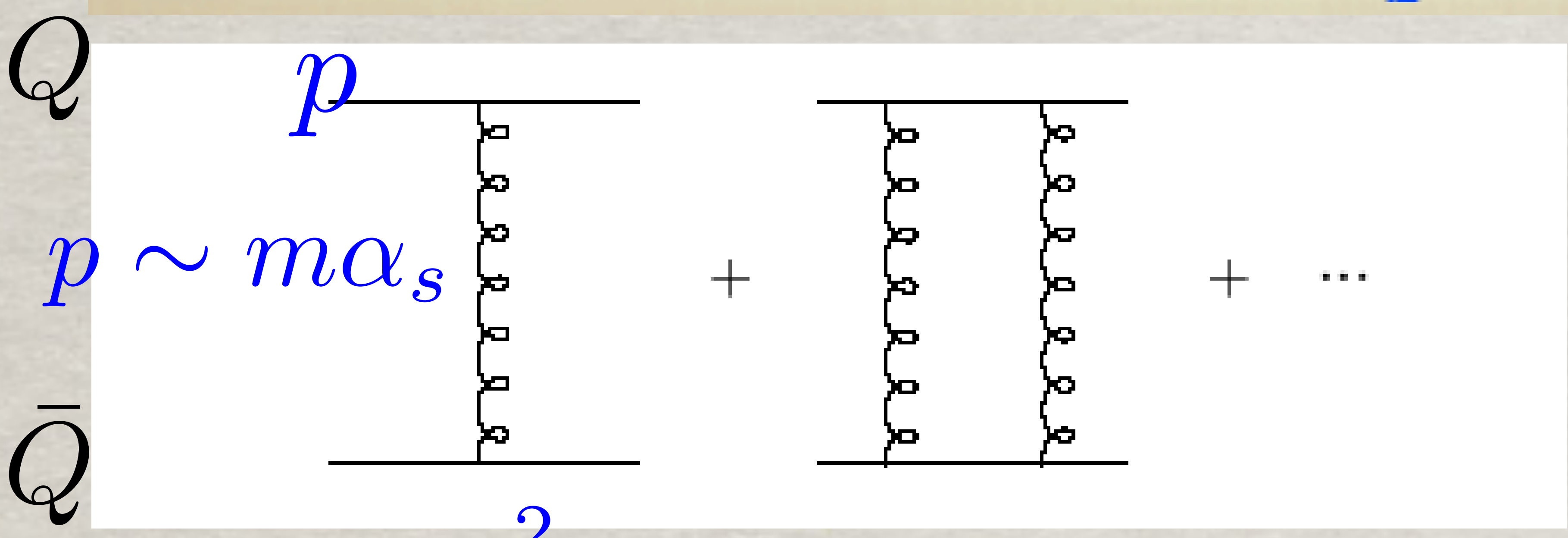

$$\frac{g^2}{p^2}\left(1 + \frac{m\alpha_s}{p}\right)$$

$$\sim \frac{1}{E - \left(\frac{p^2}{m} + V\right)}$$

- From $\left(\frac{p^2}{m} + V\right)\phi = E\phi \rightarrow p \sim mv$ and $E = \frac{p^2}{m} + V \sim mv^2$.

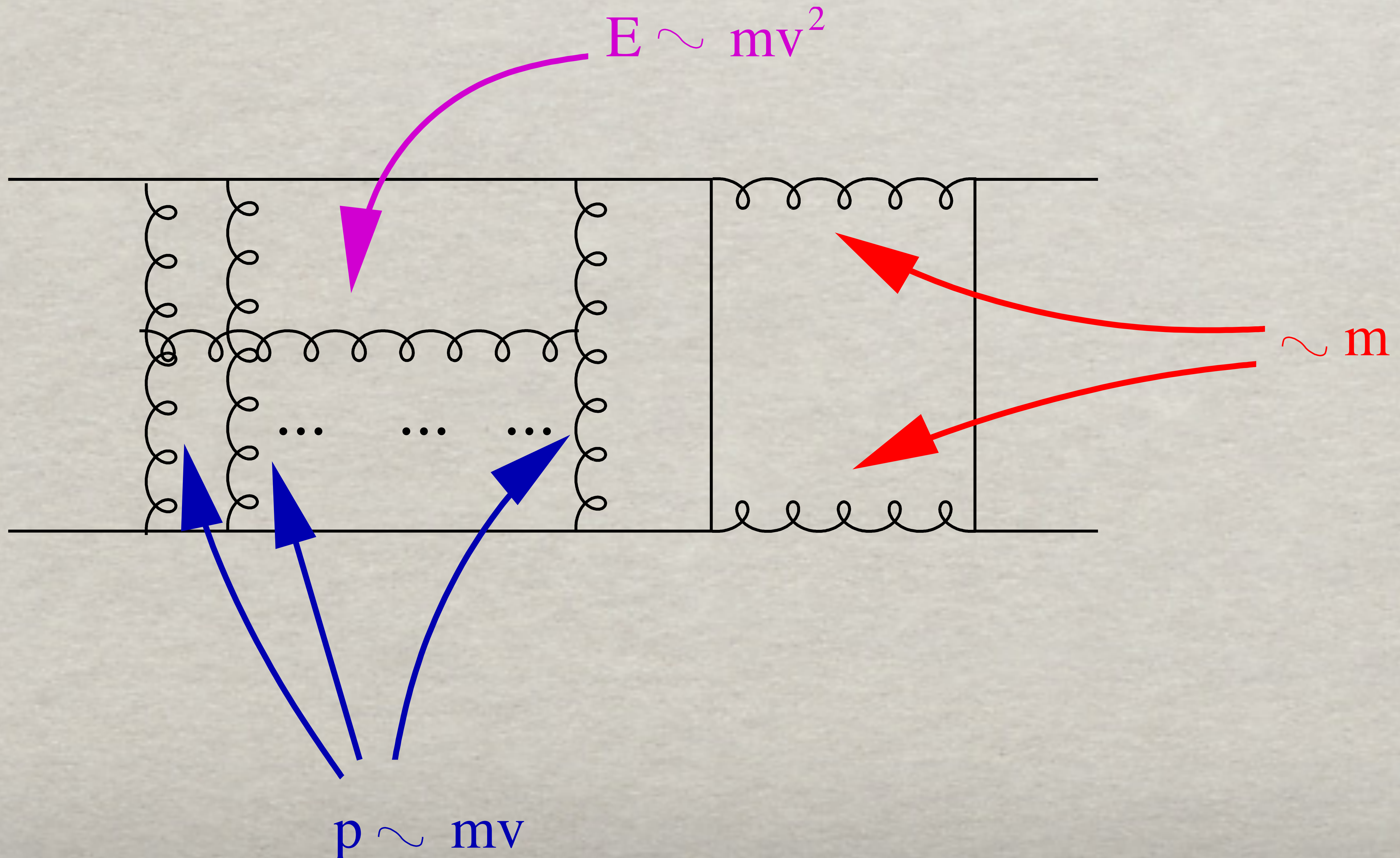

QCD theory of Quarkonium: a very hard problem even at T=0

Close to the bound state $\alpha_s \sim v$

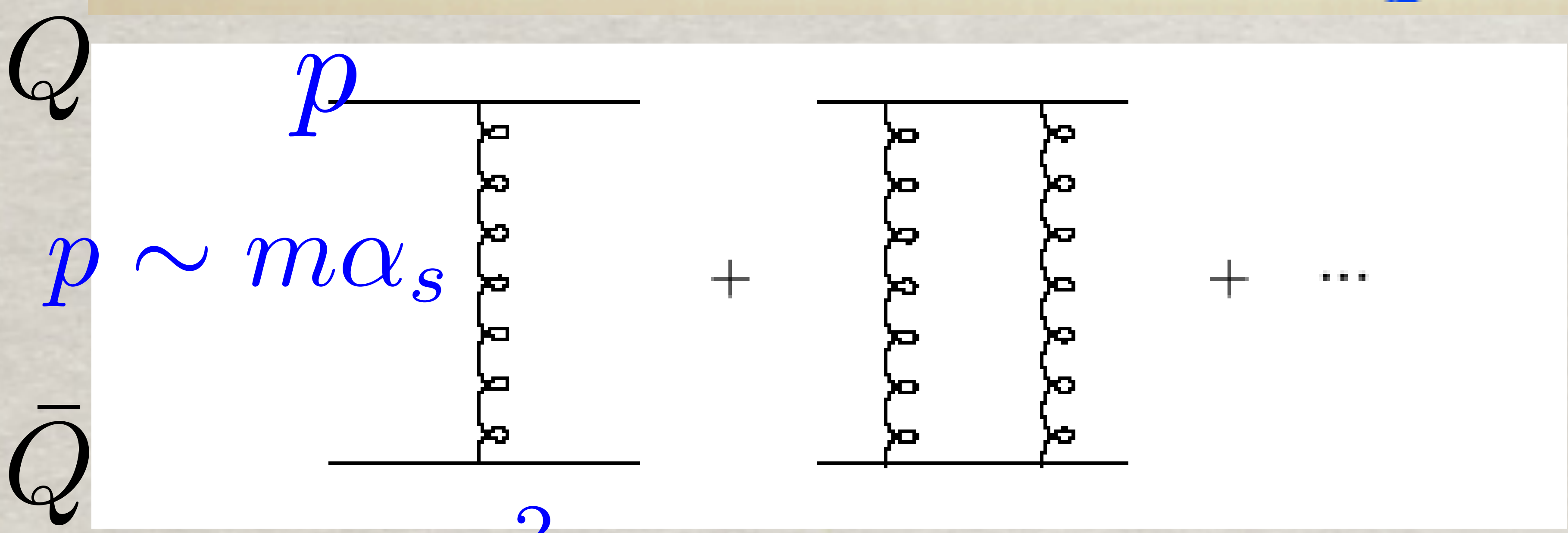

$\frac{g^2}{p^2}\left(1 + \frac{m\alpha_s}{p}\right)$

$$\sim \frac{1}{E - \left(\frac{p^2}{m} + V\right)}$$

- From $\left(\frac{p^2}{m} + V\right)\phi = E\phi \to p \sim mv$ and $E = \frac{p^2}{m} + V \sim mv^2$.

multiscale diagrams have a complicate power counting and contribute to all orders in the coupling

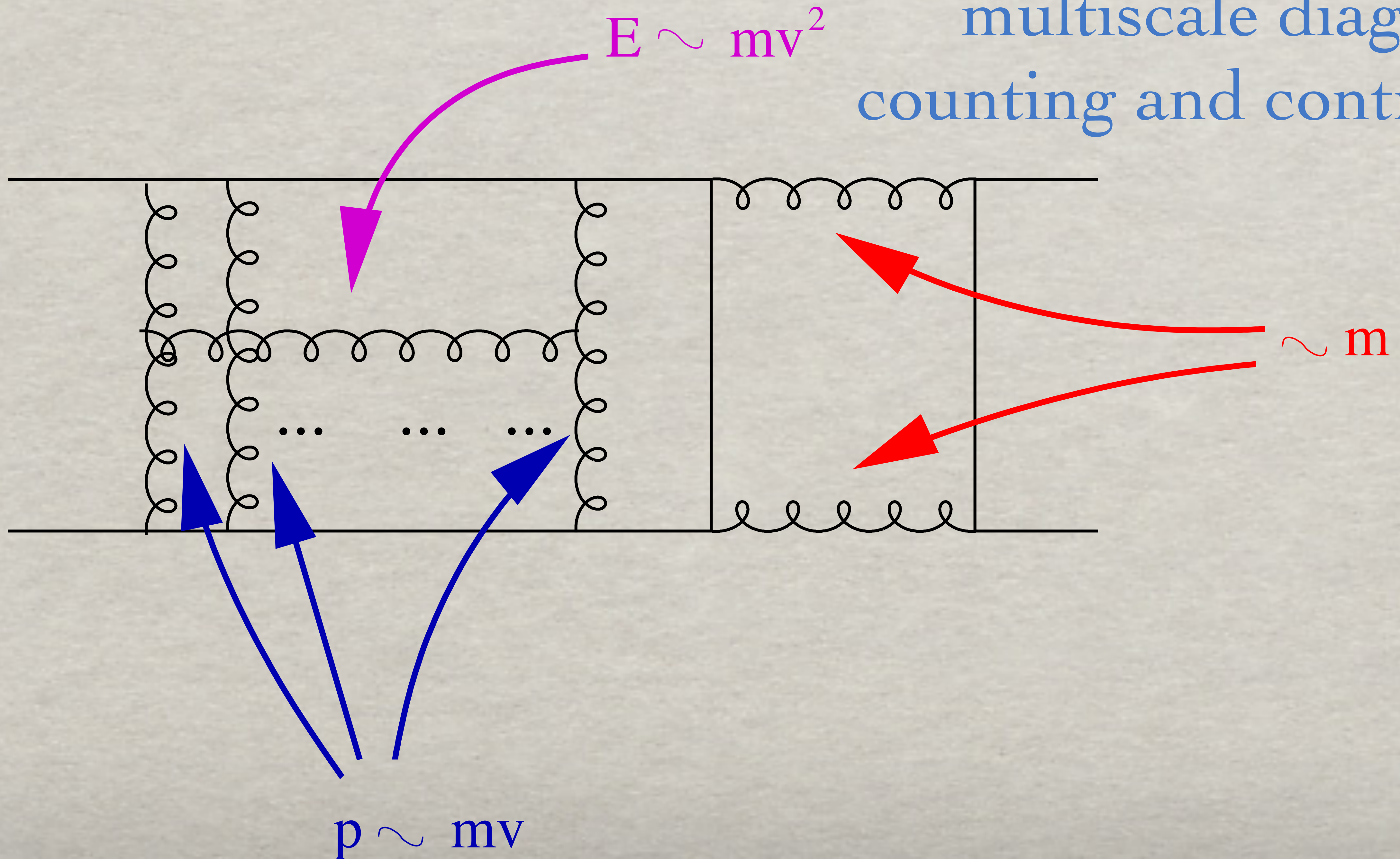

QCD theory of Quarkonium: a very hard problem even at T=0

Close to the bound state $\alpha_s \sim v$

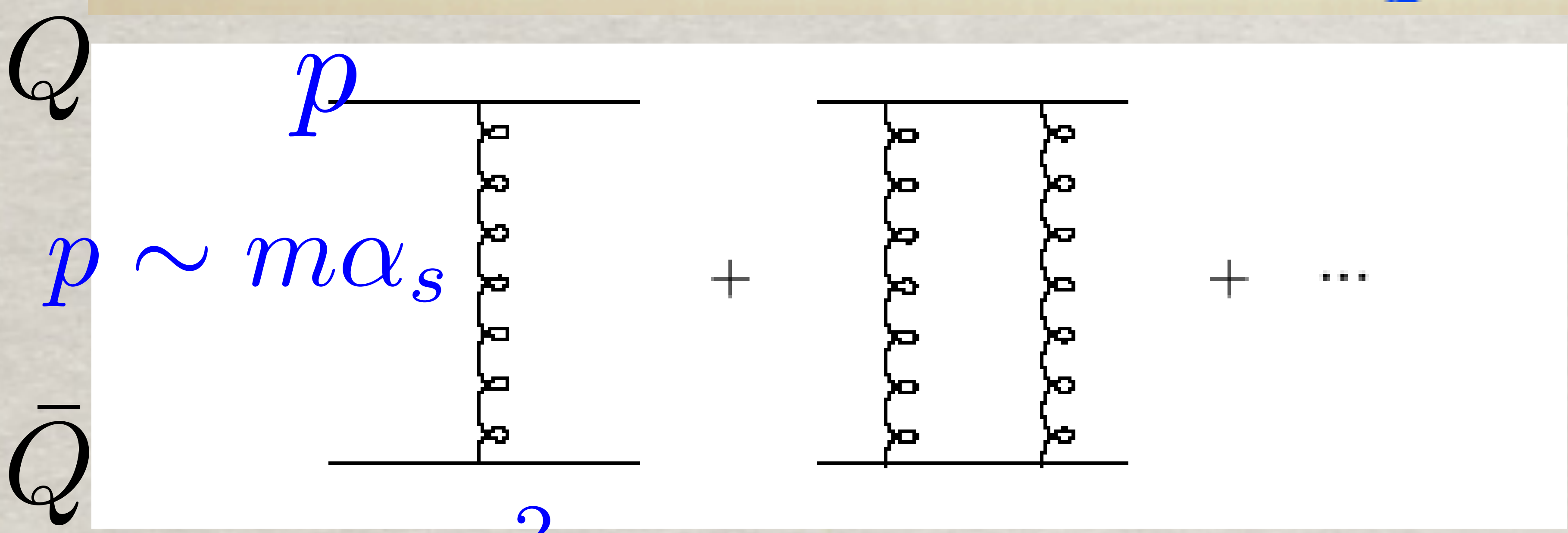

$$\frac{g^2}{p^2}\left(1 + \frac{m\alpha_s}{p}\right)$$

$$\sim \frac{1}{E - \left(\frac{p^2}{m} + V\right)}$$

- From $(\frac{p^2}{m} + V)\phi = E\phi \rightarrow p \sim mv$ and $E = \frac{p^2}{m} + V \sim mv^2$.

multiscale diagrams have a complicate power counting and contribute to all orders in the coupling

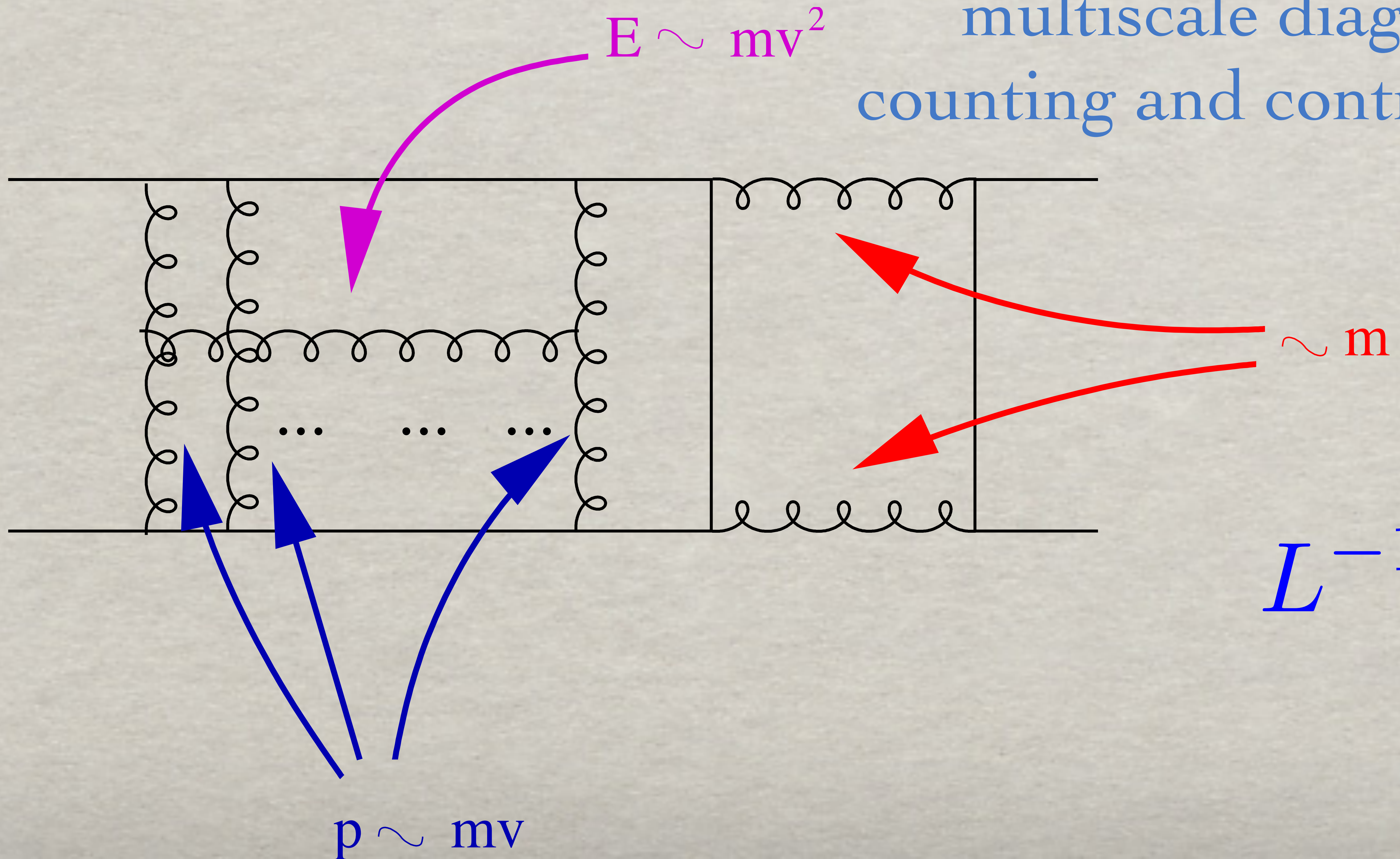

Difficult also for the lattice!

$$L^{-1} \ll \lambda \ll \Lambda \ll a^{-1}$$

QCD theory of Quarkonium: a very hard problem even at T=0

Close to the bound state $\alpha_s \sim v$

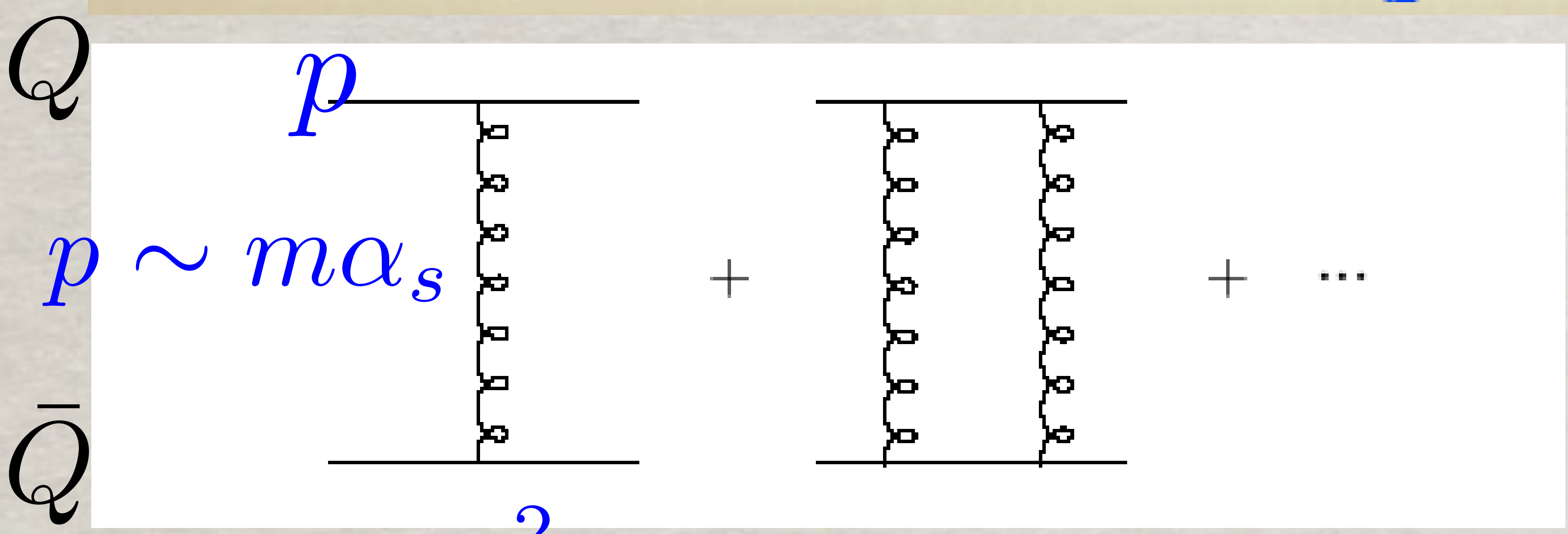

$$\frac{g^2}{p^2}\left(1 + \frac{m\alpha_s}{p}\right)$$

$$\sim \frac{1}{E - \left(\frac{p^2}{m} + V\right)}$$

- From $(\frac{p^2}{m} + V)\phi = E\phi \to p \sim mv$ and $E = \frac{p^2}{m} + V \sim mv^2$.

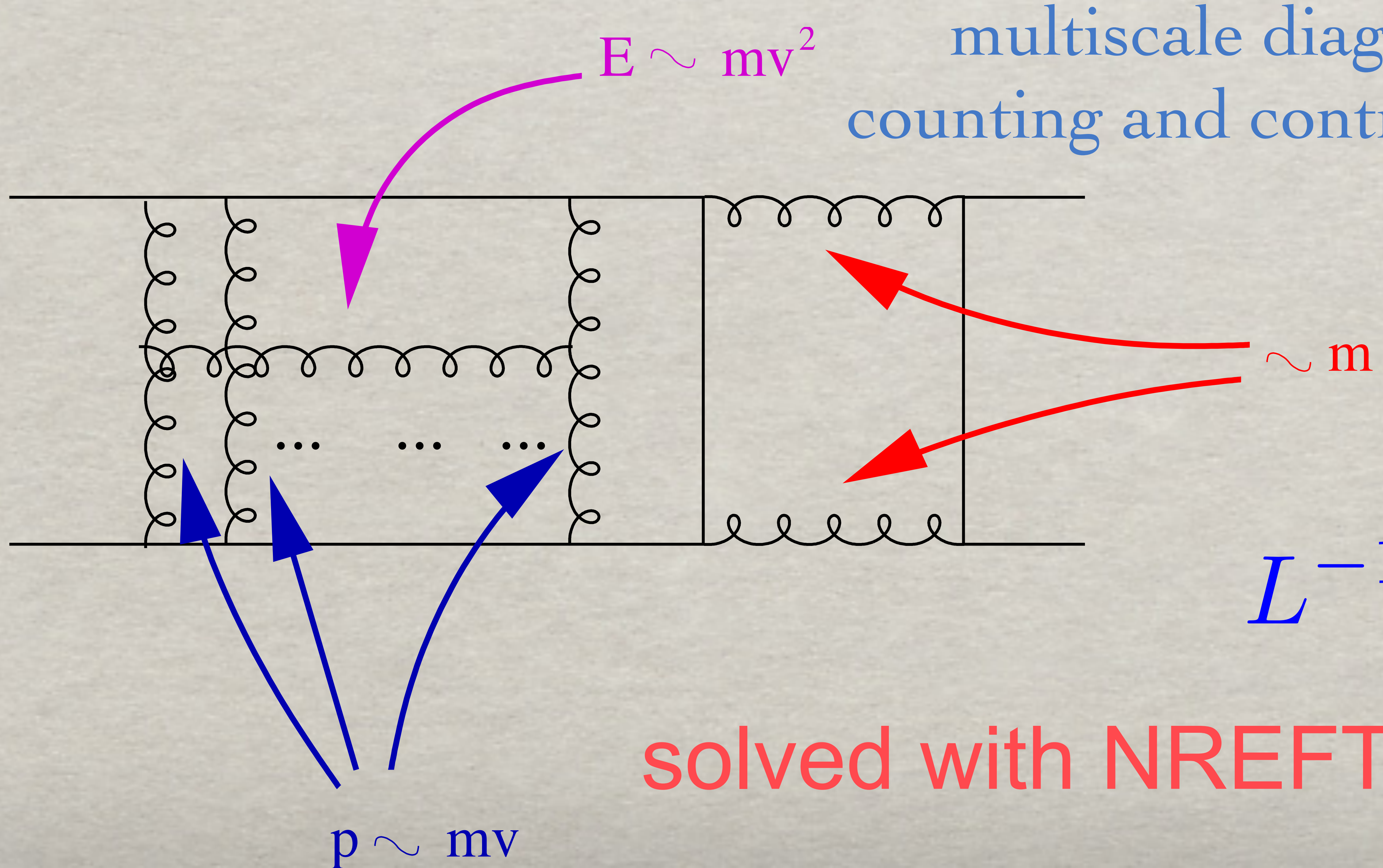

multiscale diagrams have a complicate power counting and contribute to all orders in the coupling

Difficult also for the lattice!

$$L^{-1} \ll \lambda \ll \Lambda \ll a^{-1}$$

solved with NREFT

Quarkonium with NR EFT

Color degrees of freedom
3X3=1+8
singlet and octet QQbar

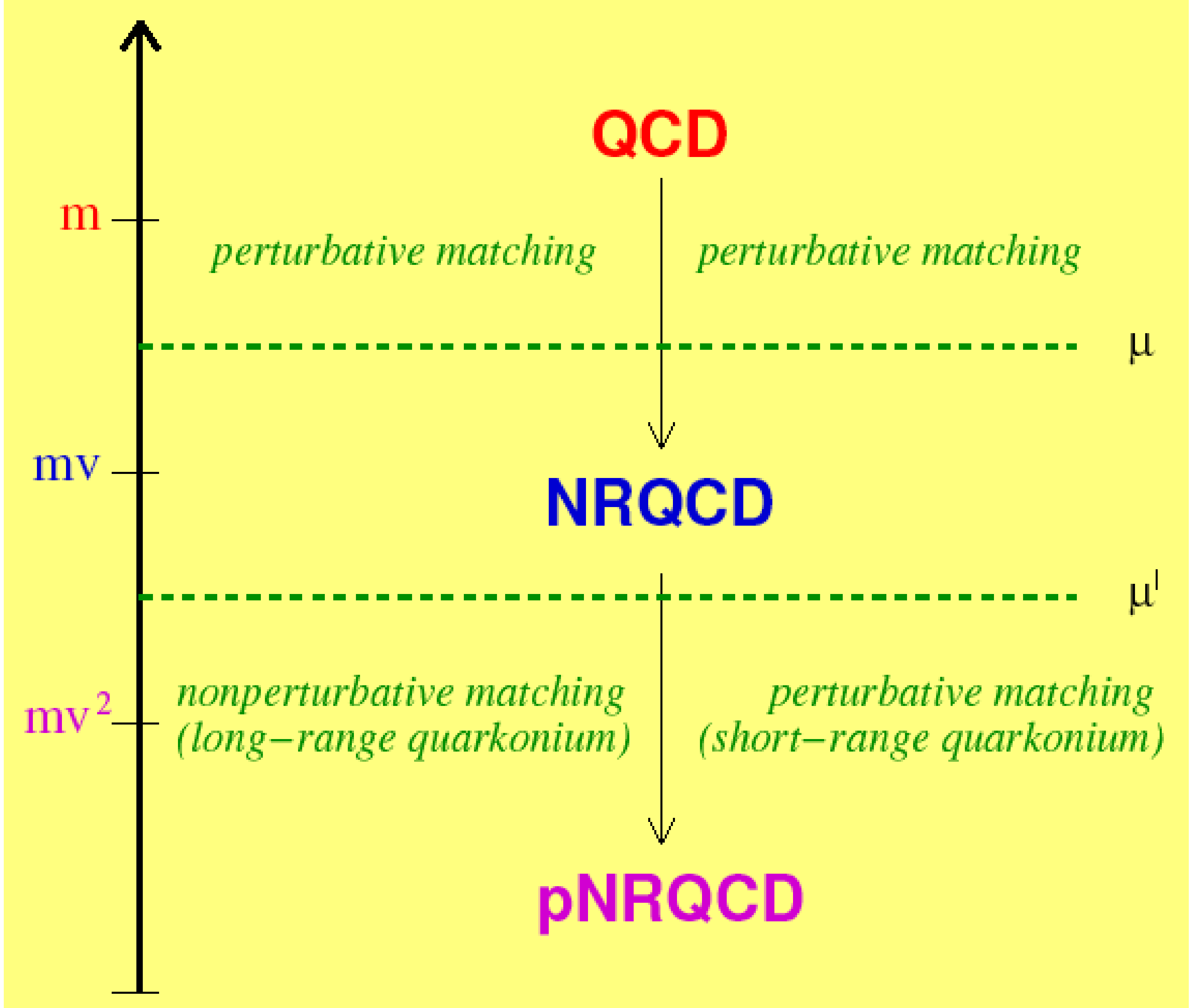

Hard

Soft
(relative
momentum)

Ultrasoft
(binding energy)

Quarkonium with NR EFT

Color degrees of freedom
3X3=1+8
singlet and octet QQbar

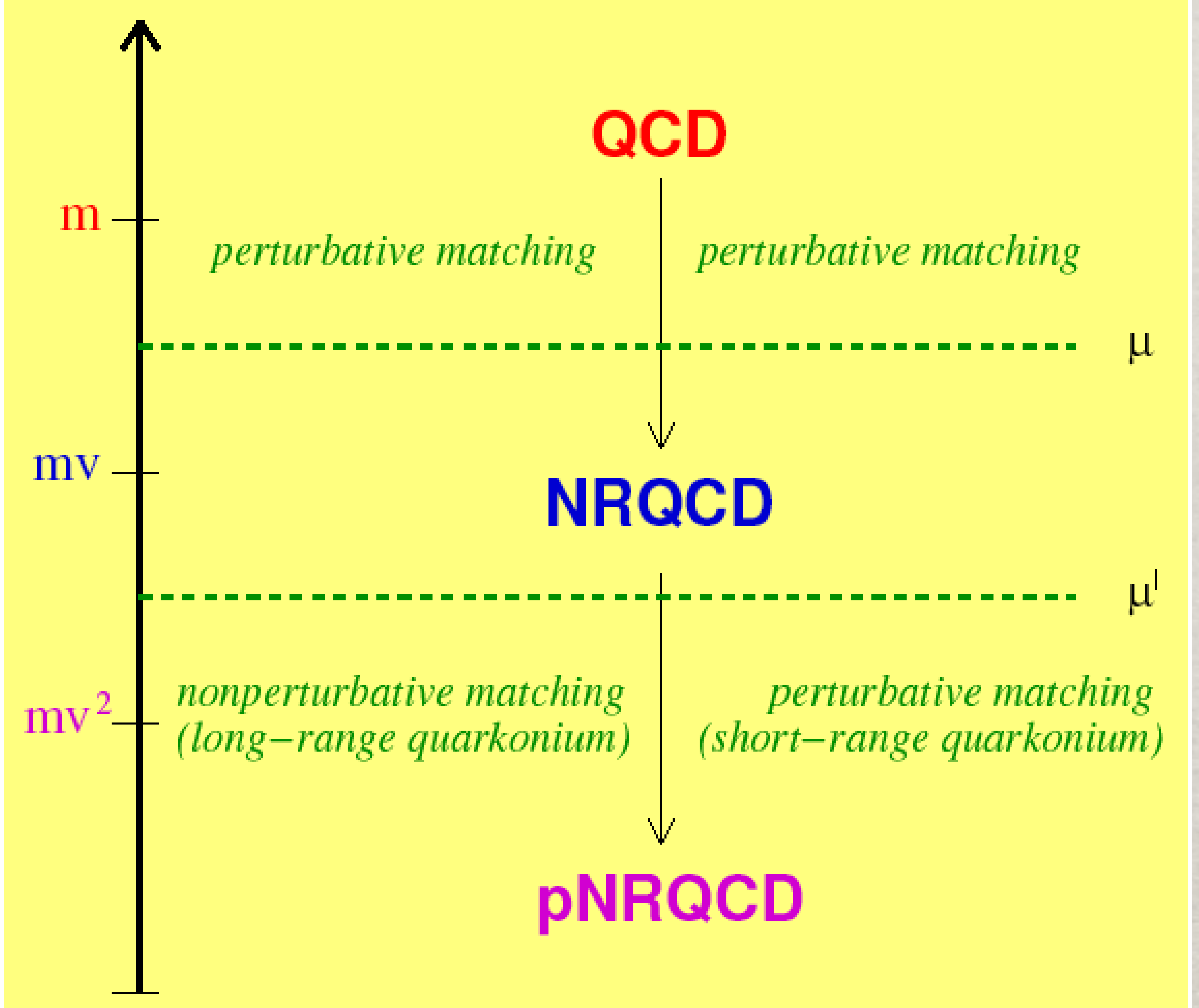

Hard

Soft
(relative
momentum)

Ultrasoft
(binding energy)

$$\mathcal{L}_{\rm EFT} = \sum_n c_n(E_\Lambda/\mu)\frac{O_n(\mu,\lambda)}{E_\Lambda}$$

Quarkonium with NR EFT

Color degrees of freedom
3X3=1+8
singlet and octet QQbar

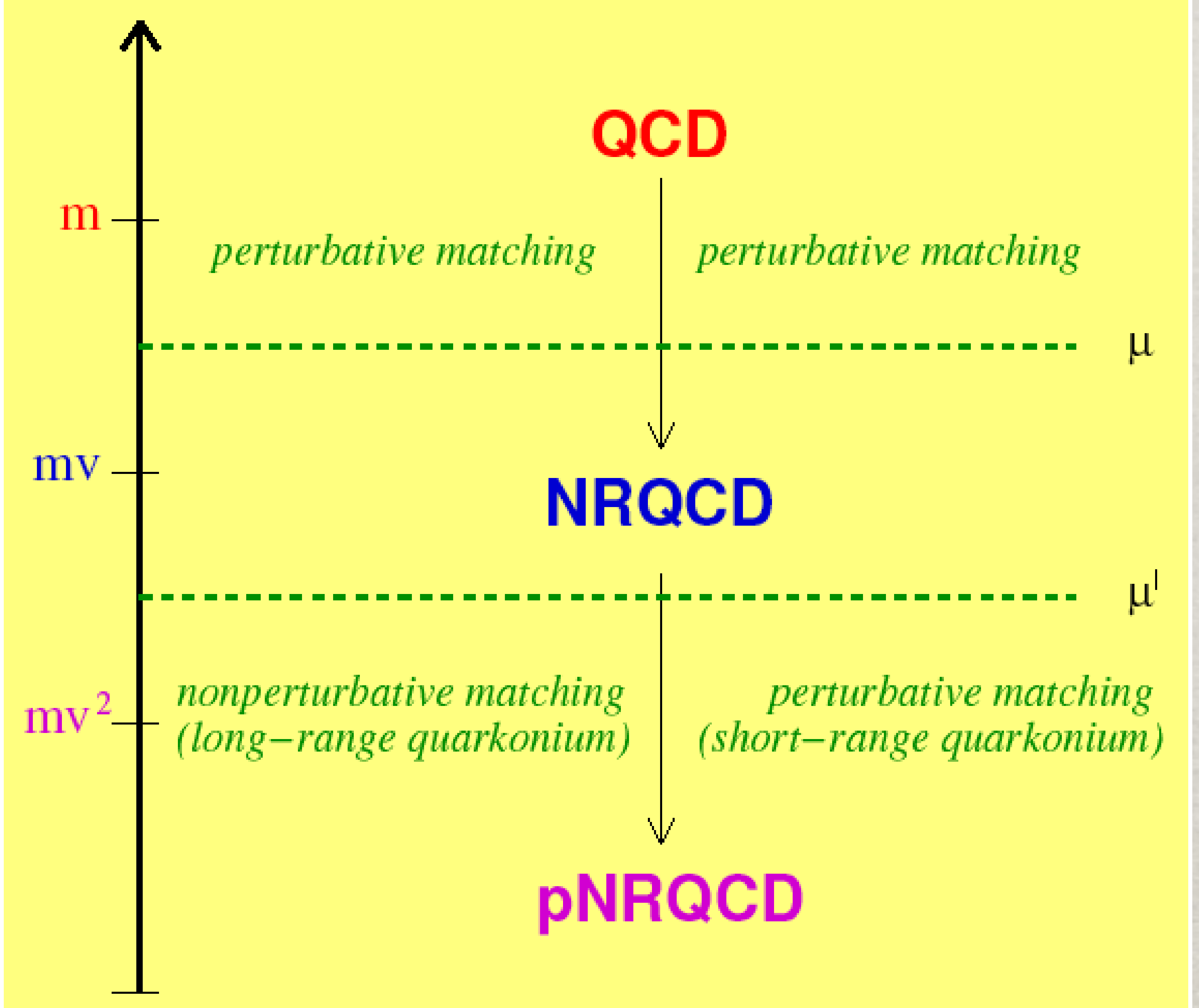

Hard

Soft
(relative
momentum)

Ultrasoft
(binding energy)

$$\mathcal{L}_{\mathrm{EFT}} = \sum_n c_n(E_\Lambda/\mu)\frac{O_n(\mu,\lambda)}{E_\Lambda}$$

$$\langle O_n \rangle \sim E_\lambda^n$$

Quarkonium with NR EFT

Color degrees of freedom
3X3=1+8
singlet and octet QQbar

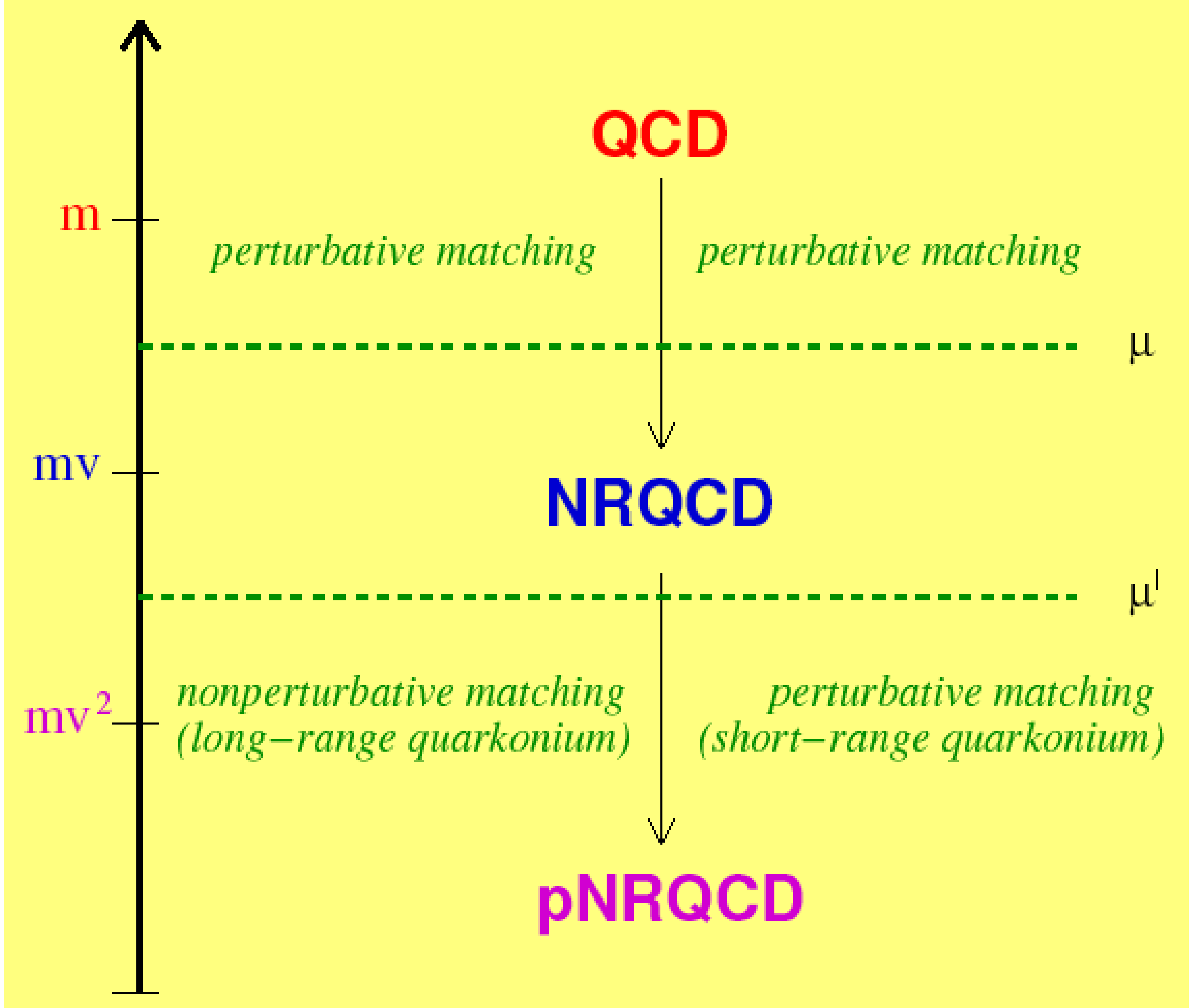

Hard

$$\frac{E_\lambda}{E_\Lambda} = \frac{mv}{m}$$

Soft
(relative
momentum)

Ultrasoft
(binding energy)

$$\mathcal{L}_{\rm EFT} = \sum_n c_n(E_\Lambda/\mu)\frac{O_n(\mu,\lambda)}{E_\Lambda}$$

$$\langle O_n \rangle \sim E_\lambda^n$$

Quarkonium with NR EFT

Color degrees of freedom
3X3=1+8
singlet and octet QQbar

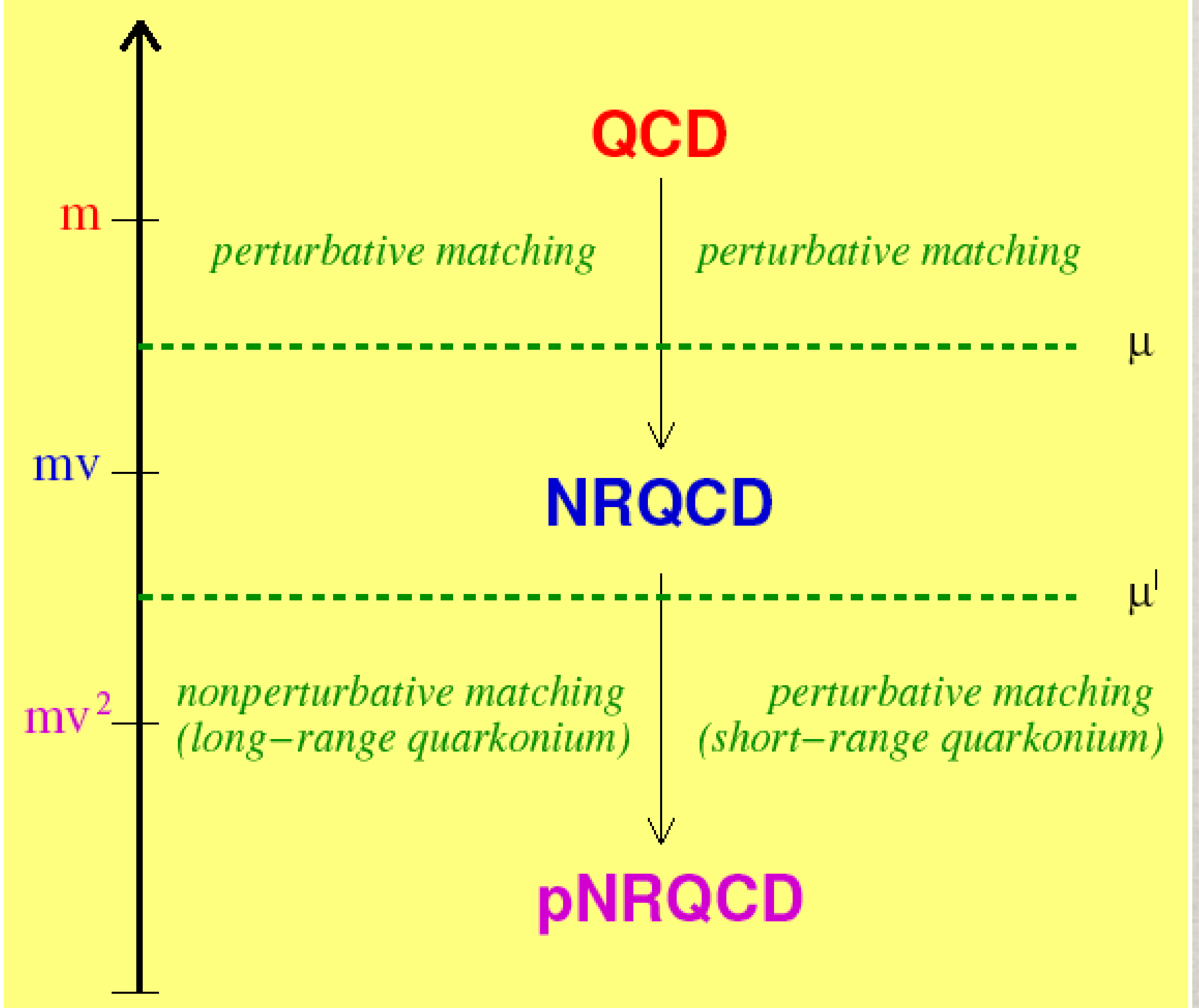

Hard

$$\frac{E_\lambda}{E_\Lambda} = \frac{mv}{m}$$

Soft
(relative momentum)

$$\frac{E_\lambda}{E_\Lambda} = \frac{mv^2}{mv}$$

Ultrasoft
(binding energy)

$$\mathcal{L}_{\rm EFT} = \sum_n c_n(E_\Lambda/\mu)\frac{O_n(\mu,\lambda)}{E_\Lambda} \qquad \langle O_n\rangle \sim E_\lambda^n$$

Quarkonium with NR EFT: Non Relativistic QCD (NRQCD)

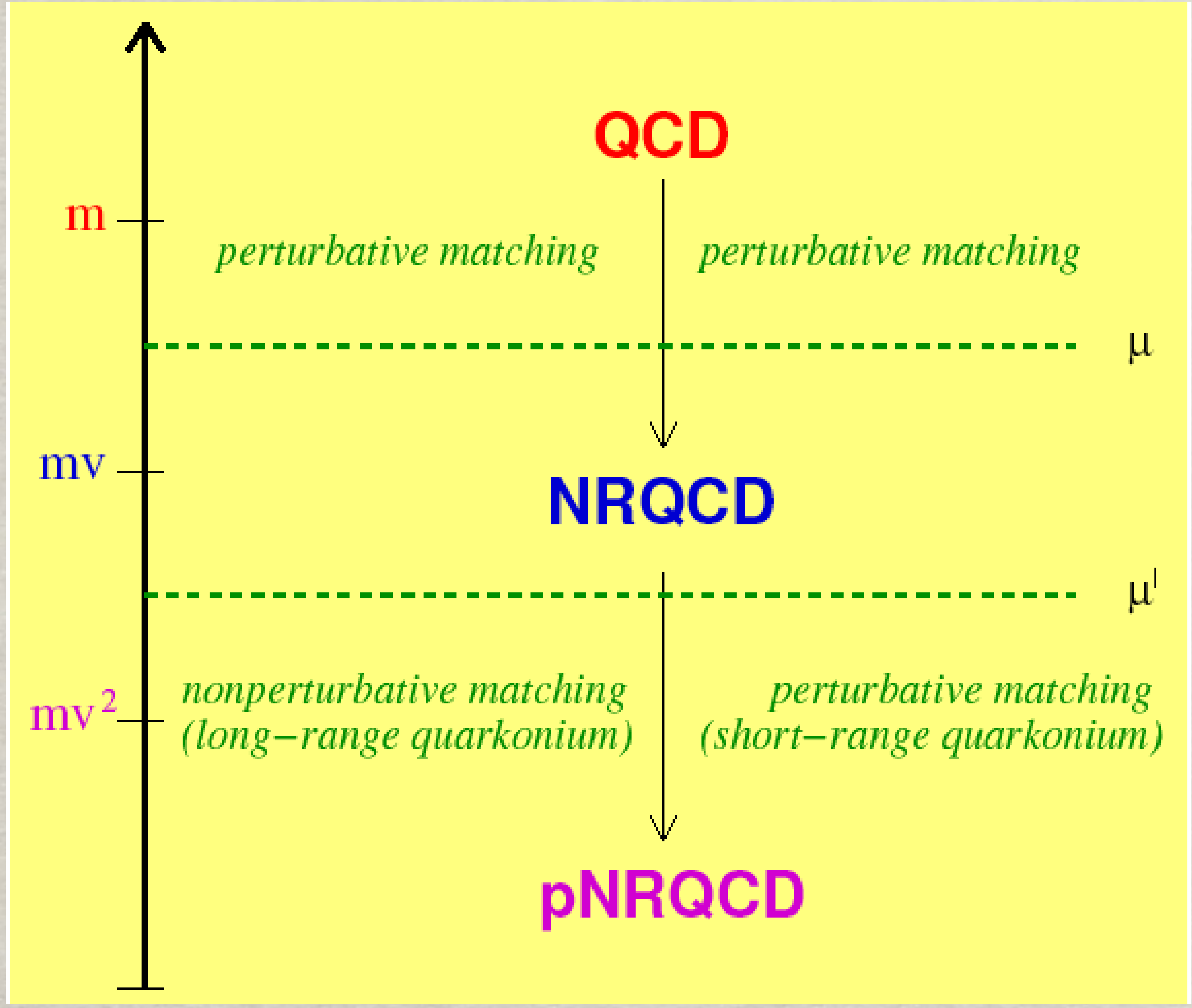

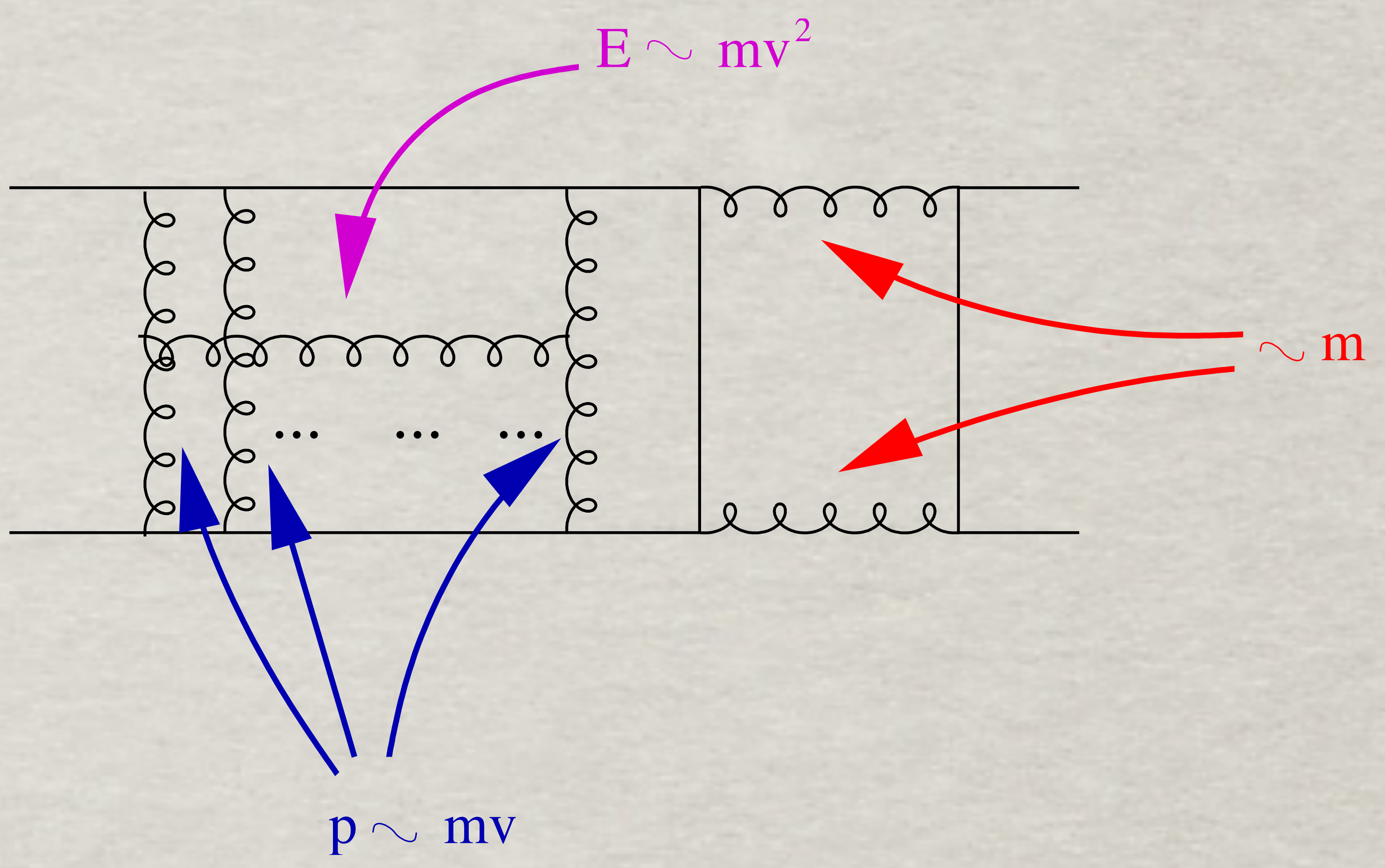

Quarkonium with NR EFT: Non Relativistic QCD (NRQCD)

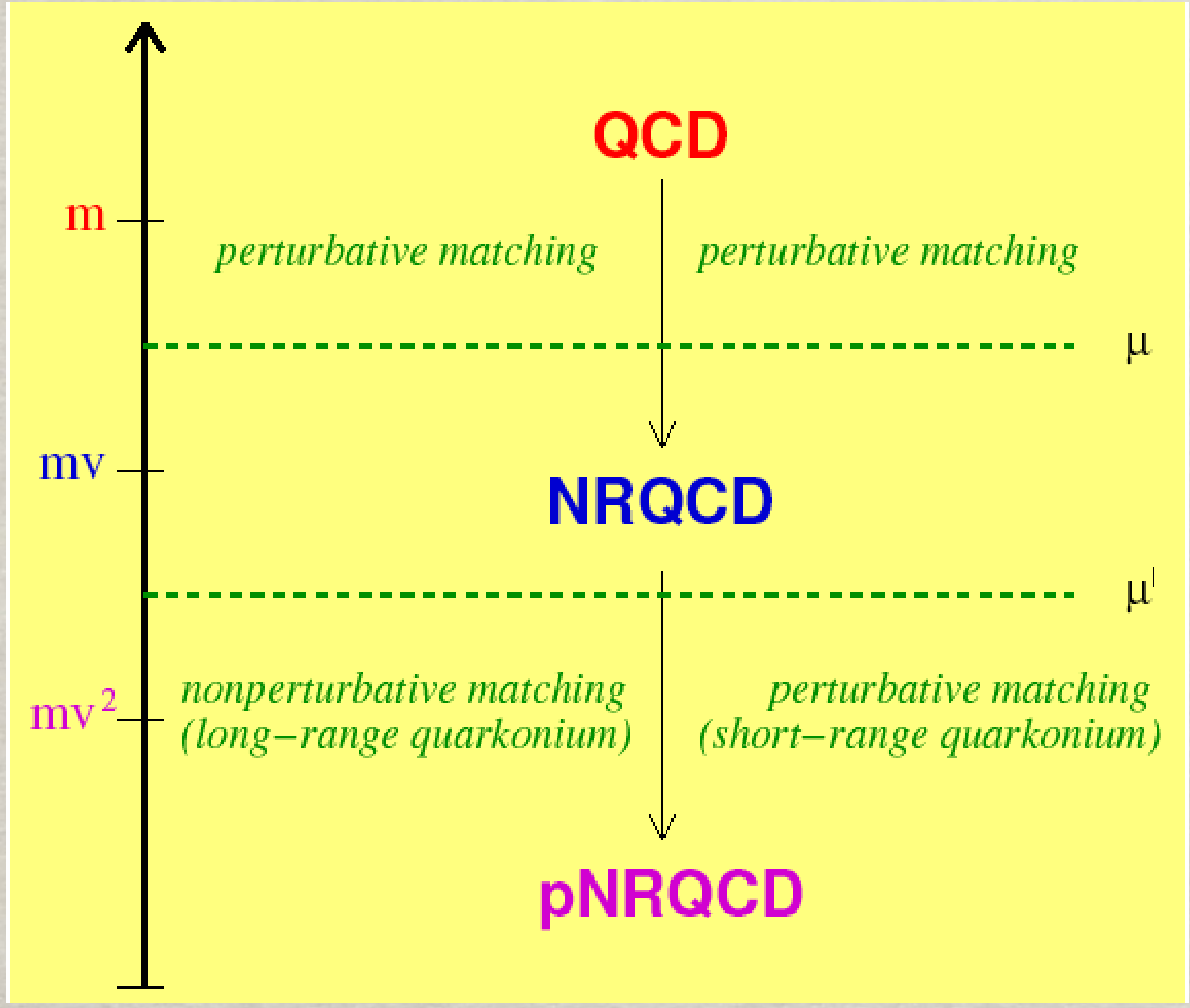

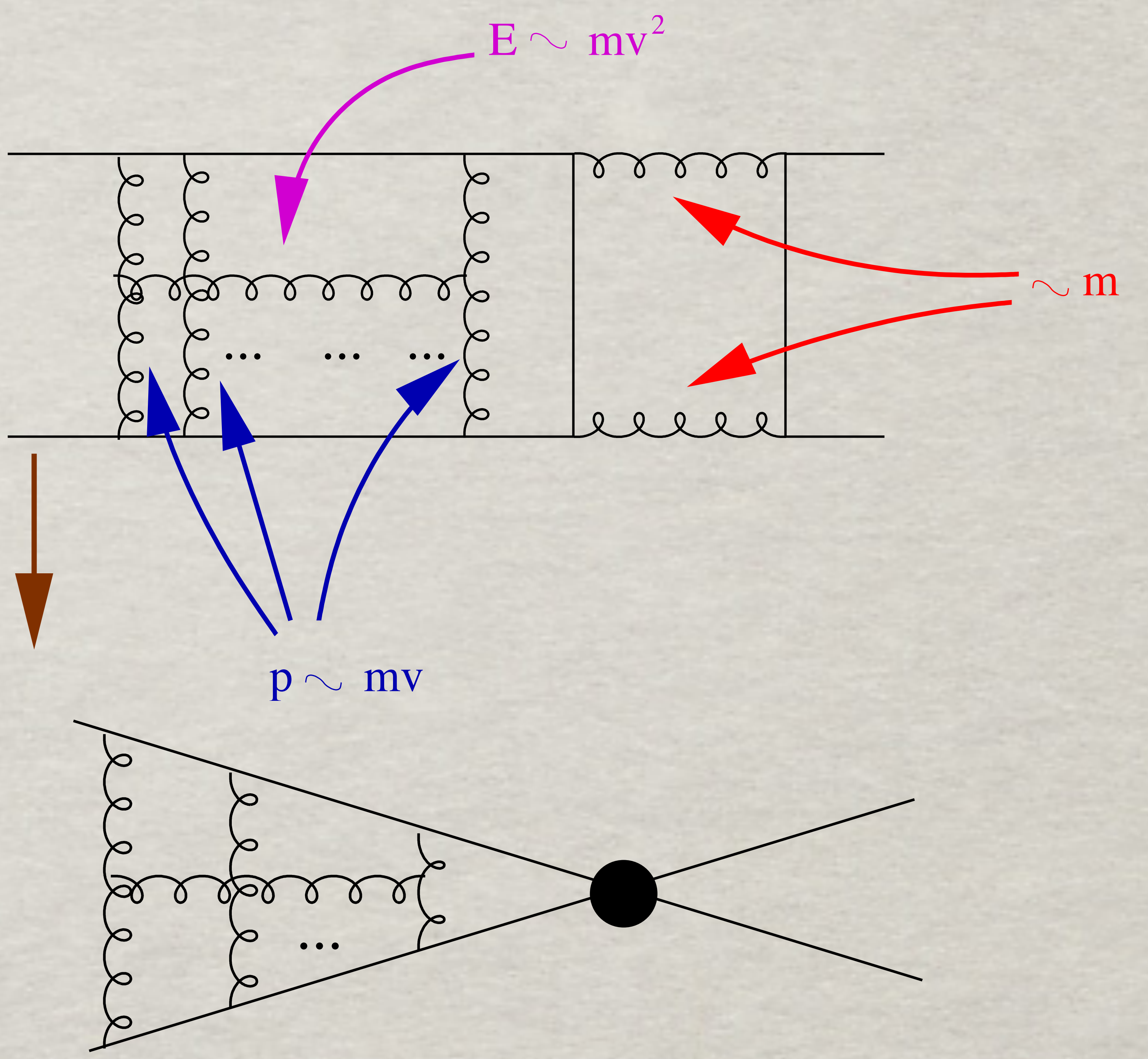

Quarkonium with NR EFT: Non Relativistic QCD (NRQCD)

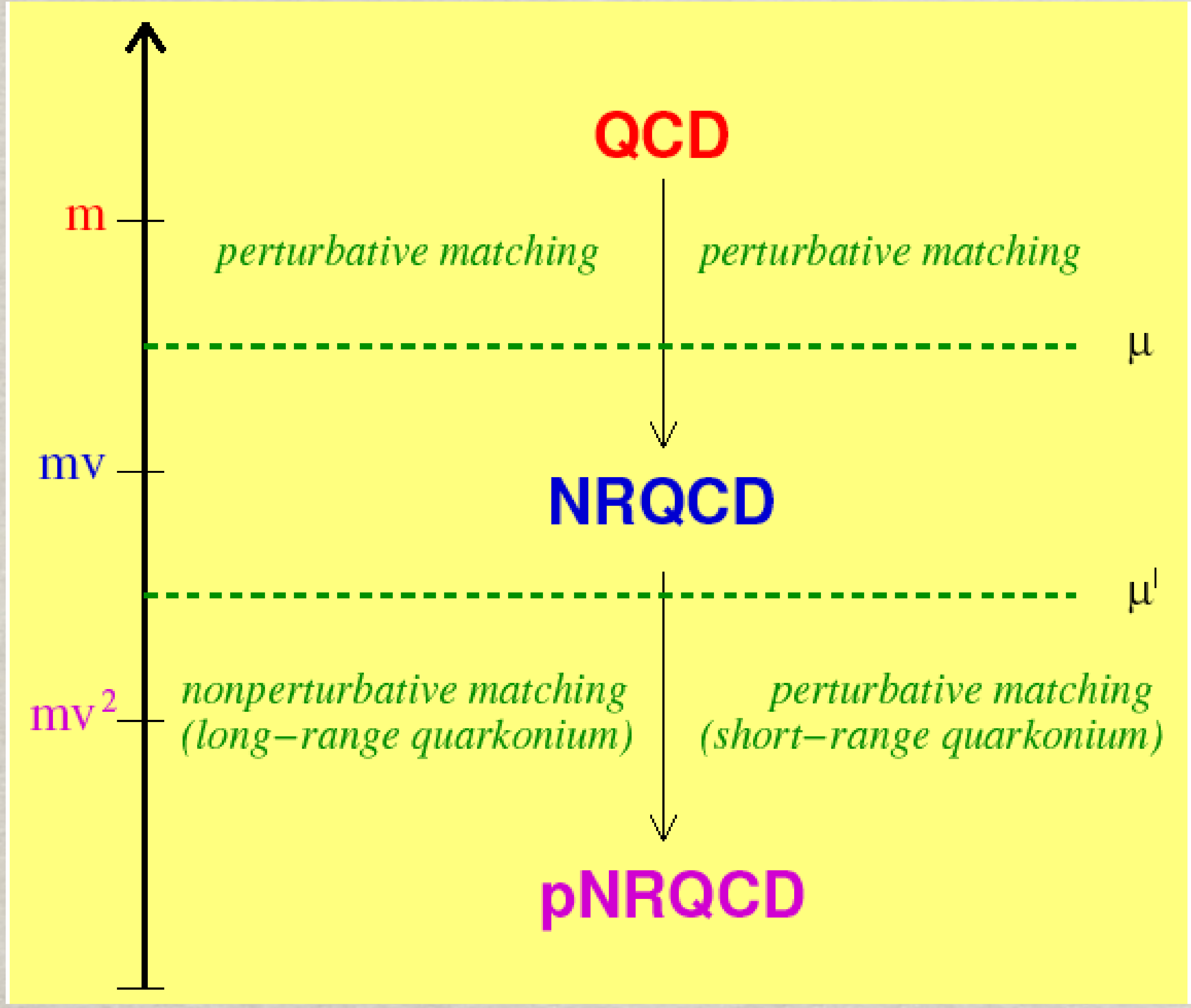

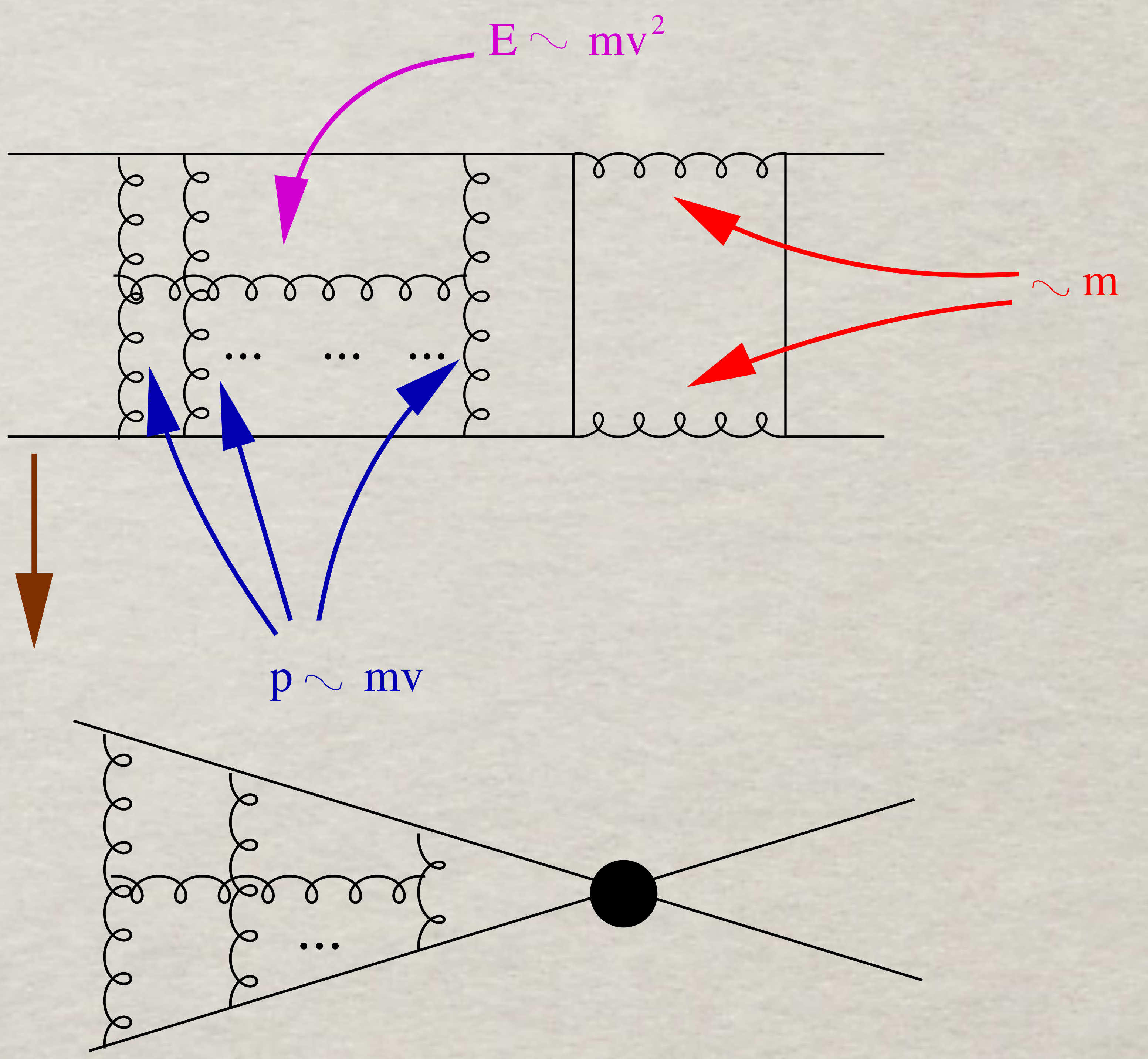

$$\mathcal{L}_{\mathrm{NRQCD}} = \sum_n c(\alpha_s(m/\mu)) \times \frac{O_n(\mu, \lambda)}{m^n}$$

Quarkonium with NR EFT: potential NonRelativistic QCD (pNRQCD)

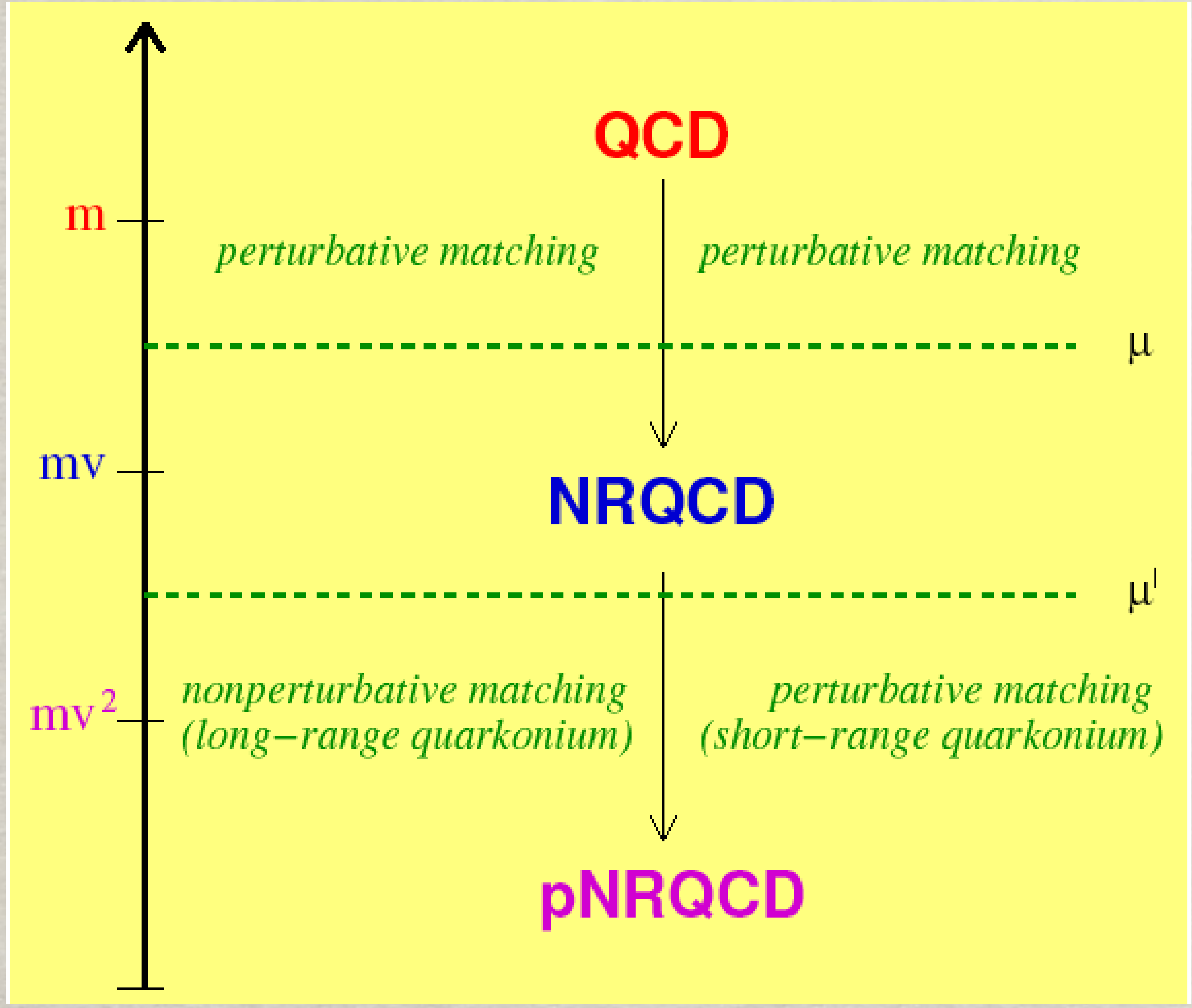

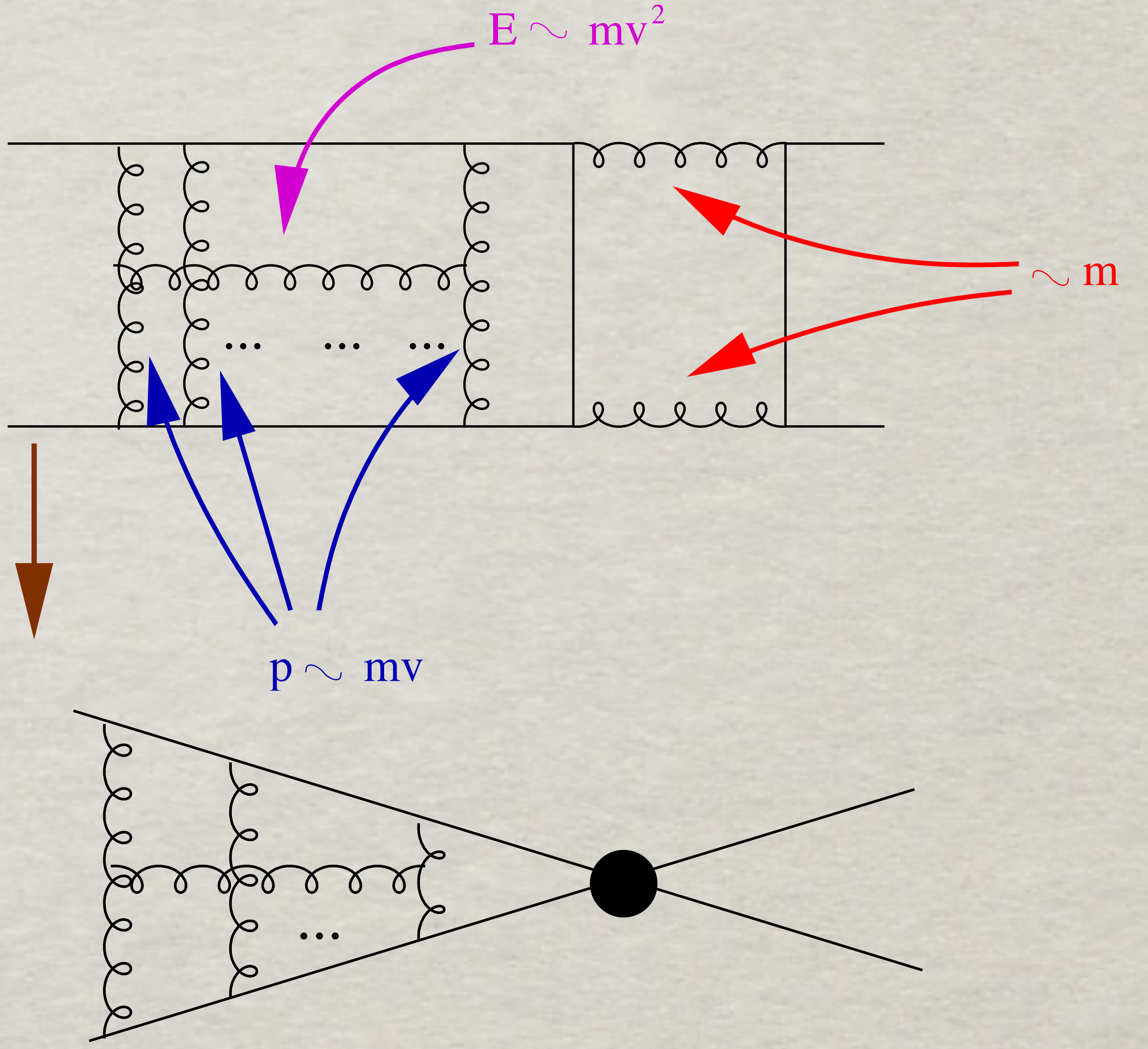

Quarkonium with NR EFT: potential NonRelativistic QCD (pNRQCD)

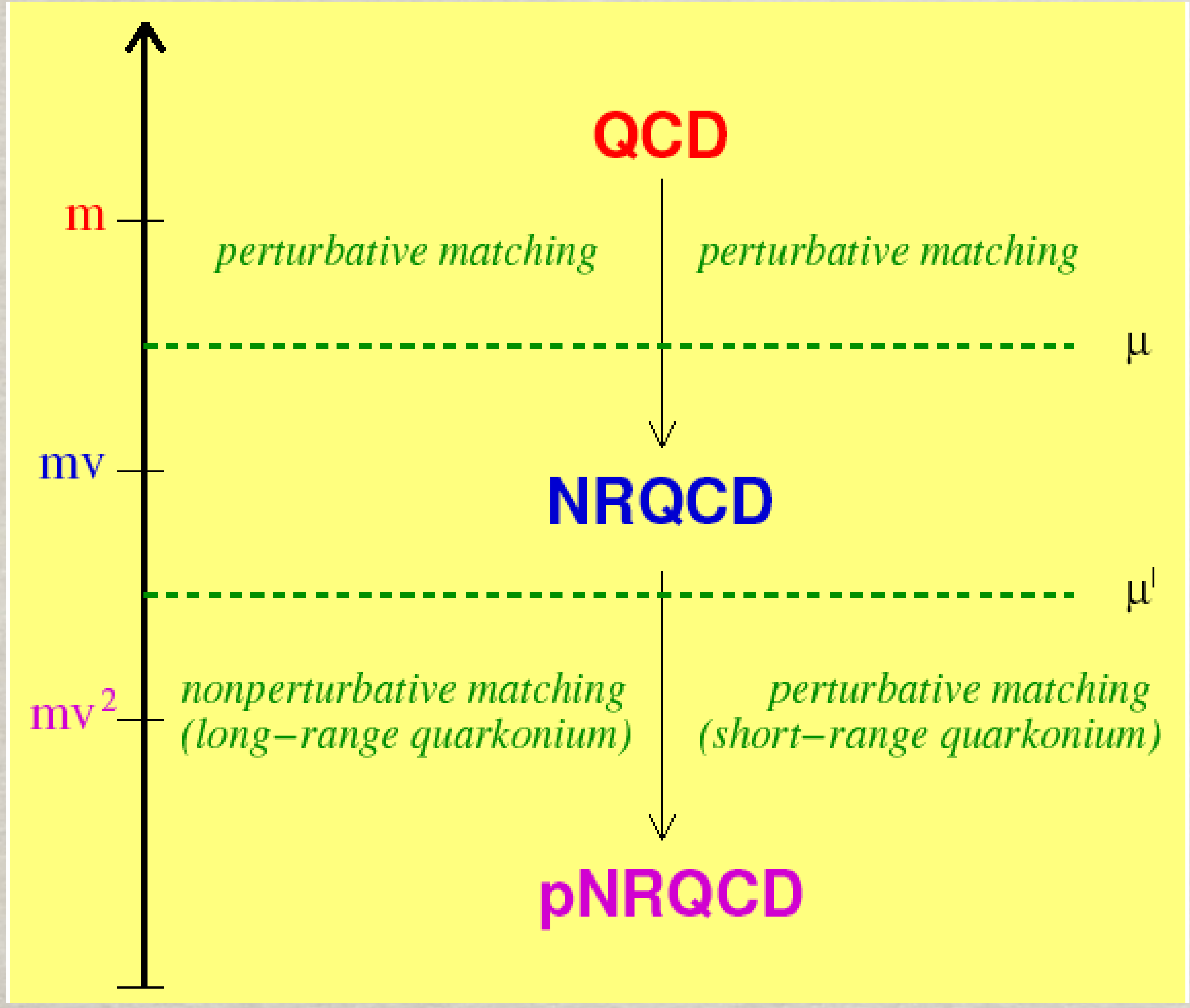

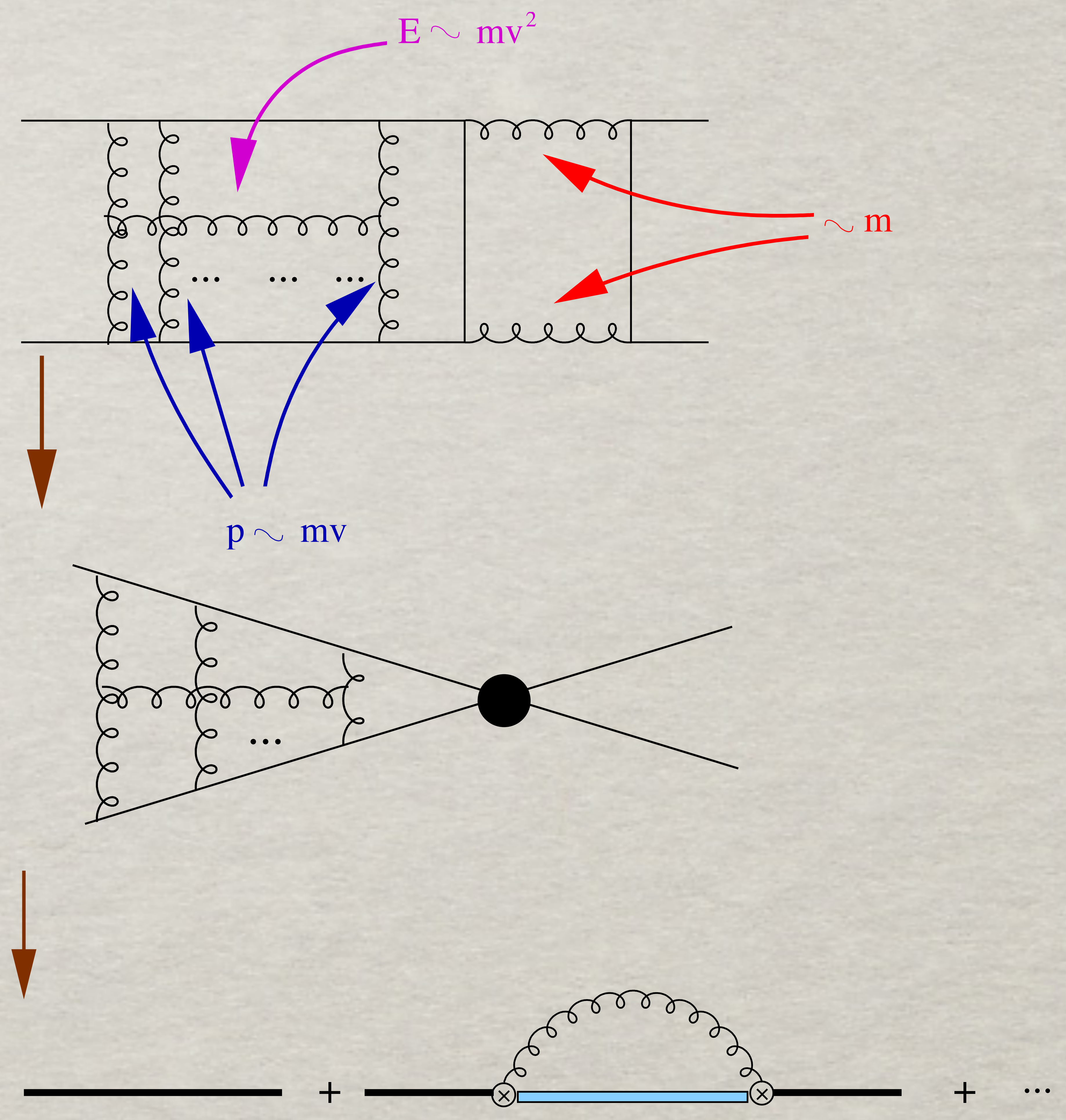

Quarkonium with NR EFT: potential NonRelativistic QCD (pNRQCD)

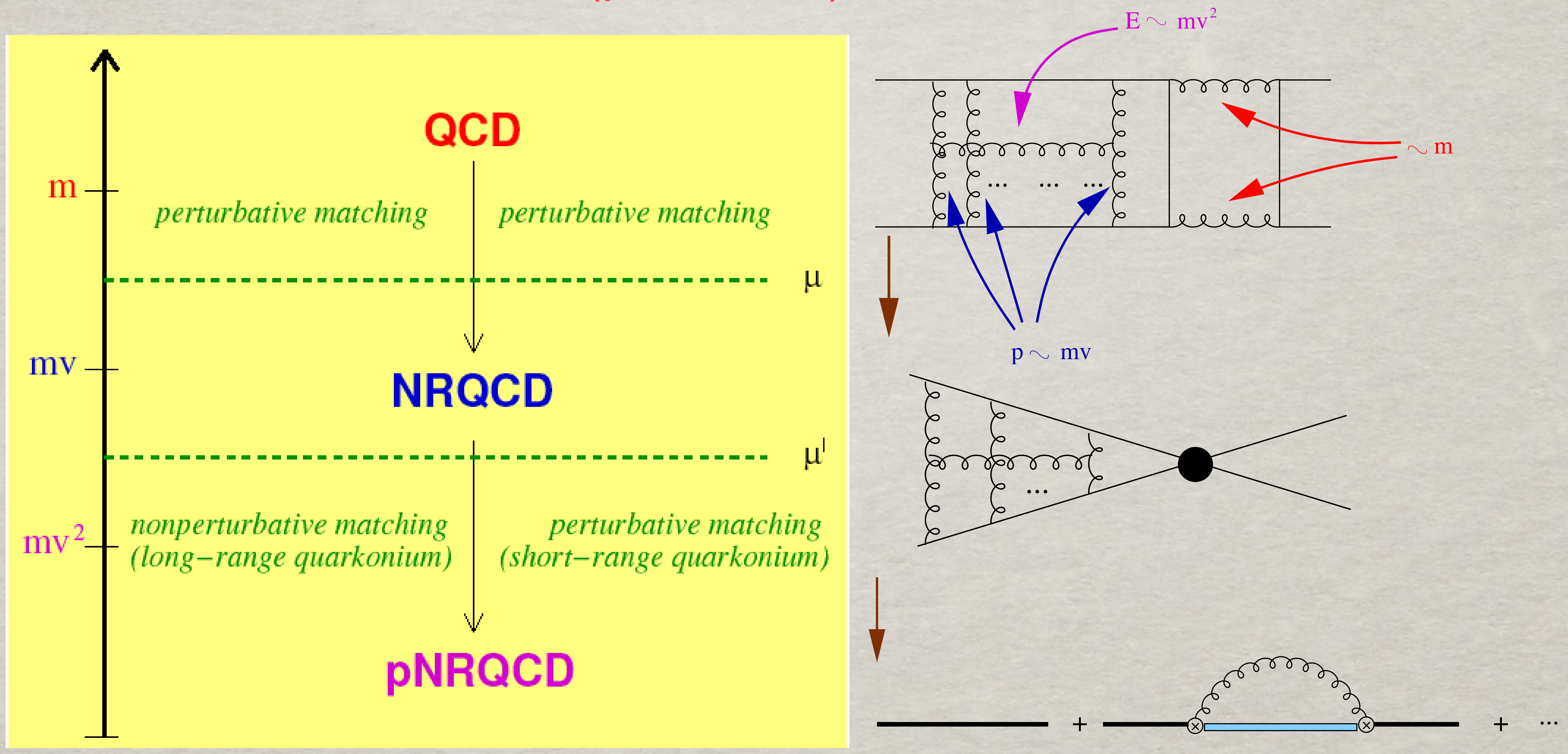

$$\mathcal{L}_{\rm pNRQCD} = \sum_k \sum_n \frac{1}{m^k} c_k(\alpha_{\rm s}(m/\mu)) \times V(r\mu', r\mu) \times O_n(\mu', \lambda)\, r^n$$

Quarkonium with NR EFT: potential NonRelativistic QCD (pNRQCD)

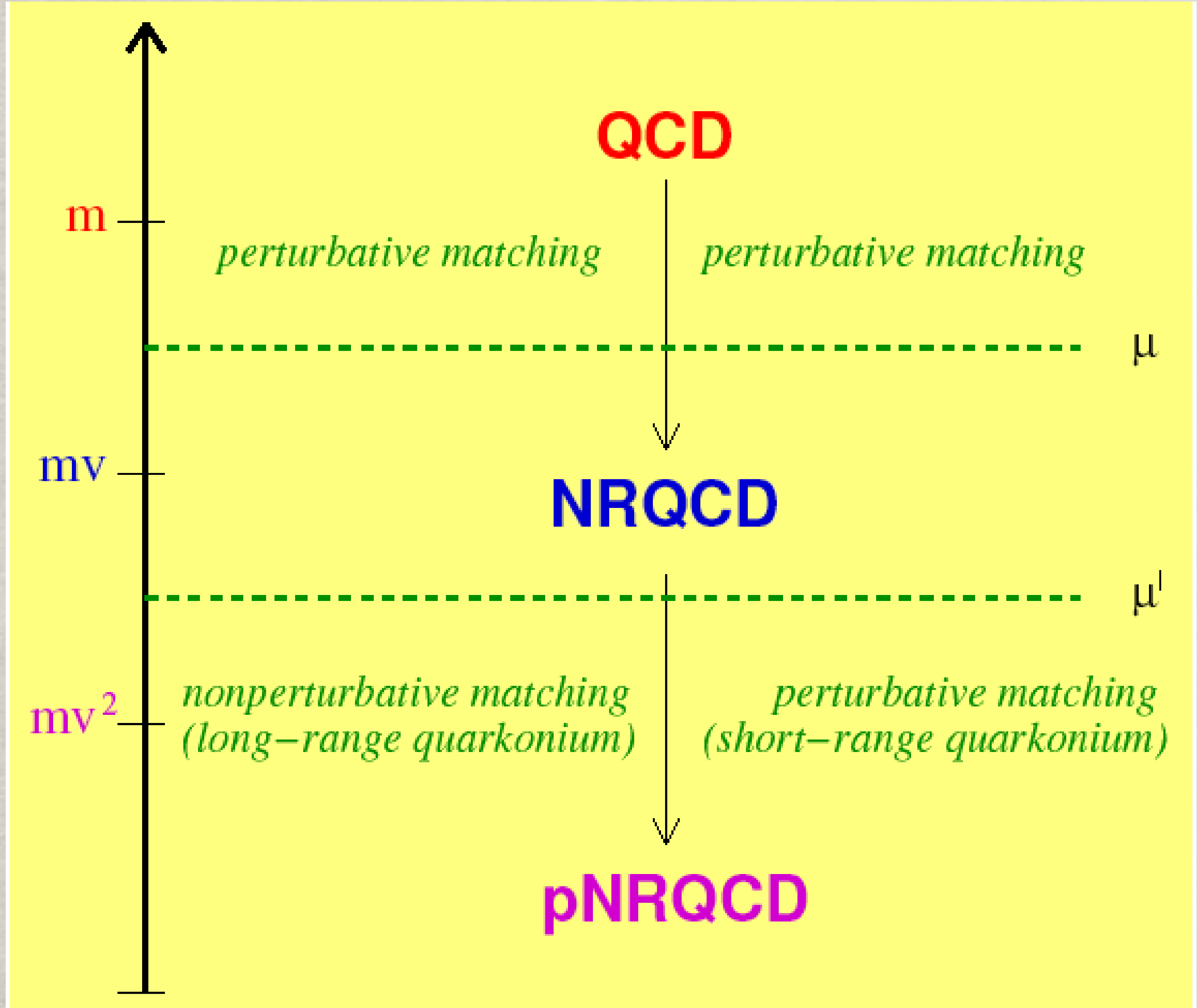

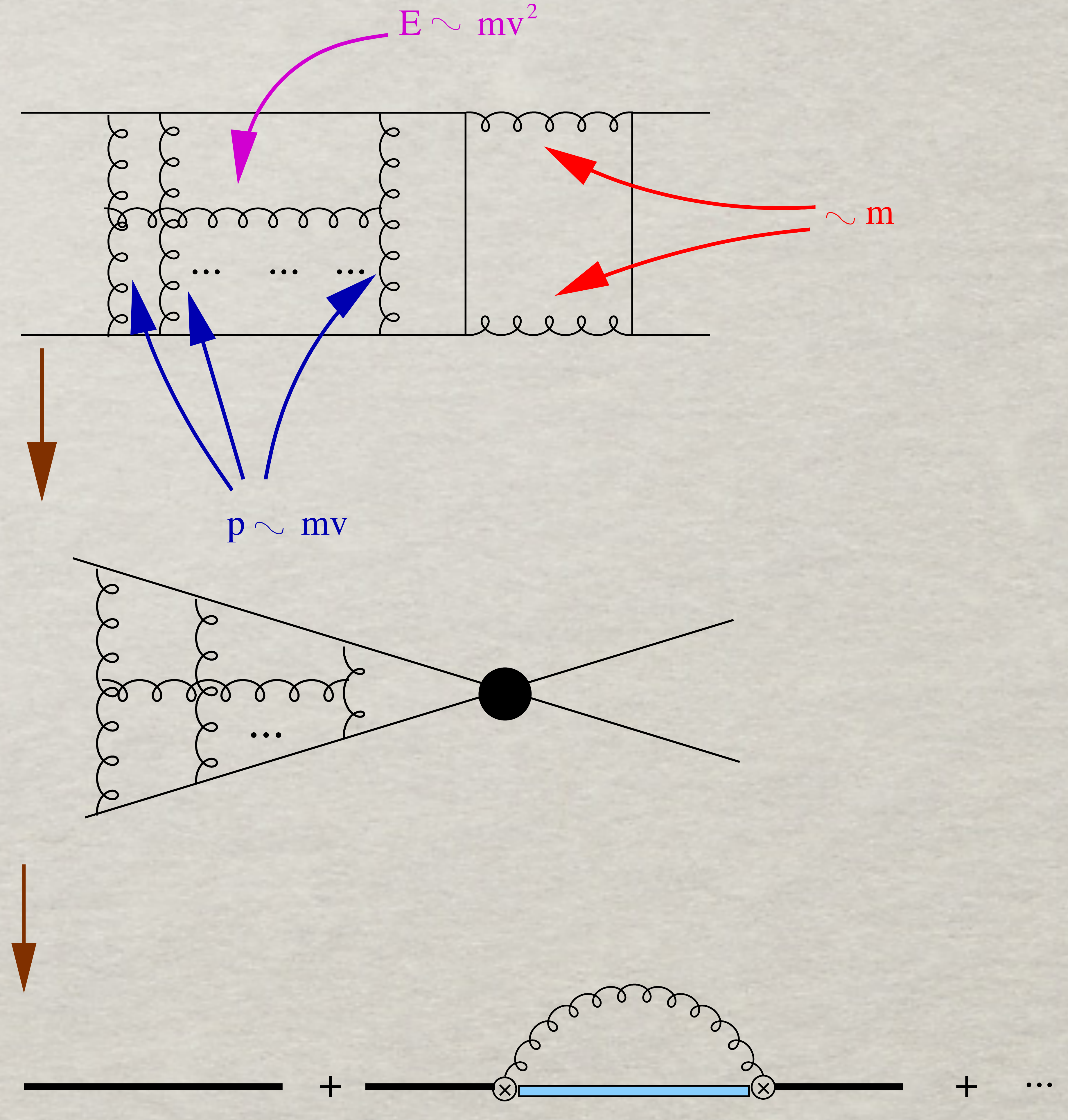

$$\mathcal{L}_{\mathrm{pNRQCD}} = \sum_k \sum_n \frac{1}{m^k} c_k(\alpha_{\mathrm{s}}(m/\mu)) \times V(r\mu', r\mu) \times O_n(\mu', \lambda)\, r^n$$

pNRQCD (potential NonRelativistic QCD) EFT for quarkonium for r<< Lambda_QCD^-1

$$\mathcal{L} = -\frac{1}{4} F^a_{\mu\nu} F^{\mu\nu\, a} + \sum_{i=1}^{n_f} \bar{q}_i \, i \not{D} q_i + \int d^3 r \mathrm{Tr} \left\{ \mathrm{S}^\dagger \left(i\partial_0 - h_s \right) \mathrm{S} + \mathrm{O}^\dagger \left(iD_0 - h_o \right) \mathrm{O} \right\}$$

- LO in r

$\theta(T)\, e^{-iTh_s}$

$\theta(T)\, e^{-iTh_o} \left(e^{-i\int dt\, A^{\mathrm{adj}}} \right)$

$$+ V_A \mathrm{Tr} \left\{ \mathrm{O}^\dagger \mathbf{r} \cdot g\mathbf{E}\, \mathrm{S} + \mathrm{S}^\dagger \mathbf{r} \cdot g\mathbf{E}\, \mathrm{O} \right\} + \frac{V_B}{2} \mathrm{Tr} \left\{ \mathrm{O}^\dagger \mathbf{r} \cdot g\mathbf{E}\, \mathrm{O} + \mathrm{O}^\dagger \mathrm{O} \mathbf{r} \cdot g\mathbf{E} \right\}$$

- NLO in r

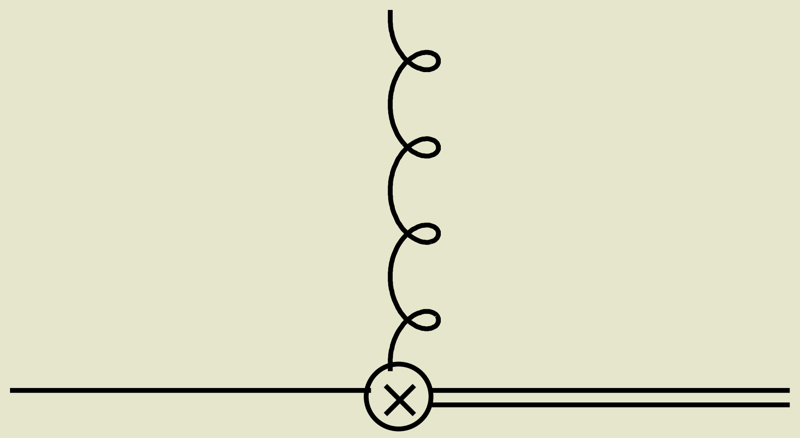

$O^\dagger \mathbf{r} \cdot g\mathbf{E}\, \mathrm{S}$

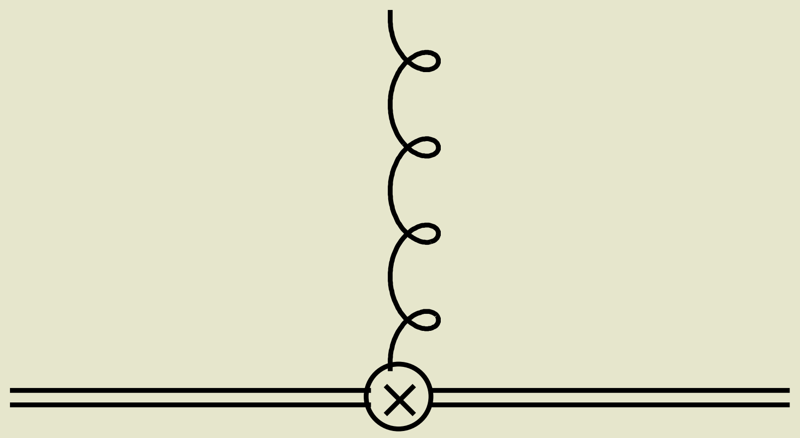

$O^\dagger \{\mathbf{r} \cdot g\mathbf{E},\, \mathrm{O}\}$

$+ \cdots$

Degrees of freedom: colour singlet S and colour octet O and low energy gluons (multipole expanded)

The potentials are the matching coefficients of pNRQCD : they are calculated via a well defined matching procedure

the finite T potential in equilibrium

the change of paradigm from the screening to the imaginary part of the potential

pNRQCD at finite T: the static potential

Finite T

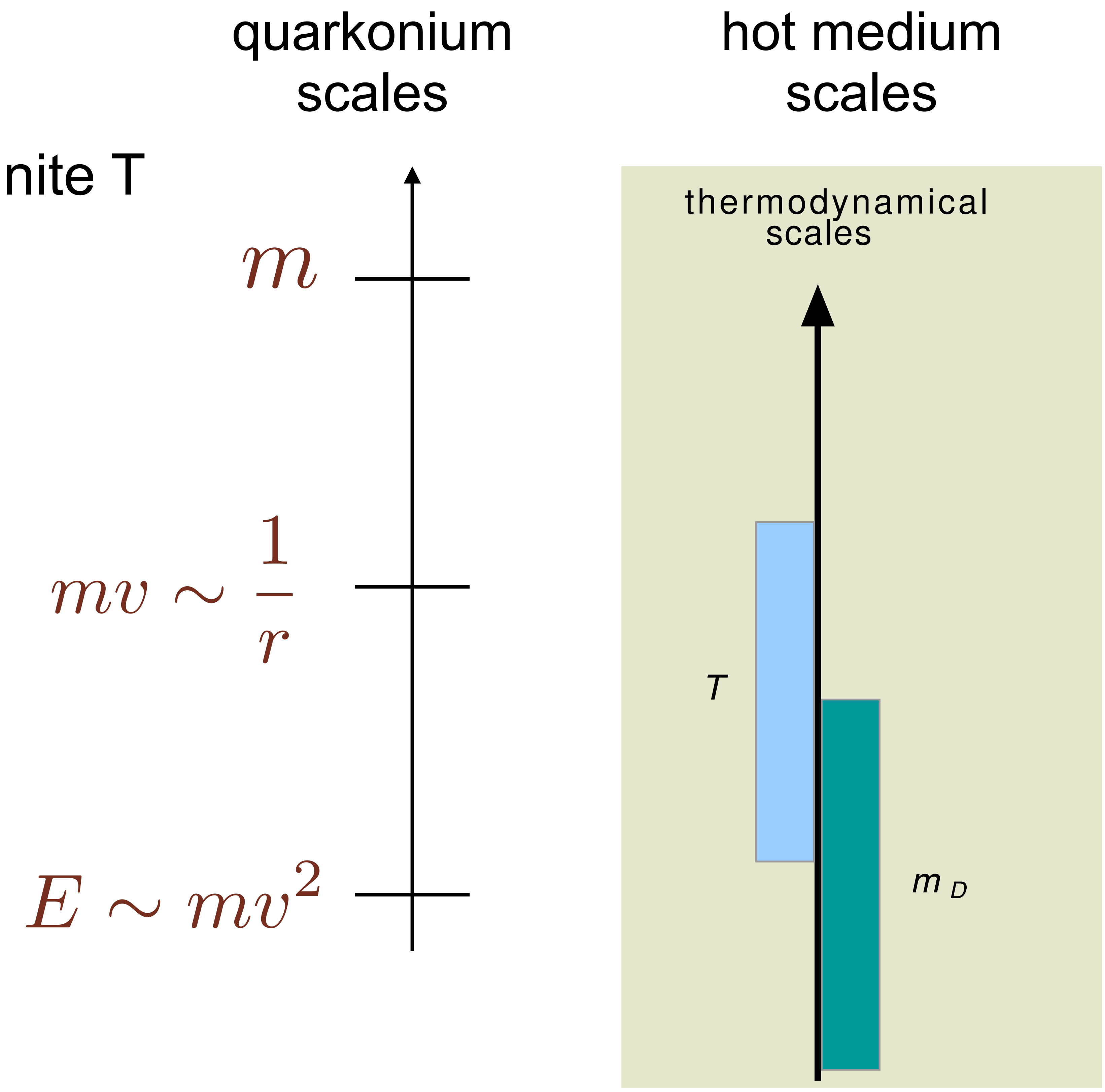

$$m \gg \Lambda_{QCD}$$

pNRQCD at finite T: the static potential

in pNRQCD the potential has a clear definition: it a matching coefficient and comes from the integration of all scales from mv up to (and not included) the energy mv^2

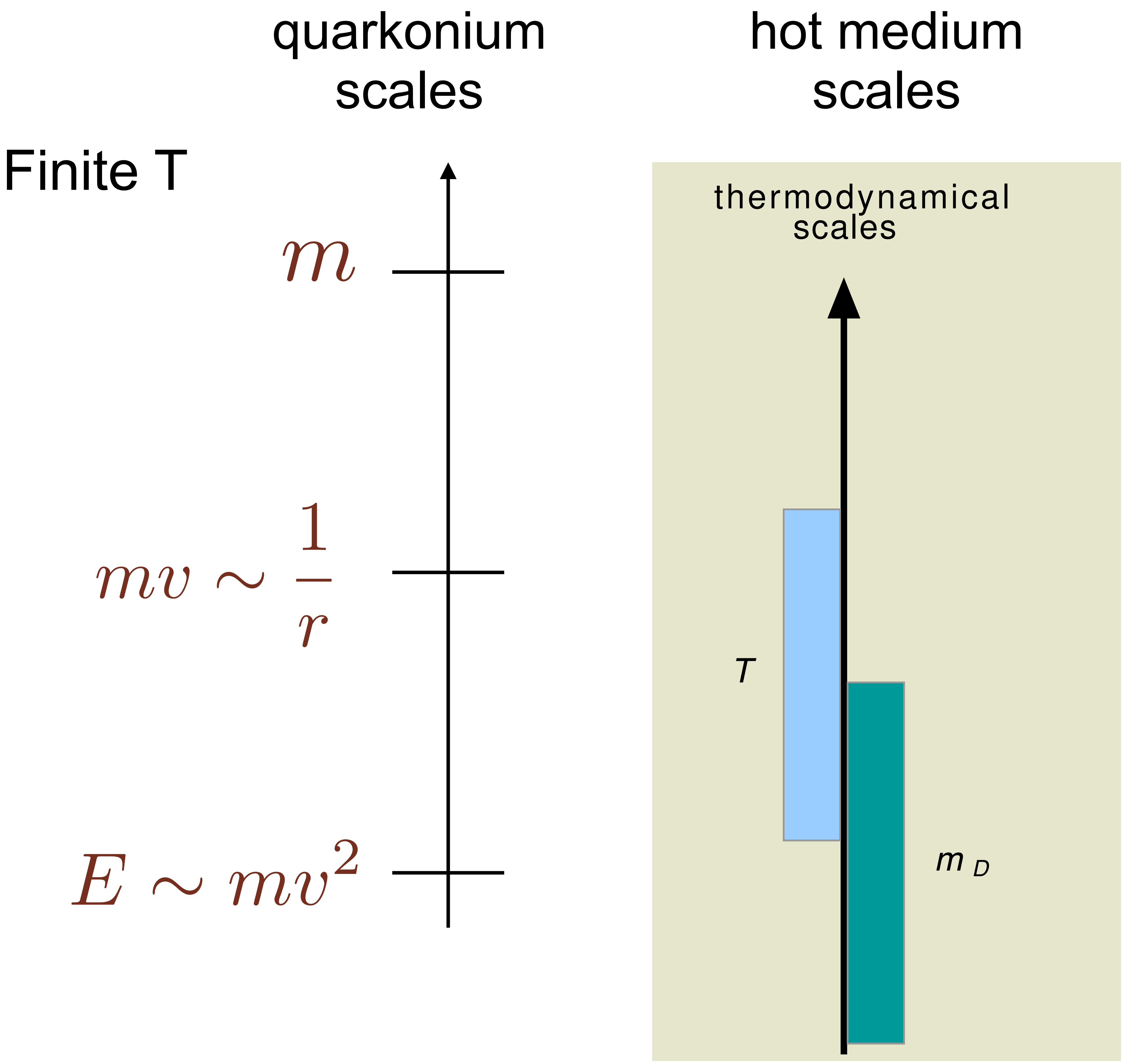

$$m \gg \Lambda_{QCD}$$

pNRQCD at finite T: the static potential

in pNRQCD the potential has a clear definition: it a matching coefficient and comes from the integration of all scales from mv up to (and not included) the energy mv^2

quarkonium scales

hot medium scales

Finite T

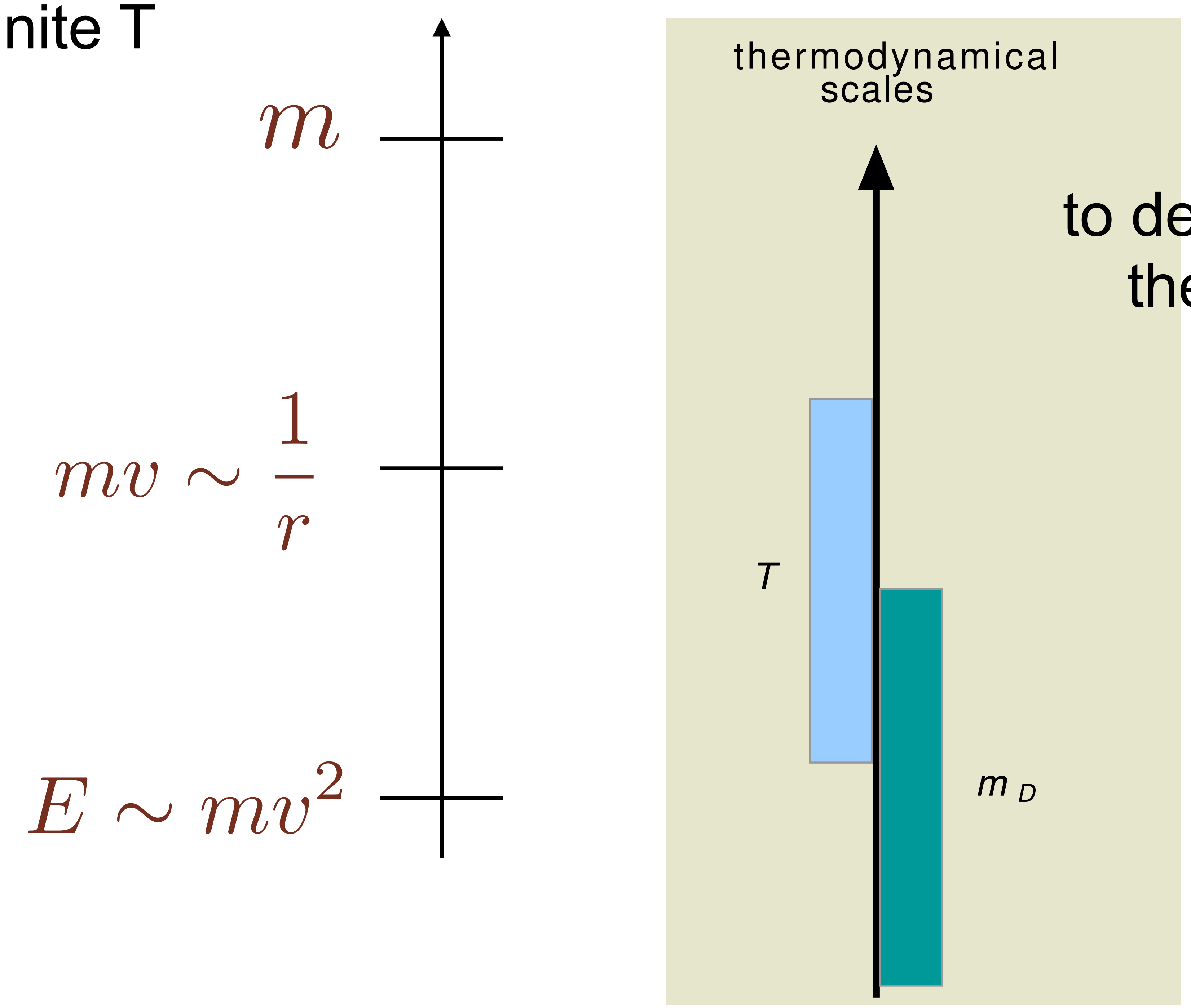

to define the potential we have to integrate out all the scales bigger than E including T and m_d

if T is of order E or less will give contribution to the energy and not to the potential

$$m \gg \Lambda_{QCD}$$

Notice:

The potential V(r,T) dictates through the Schroedinger equation the real time evolution of the QQbar in the medium

The finite T potential: how to obtain it

in pNRQCD the potential has a clear definition: it a matching coefficient and comes from the integration of all scales from mv up to (and not included) the energy mv^2

Finite T

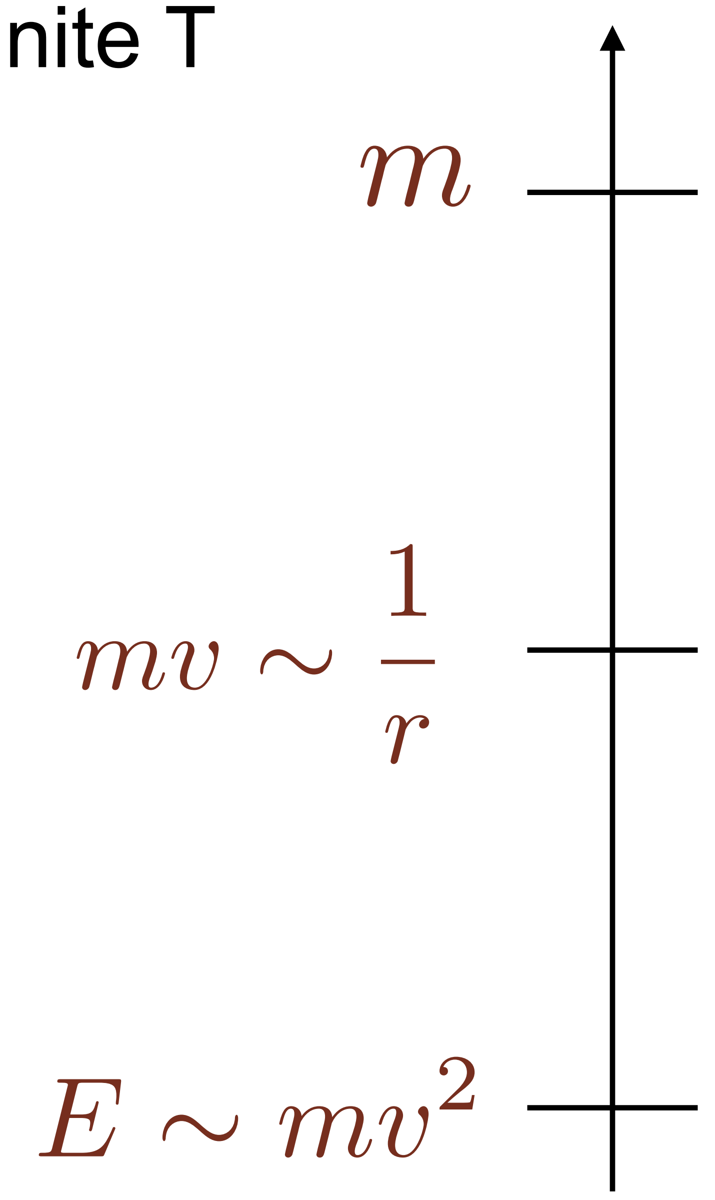

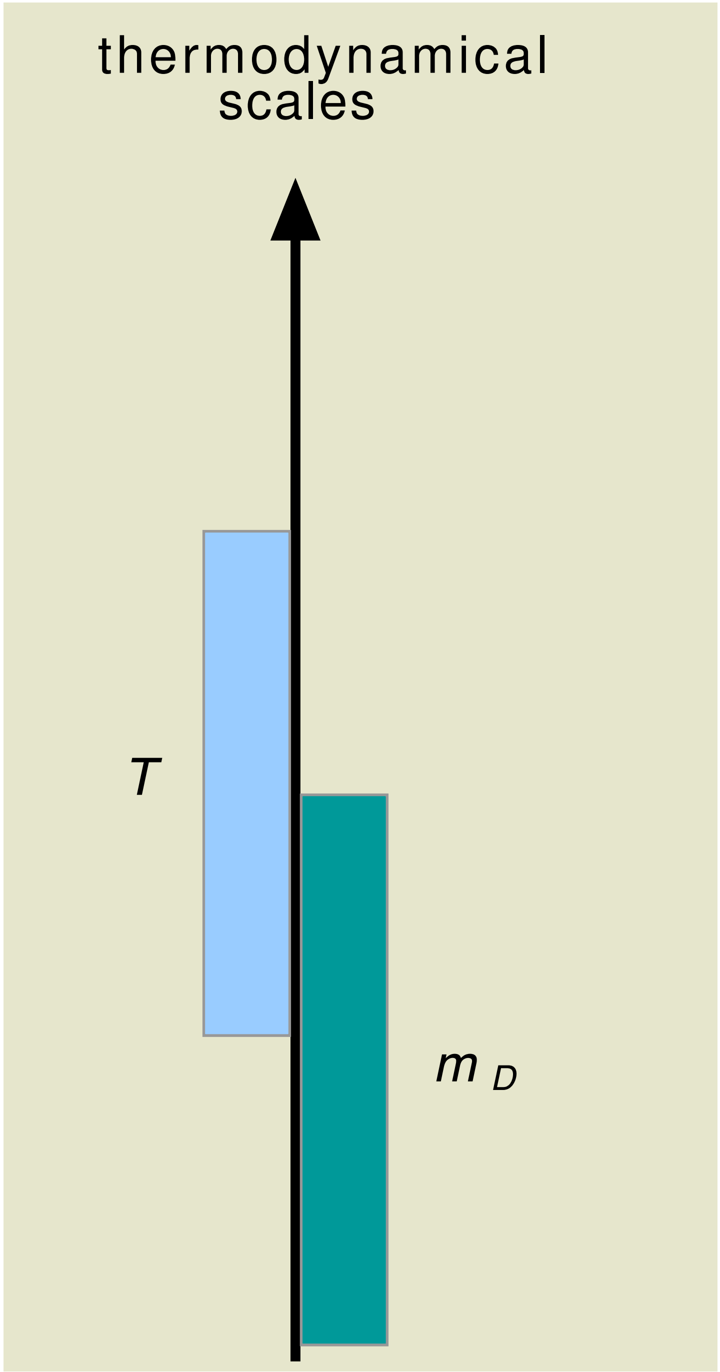

We assume that bound states exist for

- $T \ll m$
- $1/r \sim mv \gtrsim m_D$

We neglect smaller thermodynamical scales.

Inside these constraints we consider all the possible scales hierarchies

$$m \gg \Lambda_{QCD}$$

The finite T potential: how to obtain it

in pNRQCD the potential has a clear definition: it a matching coefficient and comes from the integration of all scales from mv up to (and not included) the energy mv^2

Finite T

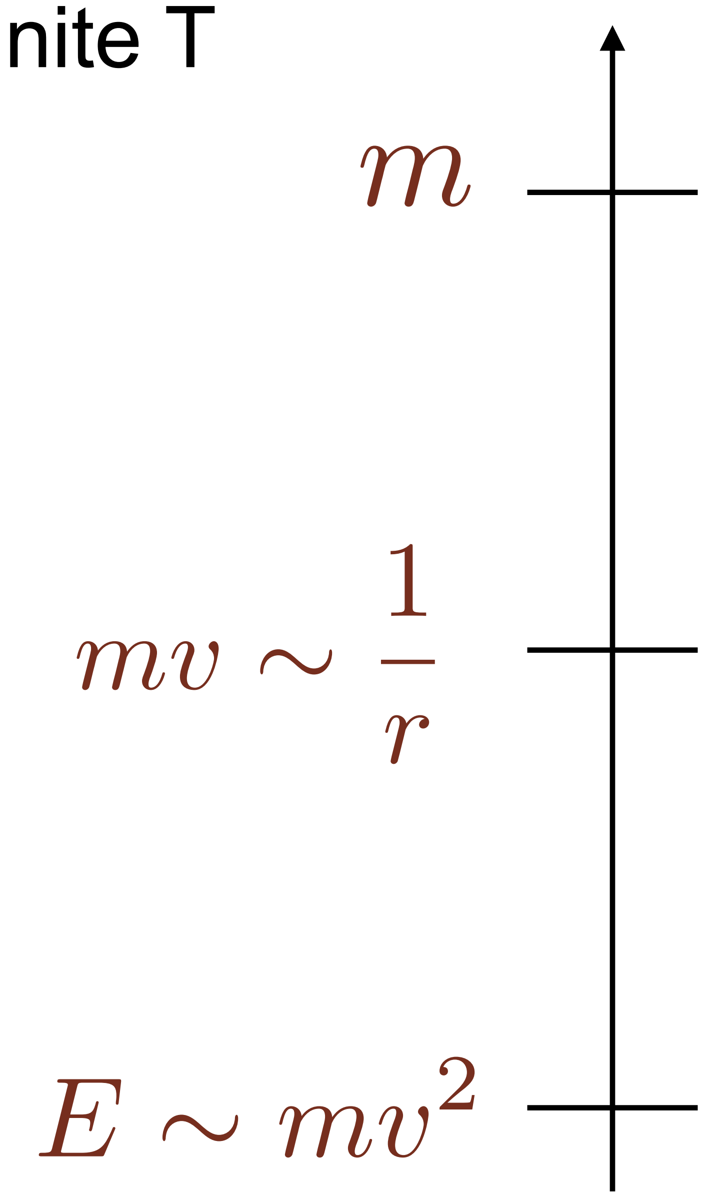

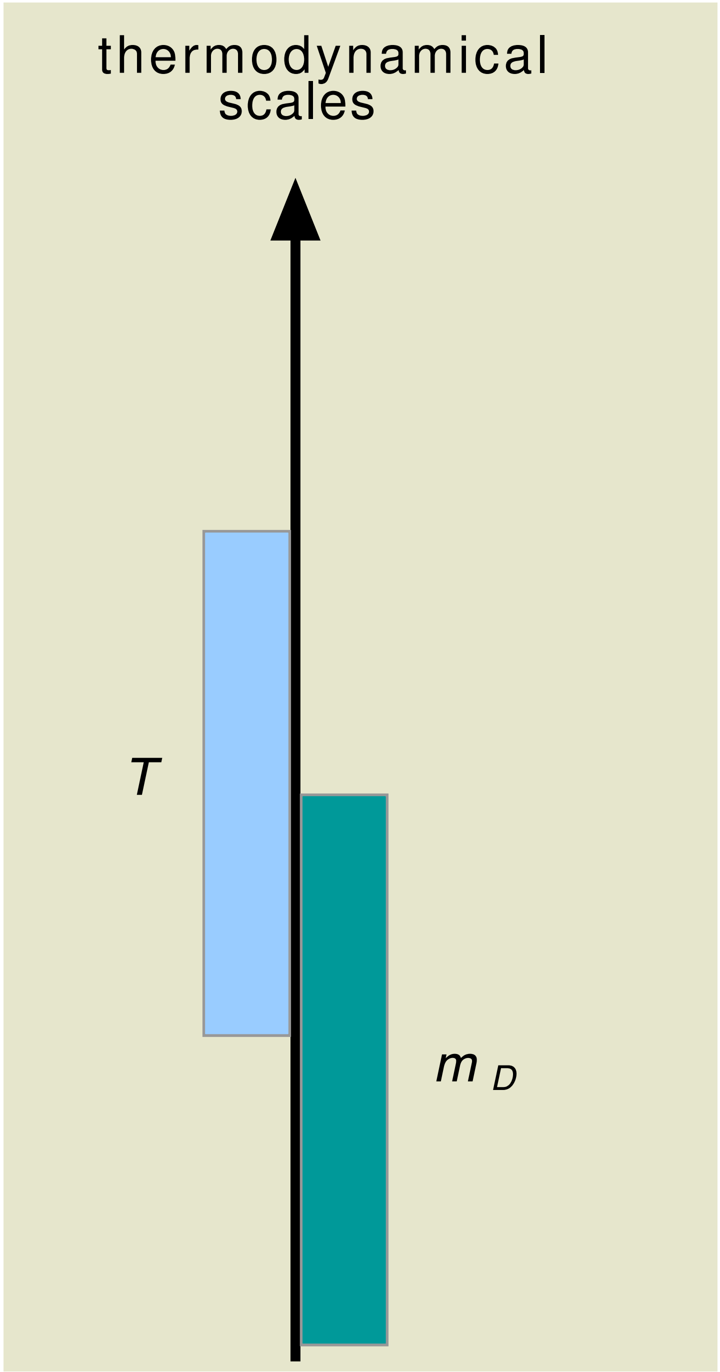

$$m \gg \Lambda_{QCD}$$

We assume that bound states exist for

- $T \ll m$
- $1/r \sim mv \gtrsim m_D$

We neglect smaller thermodynamical scales.

Inside these constraints we consider all the possible scales hierarchies

we work in the weak coupling regime

- $v \sim \alpha_s \ll 1$; valid for tightly bound states
- $T \gg gT \sim m_D$.

The finite T potential: how to obtain it

in pNRQCD the potential has a clear definition: it a matching coefficient and comes from the integration of all scales from mv up to (and not included) the energy mv^2

Finite T

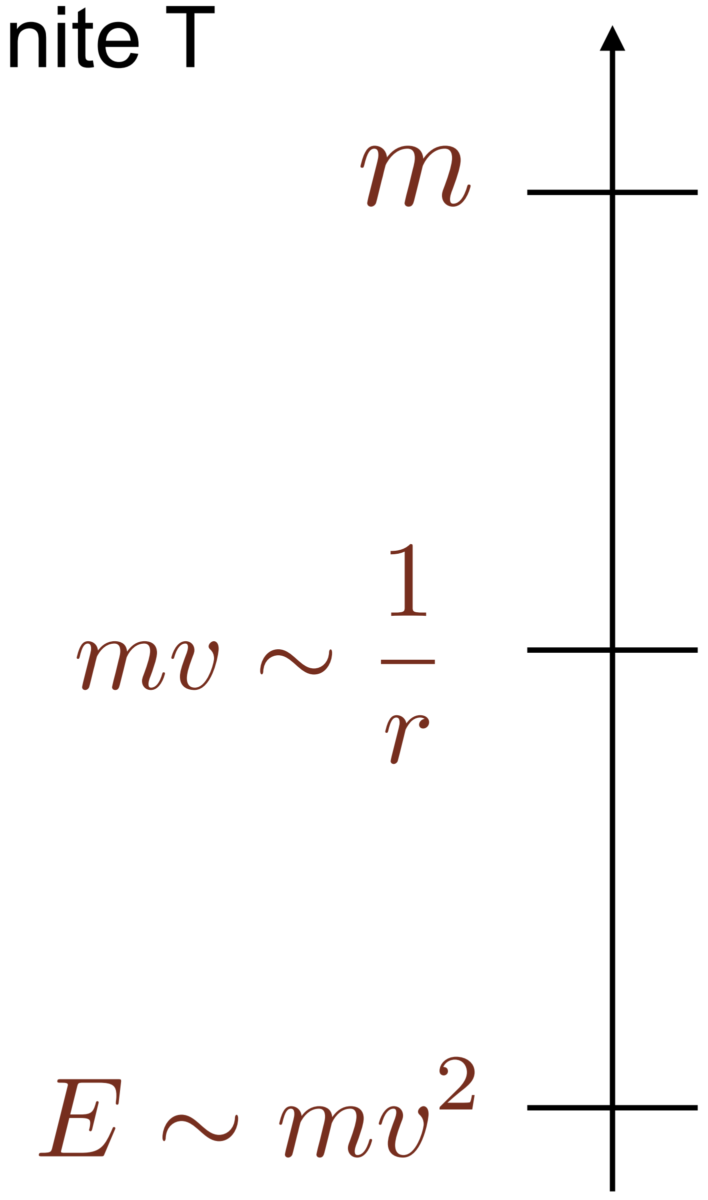

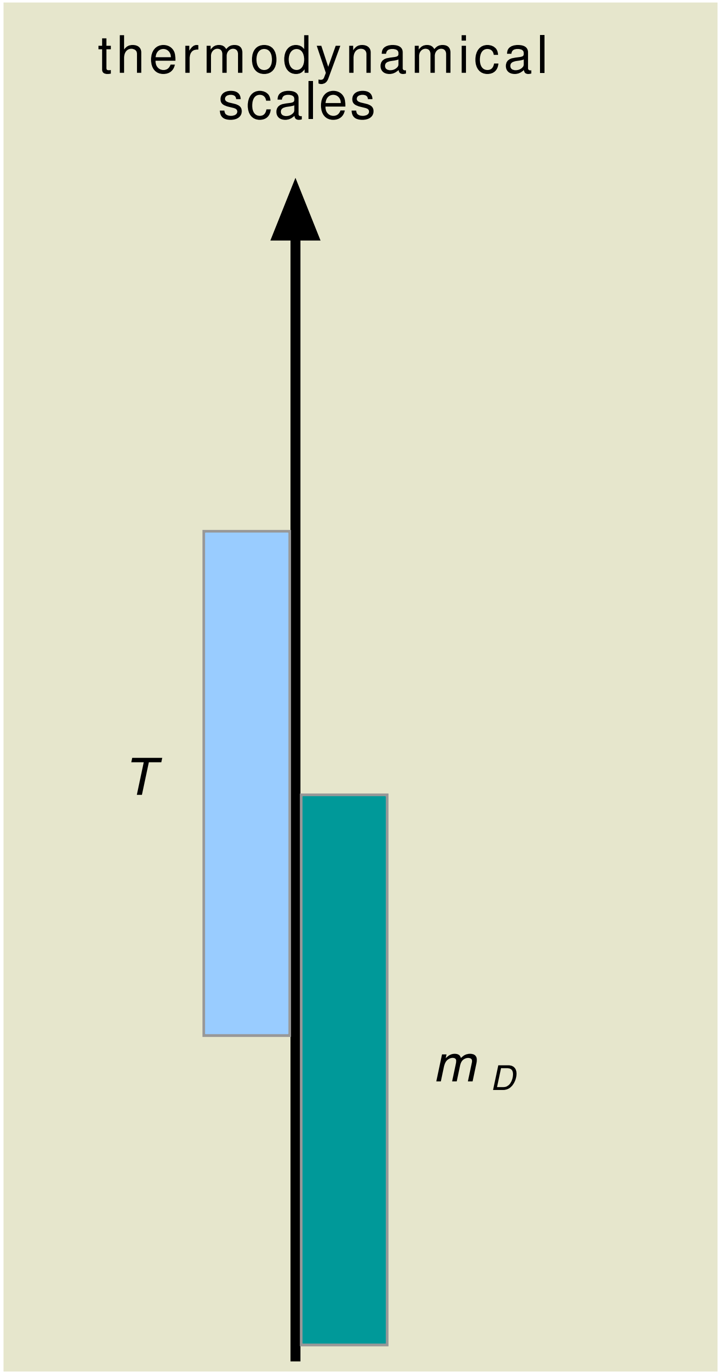

$m \gg \Lambda_{QCD}$

We assume that bound states exist for

- $T \ll m$
- $1/r \sim mv \gtrsim m_D$

We neglect smaller thermodynamical scales.

Inside these constraints we consider all the possible scales hierarchies

we work in the weak coupling regime

- $v \sim \alpha_s \ll 1$; valid for tightly bound states
- $T \gg gT \sim m_D$.

for the nonperturbative regime -> lattice calculation of the Wilson loop

The thermal part of the potential has a real and an imaginary part

$\mathrm{Re}V_s\,(r,T)$

$\mathrm{Im}V_s\,(r,T)$

thermal width of $Q\bar{Q}$

New effect, specific of QCD
dominates for E/m_D>>1

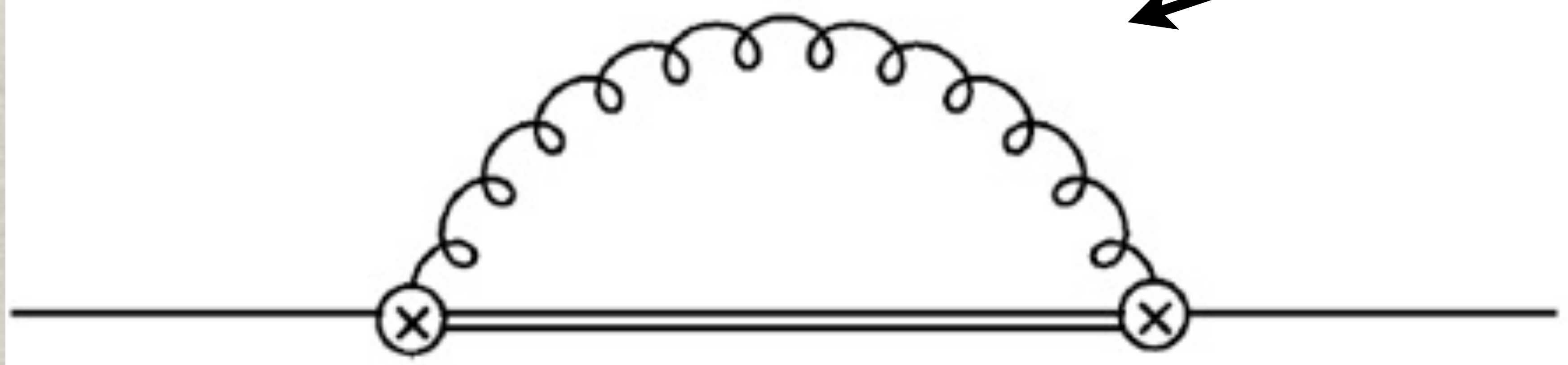

Singlet-to-octet

N.B Ghiglieri, Petreczky, Vairo 2008

Known from QED
dominates for m_D/E>>1

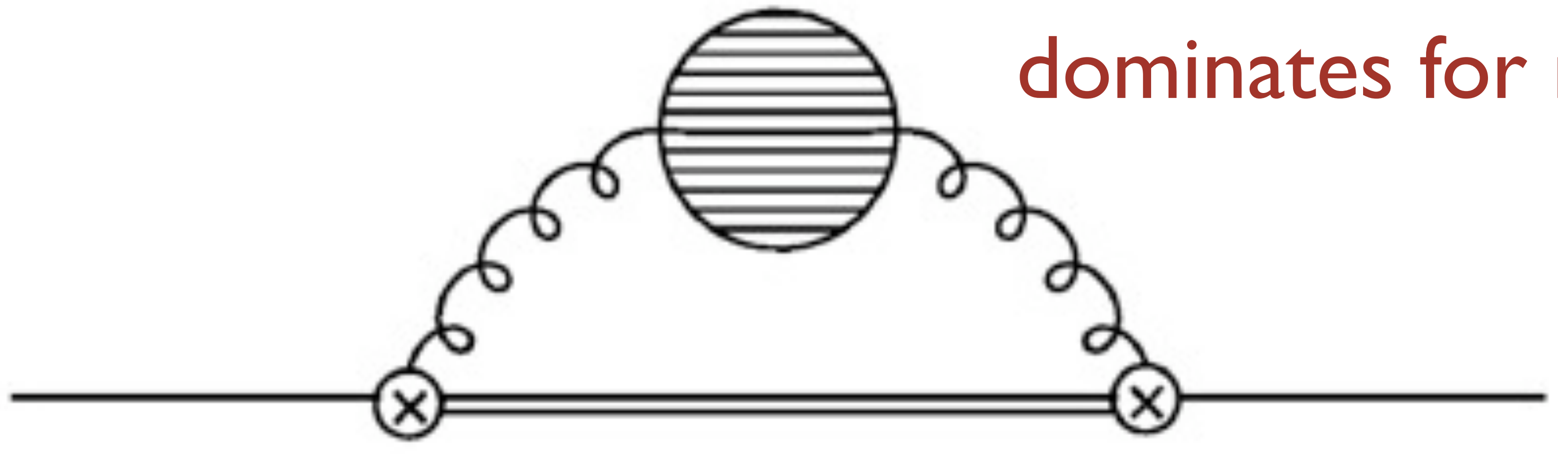

Landau damping

Laine et al 07, Escobedo Soto 07

The thermal part of the potential has a real and an imaginary part

ReVs (r,T)

ImVs (r,T)

thermal width of $Q\bar{Q}$

New effect, specific of QCD
dominates for E/m_D>>1

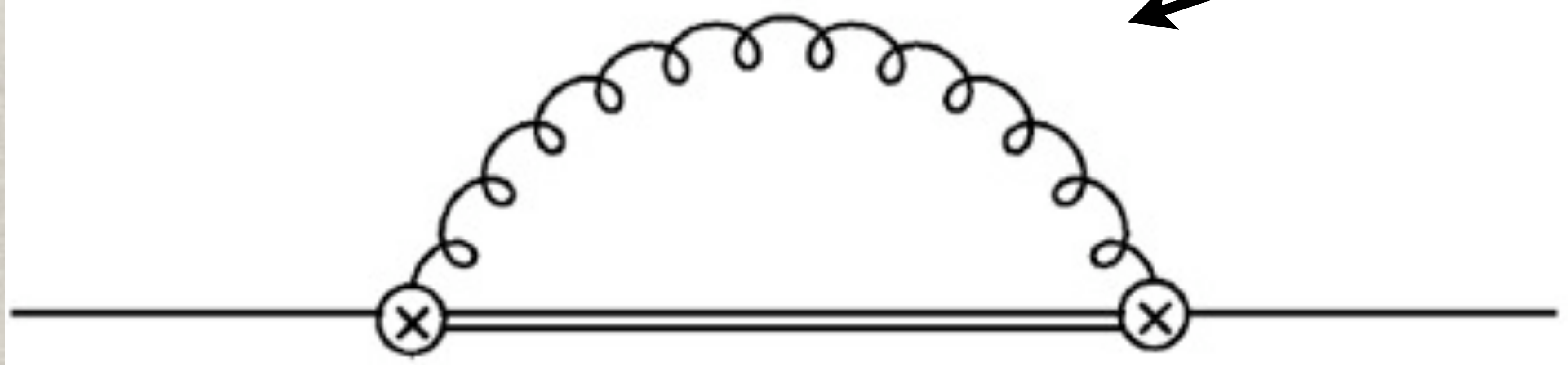

Singlet-to-octet

N.B Ghiglieri, Petreczky, Vairo 2008

(gluo dissociation)

N. B. Escobedo, Ghiglieri , Vairo 2011

Known from QED
dominates for m_D/E>>1

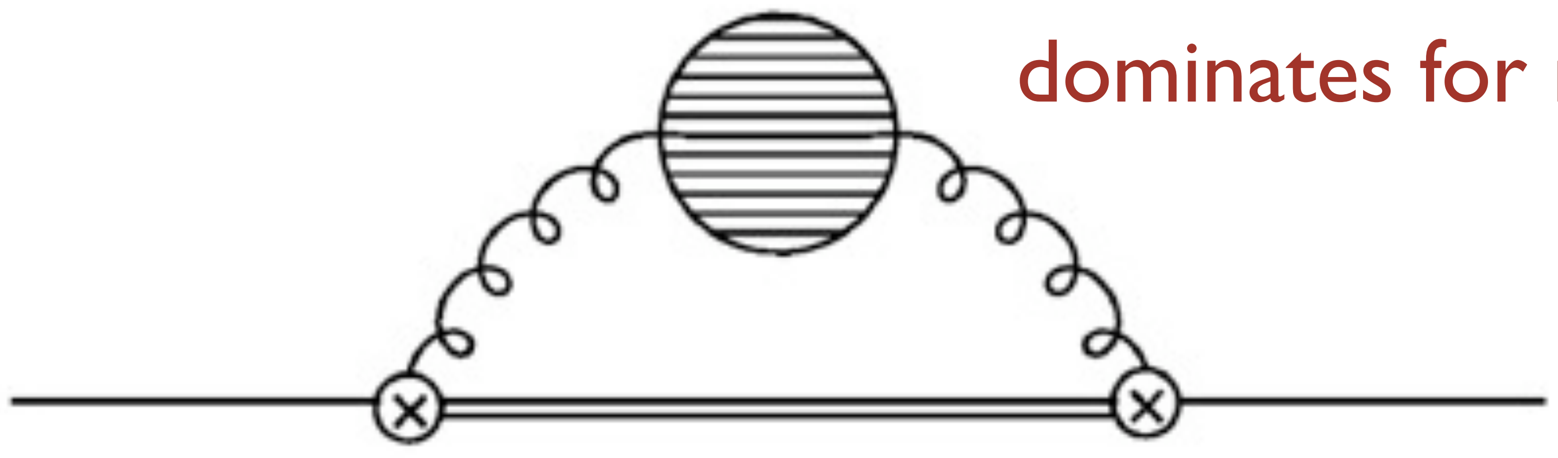

Landau damping

Laine et al 07, Escobedo Soto 07

(inelastic parton scattering)

N. B. Escobedo, Ghiglieri , Vairo 2013

The singlet static potential and the static energy

you always have a real and an imaginary part

- Temperature effects can be other than screening

$T > 1/r$ and $1/r \sim m_D \sim gT$

exponential screening but $\mathrm{Im}V \gg \mathrm{Re}V$

$T > 1/r$ and $1/r > m_D \sim gT$ or $\frac{1}{r} \gg T \gg E$

no exponential screening but power-like T corrections

$T < E_{bin}$

no corrections to the potential, corrections to the energy

for the detailed form of the potentials in each regime see: N.B Ghiglieri, Petreczky, Vairo Phys.Rev. D78 (2008) 014017

The singlet static potential and the static energy

you always have a real and an imaginary part

- Temperature effects can be other than screening

T > 1/r and 1/r ~ m_D ~ gT

exponential screening but $\mathrm{Im}V \gg \mathrm{Re}V$

T > 1/r and 1/r > m_D ~ gT

or $\frac{1}{r} \gg T \gg E$

no exponential screening but power-like T corrections

T < E_{bin}

no corrections to the potential, corrections to the energy

for the detailed form of the potentials in each regime see: N.B Ghiglieri, Petreczky, Vairo Phys.Rev. D78 (2008) 014017

imaginary parts in the potential have subsequently been found also for a strongly coupled plasma on the lattice (A. Rothkopf et al, Petreczky, Weber..) and in strings calculations

Change in the paradigm of dissociation

- The imaginary part is bigger than the real part before the screening exp{-m_D r} sets in

->the imaginary part is responsible for QQbar dissociation

$$T \gg 1/r \gg m_D \gg V$$

- Quarkonium dissociates at a temperature such that $\mathrm{Im}\, V_s(r) \sim \mathrm{Re}\, V_s(r) \sim \alpha_s/r$:

$$\pi T_{\mathrm{dissociation}} \sim m g^{4/3}$$

$E_{\mathrm{binding}} \sim \Gamma$

○ Escobedo Soto arXiv:0804.0691
Laine arXiv:0810.1112

- The interaction is screened when $\langle 1/r \rangle \sim m_D$, hence

$$\pi T_{\mathrm{screening}} \sim m g \gg \pi T_{\mathrm{dissociation}}$$

Change in the paradigm of dissociation

- The imaginary part is bigger than the real part before the screening exp{-m_D r} sets in

->the imaginary part is responsible for QQbar dissociation

$$T \gg 1/r \gg m_D \gg V$$

- Quarkonium dissociates at a temperature such that $\mathrm{Im}\, V_s(r) \sim \mathrm{Re}\, V_s(r) \sim \alpha_s/r$:

$$\pi T_{\rm dissociation} \sim m g^{4/3}$$

- The interaction is screened when $\langle 1/r \rangle \sim m_D$, hence

$$\pi T_{\rm screening} \sim m g \gg \pi T_{\rm dissociation}$$

$$E_{\rm binding} \sim \Gamma$$

o Escobedo Soto arXiv:0804.0691
Laine arXiv:0810.1112

the EFT offers a systematic framework to do the calculations of the energy and width in a hot medium

Change in the paradigm of dissociation

- The imaginary part is bigger than the real part before the screening exp{-m_D r} sets in

->the imaginary part is responsible for QQbar dissociation

$$T \gg 1/r \gg m_D \gg V$$

- Quarkonium dissociates at a temperature such that $\mathrm{Im}\, V_s(r) \sim \mathrm{Re}\, V_s(r) \sim \alpha_s/r$:

$$\pi T_{\text{dissociation}} \sim m g^{4/3}$$

$E_{\text{binding}} \sim \Gamma$

○ Escobedo Soto arXiv:0804.0691
Laine arXiv:0810.1112

- The interaction is screened when $\langle 1/r \rangle \sim m_D$, hence

$$\pi T_{\text{screening}} \sim m g \gg \pi T_{\text{dissociation}}$$

the EFT offers a systematic framework to do the calculations of the energy and width in a hot medium

The bottomonium ground state , which is a weakly coupled non-relativistic bound state: $mv \sim m\alpha_s,\, mv^2 \sim m\alpha_s^2 \gtrsim \Lambda_{\mathrm{QCD}}$, produced in the QCD medium of heavy-ion collisions at the LHC may possibly realize the hierarchy

$$m \approx 5\ \text{GeV} > m\alpha_s \approx 1.5\ \text{GeV} > \pi T \approx 1\ \text{GeV} > m\alpha_s^2 \approx 0.5\ \text{GeV} \gtrsim m_D, \Lambda_{\mathrm{QCD}}$$

T_dissociation in the $\Upsilon(1S)$ case is about 450 MeV.

bottomonium 1S below the melting temperature T_d

The complete mass and width up to $\mathcal{O}(m\alpha_s^5)$

$$\delta E_{1S}^{(\mathrm{thermal})} = \frac{34\pi}{27}\alpha_s^2\,T^2 a_0 + \frac{7225}{324}\frac{E_1\alpha_s^3}{\pi}\left[\ln\left(\frac{2\pi T}{E_1}\right)^2 - 2\gamma_E\right] + \frac{128 E_1\alpha_s^3}{81\pi}L_{1,0} - 3a_0^2\left\{\left[\frac{6}{\pi}\zeta(3) + \frac{4\pi}{3}\right]\alpha_s\,T\,m_D^2 - \frac{8}{3}\zeta(3)\,\alpha_s^2\,T^3\right\}$$

$$\Gamma_{1S}^{(\mathrm{thermal})} = \frac{1156}{81}\alpha_s^3 T + \frac{7225}{162}E_1\alpha_s^3 + \frac{32}{9}\alpha_s\,T m_D^2\,a_0^2\,I_{1,0} - \left[\frac{4}{3}\alpha_s T m_D^2\left(\ln\frac{E_1^2}{T^2} + 2\gamma_E - 3 - \ln 4 - 2\frac{\zeta'(2)}{\zeta(2)}\right) + \frac{32\pi}{3}\ln 2\,\alpha_s^2\,T^3\right]a_0^2$$

where $E_1 = -\frac{4m\alpha_s^2}{9}$, $a_0 = \frac{3}{2m\alpha_s}$ and $L_{1,0}$ (similar $I_{1,0}$) is the Bethe logarithm.

- Brambilla Escobedo Ghiglieri Soto Vairo JHEP 1009 (2010) 038

first systematic calculation of the thermal contributions to quarkonium mass and width

Consistent with lattice calculations of spectral functions

- Aarts Allton Kim Lombardo Oktay Ryan Sinclair Skullerud JHEP 1111 (2011) 103

To describe quarkonium in QGP we should account for: screening,
dissociation effects (singlet to octet, inelastic parton scattering),
recombination effects

To describe quarkonium in QGP we should account for: screening, dissociation effects (singlet to octet, inelastic parton scattering), recombination effects

—->The non equilibrium evolution of quarkonium in QGP

Using pNRQCD and Open Quantum Systems (OQS) we could use bottomonium as a probe of a strongly coupled QGP and obtain master equations for the singlet and octet matrix density evolution

The equations are quantum, nonabelian and conserve the number of heavy quarks

Quarkonium in the fireball

- After the heavy-ion collisions, heavy quark-antiquarks propagate freely up to 0.6 fm.
- From 0.6 fm to the freeze-out time t_F they propagate in the medium.
- We assume the medium infinite, homogeneous and isotropic.
- We assume the heavy quarks comoving with the medium.
- We assume the medium to be locally in thermal equilibrium,

  i.e., the temperature T of the medium changes (slowly) with time:

Quarkonium in the fireball

- After the heavy-ion collisions, heavy quark-antiquarks propagate freely up to 0.6 fm.
- From 0.6 fm to the freeze-out time t_F they propagate in the medium.
- We assume the medium infinite, homogeneous and isotropic.
- We assume the heavy quarks comoving with the medium.
- We assume the medium to be locally in thermal equilibrium,

  i.e., the temperature T of the medium changes (slowly) with time:

Quarkonium as a small radius probe: bottomonium

Hierarchy of scales:

$$m \gg 1/r \sim m\alpha_s \gg T \sim gT \gg E$$

Coulombic bound state:

quark-antiquark color singlet Hamiltonian $$h_s = \frac{\mathbf{p}^2}{m} - \frac{4}{3}\frac{\alpha_s}{r}$$

quark-antiquark color octet Hamiltonian $$h_o = \frac{\mathbf{p}^2}{m} + \frac{1}{6}\frac{\alpha_s}{r}$$

The octet potential describes an unbound quark-antiquark pair.

Quarkonium in the fireball

- After the heavy-ion collisions, heavy quark-antiquarks propagate freely up to 0.6 fm.
- From 0.6 fm to the freeze-out time t_F they propagate in the medium.
- We assume the medium infinite, homogeneous and isotropic.
- We assume the heavy quarks comoving with the medium.
- We assume the medium to be locally in thermal equilibrium,

  i.e., the temperature T of the medium changes (slowly) with time:

Open Quantum system

- Subsystem: heavy quarks/quarkonium
- Environment: quark gluon plasma

N.B., J. Soto, M. Escobedo, A. Vairo 2016, 2018 (1612.07248, 1711.04515)

Quarkonium as a small radius probe: bottomonium

Hierarchy of scales:

$$m \gg 1/r \sim m\alpha_s \gg T \sim gT \gg E$$

Coulombic bound state:

quark-antiquark color singlet Hamiltonian $\quad h_s = \frac{\mathbf{p}^2}{m} - \frac{4}{3}\frac{\alpha_s}{r}$

quark-antiquark color octet Hamiltonian $\quad h_o = \frac{\mathbf{p}^2}{m} + \frac{1}{6}\frac{\alpha_s}{r}$

The octet potential describes an unbound quark-antiquark pair.

We may define a density matrix in pNRQCD for the heavy quark-antiquark pair in a singlet and octet configuration:

$$\langle \mathbf{r}', \mathbf{R}' | \rho_s(t';t) | \mathbf{r}, \mathbf{R}\rangle \equiv \mathrm{Tr}\{\rho_{\mathrm{full}}(t_0)\, S^\dagger(t,\mathbf{r},\mathbf{R}) S(t',\mathbf{r}',\mathbf{R}')\}$$

$$\langle \mathbf{r}', \mathbf{R}' | \rho_o(t';t) | \mathbf{r}, \mathbf{R}\rangle \frac{\delta^{ab}}{8} \equiv \mathrm{Tr}\{\rho_{\mathrm{full}}(t_0)\, O^{a\dagger}(t,\mathbf{r},\mathbf{R}) O^b(t',\mathbf{r}',\mathbf{R}')\}$$

Quarkonium in the fireball

- After the heavy-ion collisions, heavy quark-antiquarks propagate freely up to 0.6 fm.
- From 0.6 fm to the freeze-out time t_F they propagate in the medium.
- We assume the medium infinite, homogeneous and isotropic.
- We assume the heavy quarks comoving with the medium.
- We assume the medium to be locally in thermal equilibrium,

  i.e., the temperature T of the medium changes (slowly) with time:

Open Quantum system

- Subsystem: heavy quarks/quarkonium
- Environment: quark gluon plasma

N.B., J. Soto, M. Escobedo, A. Vairo 2016, 2018 (1612.07248, 1711.04515)

Quarkonium as a small radius probe: bottomonium

Hierarchy of scales:

$$m \gg 1/r \sim m\alpha_s \gg T \sim gT \gg E$$

Coulombic bound state:

quark-antiquark color singlet Hamiltonian $\quad h_s = \frac{\mathbf{p}^2}{m} - \frac{4}{3}\frac{\alpha_s}{r}$

quark-antiquark color octet Hamiltonian $\quad h_o = \frac{\mathbf{p}^2}{m} + \frac{1}{6}\frac{\alpha_s}{r}$

The octet potential describes an unbound quark-antiquark pair.

We may define a density matrix in pNRQCD for the heavy quark-antiquark pair in a singlet and octet configuration:

$$\begin{aligned}
\langle \mathbf{r}', \mathbf{R}' | \rho_s(t';t) | \mathbf{r}, \mathbf{R} \rangle &\equiv \mathrm{Tr}\{\rho_{\mathrm{full}}(t_0)\, S^\dagger(t,\mathbf{r},\mathbf{R}) S(t',\mathbf{r}',\mathbf{R}')\} \\
\langle \mathbf{r}', \mathbf{R}' | \rho_o(t';t) | \mathbf{r}, \mathbf{R} \rangle \frac{\delta^{ab}}{8} &\equiv \mathrm{Tr}\{\rho_{\mathrm{full}}(t_0)\, O^{a\dagger}(t,\mathbf{r},\mathbf{R}) O^b(t',\mathbf{r}',\mathbf{R}')\}
\end{aligned}$$

The system is in non-equilibrium because through interaction with the environment (quark gluon plasma) singlet and octet quark-antiquark states continuously transform in each other although the number of heavy quarks is conserved: $\mathrm{Tr}\{\rho_s\} + \mathrm{Tr}\{\rho_o\} = 1$.

Closed time path formalism

In the closed-time path formalism we can represent the density matrices as 12 propagators on a closed time path:

$$\begin{aligned}\langle \mathbf{r}', \mathbf{R}' | \rho_s(t';t) | \mathbf{r}, \mathbf{R}\rangle &= \langle S_1(t', \mathbf{r}', \mathbf{R}') S_2^\dagger(t, \mathbf{r}, \mathbf{R})\rangle \\ \langle \mathbf{r}', \mathbf{R}' | \rho_o(t';t) | \mathbf{r}, \mathbf{R}\rangle \frac{\delta^{ab}}{8} &= \langle O_1^b(t', \mathbf{r}', \mathbf{R}') O_2^{a\dagger}(t, \mathbf{r}, \mathbf{R})\rangle\end{aligned}$$

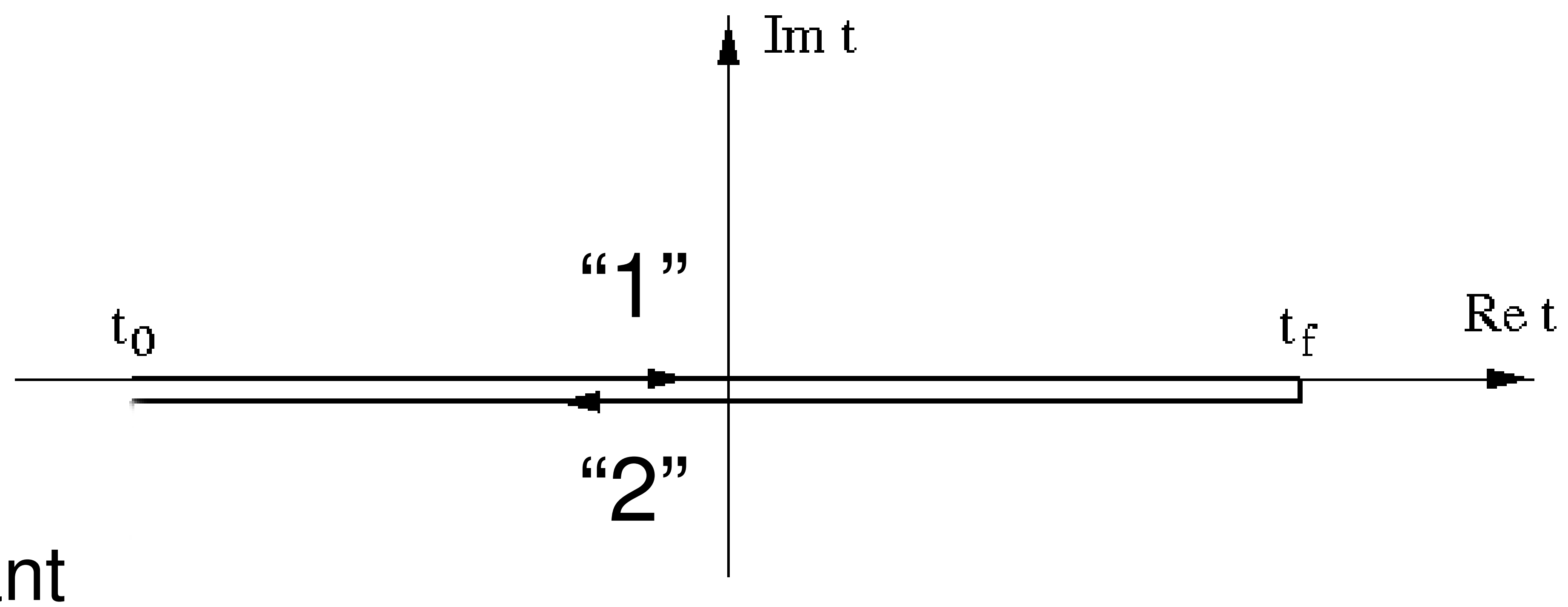

Differently from the thermal equilibrium case 12 propagators are relevant (in thermal equilibrium they are exponentially suppressed).

12 propagators are not time ordered, while 11 and 22 operators select the forward time direction $\propto \theta(t-t')$, $\theta(t'-t)$.

Closed time path formalism

In the closed-time path formalism we can represent the density matrices as 12 propagators on a closed time path:

$$\langle \mathbf{r}', \mathbf{R}' | \rho_s(t';t) | \mathbf{r}, \mathbf{R} \rangle = \langle S_1(t', \mathbf{r}', \mathbf{R}') S_2^\dagger(t, \mathbf{r}, \mathbf{R}) \rangle$$

$$\langle \mathbf{r}', \mathbf{R}' | \rho_o(t';t) | \mathbf{r}, \mathbf{R} \rangle \frac{\delta^{ab}}{8} = \langle O_1^b(t', \mathbf{r}', \mathbf{R}') O_2^{a\dagger}(t, \mathbf{r}, \mathbf{R}) \rangle$$

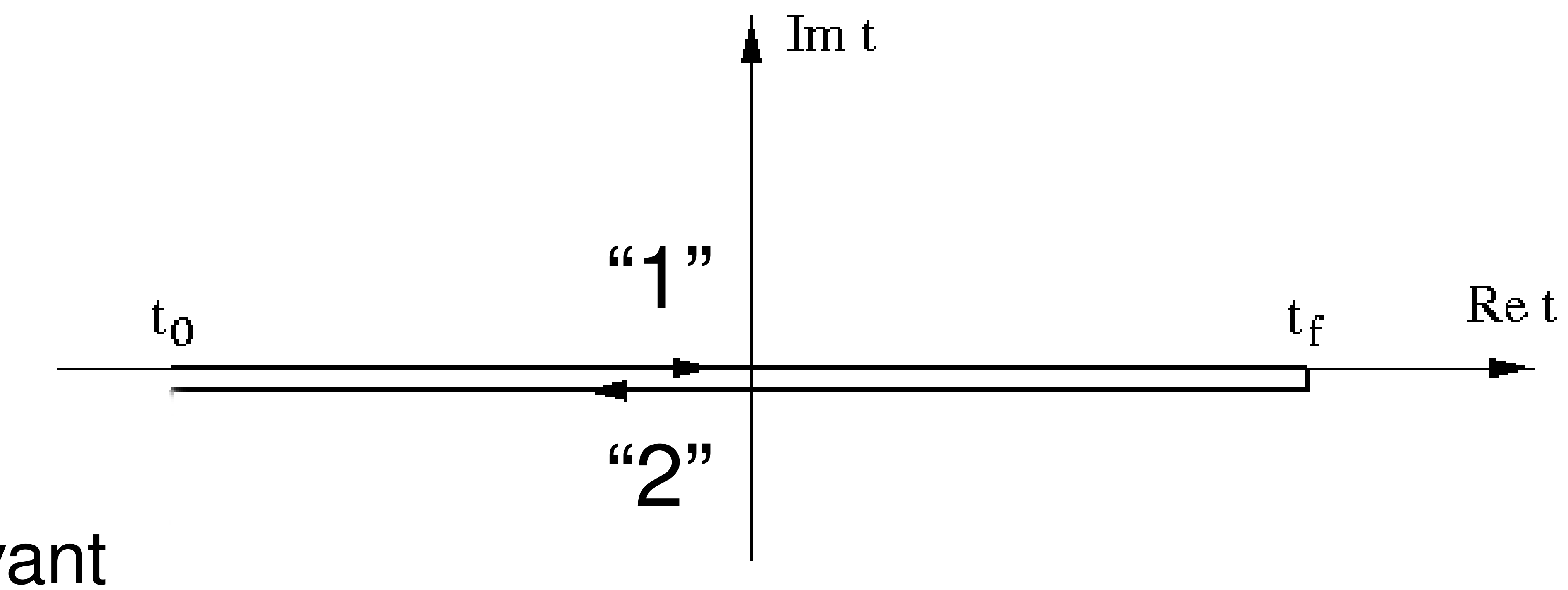

Differently from the thermal equilibrium case 12 propagators are relevant (in thermal equilibrium they are exponentially suppressed).

12 propagators are not time ordered, while 11 and 22 operators select the forward time direction $\propto \theta(t-t')$, $\theta(t'-t)$.

Expansions

- The density of heavy quarks is much smaller than the one of light quarks: we expand at first order in the heavy quark-antiquark density.
- We consider T much smaller than the Bohr radius of the quarkonium: we expand up to order r^2 in the multipole expansion.

LO and NLO evolution

For $t > t_0$, the LO singlet density matrix is

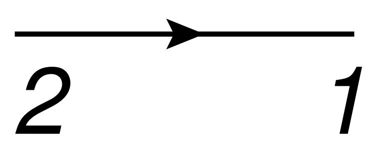

$$= e^{-ih_s(t-t_0)}\rho_s(t_0;t_0)e^{ih_s(t-t_0)}$$

($h_{s,o}$ = singlet/octet pNRQCD Hamiltonian $= V_{s,o}$ in the static limit)

and the NLO (in the multipole expansion) corrections are at first order in the density

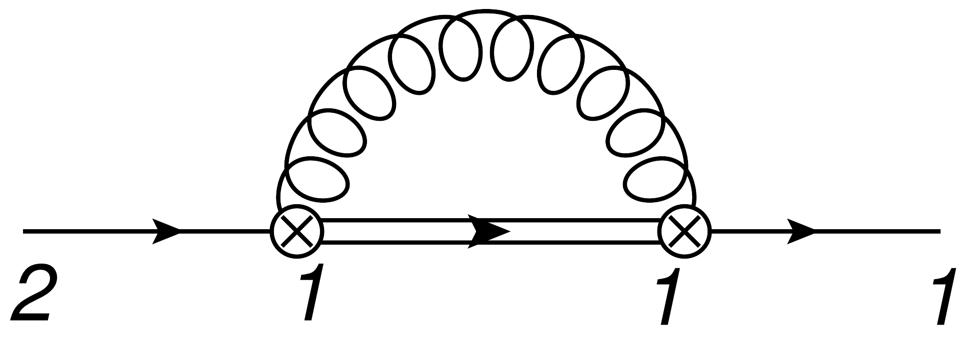

$$= -\int_{t_0}^{t} dt_1\, e^{-ih_s(t-t_1)}\,\Sigma_s(t_1)\,e^{-ih_s(t_1-t_0)}\,\rho_s(t_0;t_0)\,e^{ih_s(t-t_0)}$$

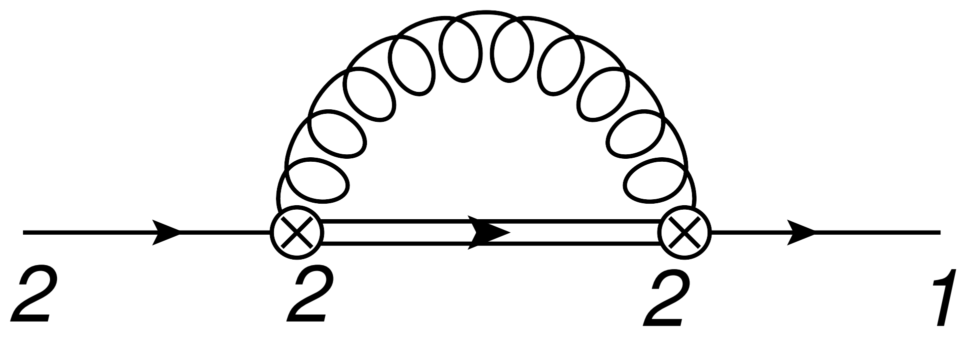

$$= -\int_{t_0}^{t} dt_1\, e^{-ih_s(t-t_0)}\,\rho_s(t_0;t_0)\,e^{ih_s(t_1-t_0)}\,\Sigma_s^\dagger(t_1)\,e^{ih_s(t-t_1)}$$

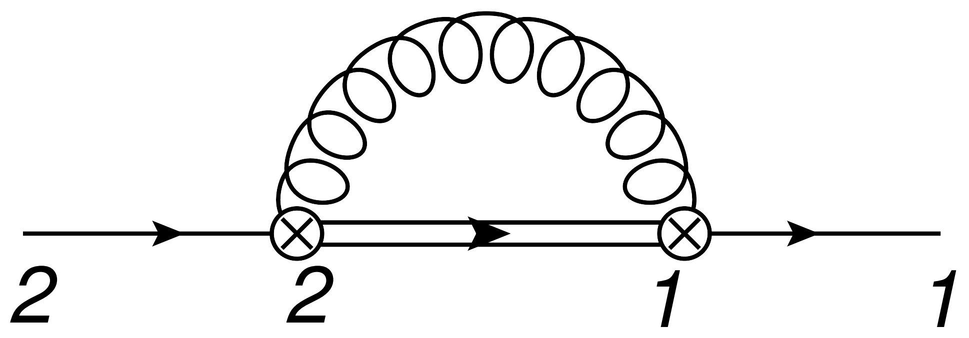

$$= \int_{t_0}^{t} dt_1\, e^{-ih_s(t-t_1)}\,\Xi_{so}(\rho_o(t_0;t_0),t_1)\,e^{ih_s(t-t_1)}$$

and similar for the octet

$$
\Sigma_s(t) = \frac{g^2}{2N_c}\int_{t_0}^{t} dt_2\, r^i\, e^{-ih_o(t-t_2)}\, r^j\, e^{ih_s(t-t_2)}\, \langle E^{a,i}(t,\mathbf{0})E^{a,j}(t_2,\mathbf{0})\rangle
$$

$$
\Xi_{so}(\rho_o(t_0;t_0),t) = \frac{g^2}{2N_c(N_c^2-1)}\int_{t_0}^{t} dt_2\, \Big[r^i\, e^{-ih_o(t-t_0)}\, \rho_o(t_0;t_0)\, e^{ih_o(t_2-t_0)} \times r^j\, e^{ih_s(t-t_2)}\, \langle E^{a,j}(t_2,\mathbf{0})E^{a,i}(t,\mathbf{0})\rangle + \text{H.c.}\Big]
$$

and similar for the octet

A Wilson line in the adjoint representation is understood in the chromoelectric correlators.

$$\Sigma_s(t) = \frac{g^2}{2N_c}\int_{t_0}^{t} dt_2\, r^i\, e^{-ih_o(t-t_2)}\, r^j\, e^{ih_s(t-t_2)}\, \langle E^{a,i}(t,\mathbf{0})E^{a,j}(t_2,\mathbf{0})\rangle$$

$$\Xi_{so}(\rho_o(t_0;t_0),t) = \frac{g^2}{2N_c(N_c^2-1)}\int_{t_0}^{t} dt_2\, \Big[r^i\, e^{-ih_o(t-t_0)}\, \rho_o(t_0;t_0)\, e^{ih_o(t_2-t_0)} \times r^j\, e^{ih_s(t-t_2)}\, \langle E^{a,j}(t_2,\mathbf{0})E^{a,i}(t,\mathbf{0})\rangle + \text{H.c.}\Big]$$

and similar for the octet

A Wilson line in the adjoint representation is understood in the chromoelectric correlators.

Diagrams and resummation

Resumming $(t-t_0)\times$ self-energy contributions à la Schwinger–Dyson ...

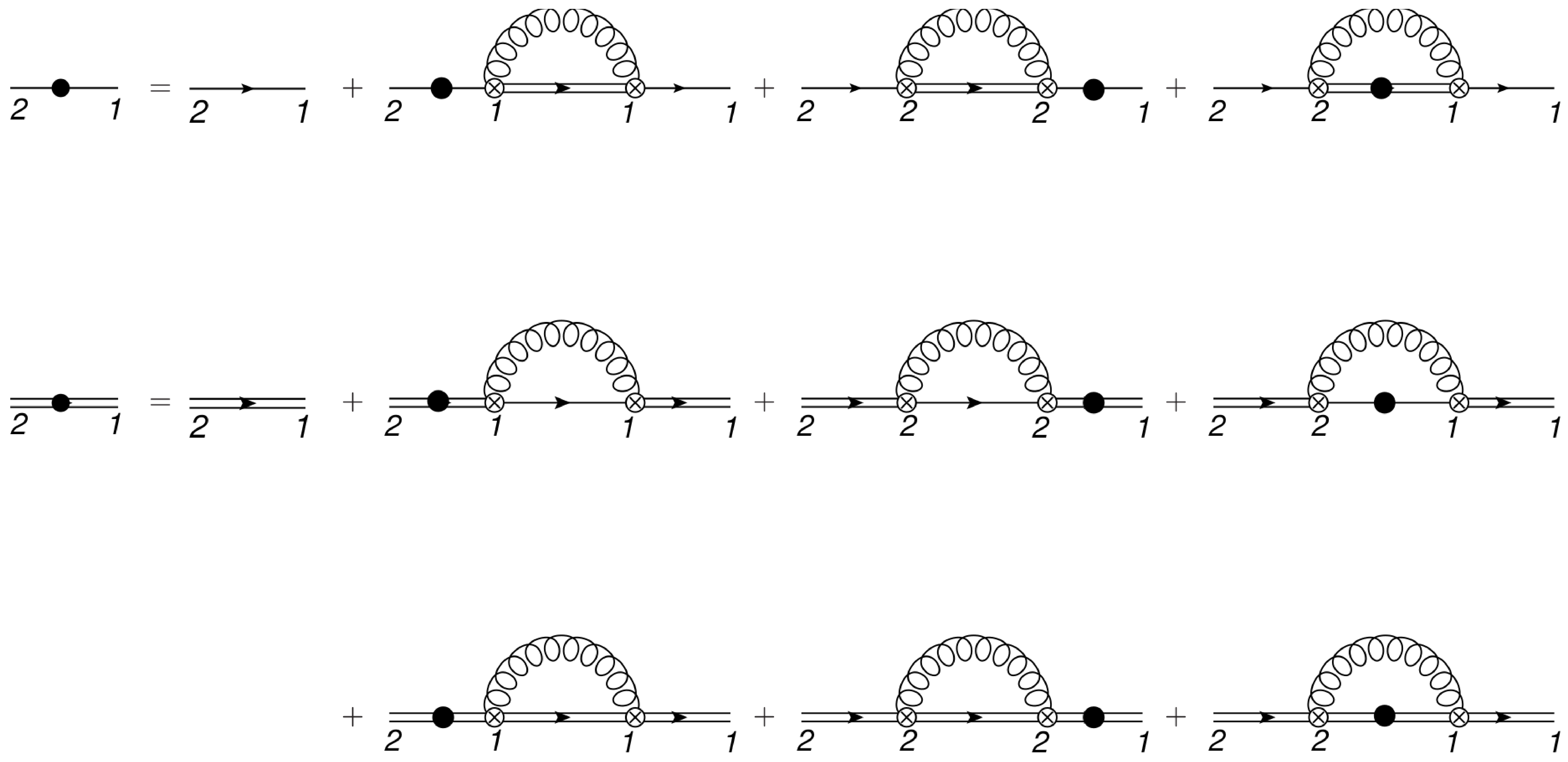

Singlet and octet density matrix evolution equations

... and differentiating over time we obtain the coupled evolution equations:

$$\frac{d\rho_s(t;t)}{dt} = -i[h_s, \rho_s(t;t)] - \Sigma_s(t)\rho_s(t;t) - \rho_s(t;t)\Sigma_s^\dagger(t) + \Xi_{so}(\rho_o(t;t), t)$$

$$\frac{d\rho_o(t;t)}{dt} = -i[h_o, \rho_o(t;t)] - \Sigma_o(t)\rho_o(t;t) - \rho_o(t;t)\Sigma_o^\dagger(t) + \Xi_{os}(\rho_s(t;t), t) + \Xi_{oo}(\rho_o(t;t), t)$$

The evolution equations are Markovian.

Singlet and octet density matrix evolution equations

... and differentiating over time we obtain the coupled evolution equations:

$$
\begin{aligned}
\frac{d\rho_s(t;t)}{dt} &= -i[h_s, \rho_s(t;t)] - \Sigma_s(t)\rho_s(t;t) - \rho_s(t;t)\Sigma_s^\dagger(t) + \Xi_{so}(\rho_o(t;t), t) \\
\frac{d\rho_o(t;t)}{dt} &= -i[h_o, \rho_o(t;t)] - \Sigma_o(t)\rho_o(t;t) - \rho_o(t;t)\Sigma_o^\dagger(t) + \Xi_{os}(\rho_s(t;t), t) \\
&\quad +\Xi_{oo}(\rho_o(t;t), t)
\end{aligned}
$$

The evolution equations are Markovian.

Interpretation

- The self energies Σ_s and Σ_o provide the in-medium induced mass shifts, $\delta m_{s,o}$, and widths, $\Gamma_{s,o}$, for the color-singlet and color-octet heavy quark-antiquark systems respectively:

$$
\begin{aligned}
-i\Sigma_{s,o}(t) + i\Sigma^\dagger_{s,o}(t) &= 2\,\mathrm{Re}\left(-i\Sigma_{s,o}(t)\right) = 2\delta m_{s,o}(t) \\
\Sigma_{s,o}(t) + \Sigma^\dagger_{s,o}(t) &= -2\,\mathrm{Im}\left(-i\Sigma_{s,o}(t)\right) = \Gamma_{s,o}(t)
\end{aligned}
$$

- Ξ_{so} accounts for the production of singlets through the decay of octets, and Ξ_{os} and Ξ_{oo} account for the production of octets through the decays of singlets and octets respectively. There are two octet production mechanisms/octet chromoelectric dipole vertices in the pNRQCD Lagrangian.

Singlet and octet density matrix evolution equations

... and differentiating over time we obtain the coupled evolution equations:

The conservation of the trace of the sum of the densities, i.e., the conservation of the number of heavy quarks, follows from

$$
\begin{aligned}
\mathrm{Tr}\left\{\rho_s(t;t)\left(\Sigma_s(t)+\Sigma_s^\dagger(t)\right)\right\} &= \mathrm{Tr}\left\{\Xi_{os}(\rho_s(t;t),t)\right\} \\
\mathrm{Tr}\left\{\rho_o(t;t)\left(\Sigma_o(t)+\Sigma_o^\dagger(t)\right)\right\} &= \mathrm{Tr}\left\{\Xi_{so}(\rho_o(t;t),t)+\Xi_{oo}(\rho_o(t;t),t)\right\}
\end{aligned}
$$

s are Markovian.

Interpretation

- The self energies Σ_s and Σ_o provide the in-medium induced mass shifts, $\delta m_{s,o}$, and widths, $\Gamma_{s,o}$, for the color-singlet and color-octet heavy quark-antiquark systems respectively:

$$
\begin{aligned}
-i\Sigma_{s,o}(t)+i\Sigma^\dagger_{s,o}(t) &= 2\,\mathrm{Re}\left(-i\Sigma_{s,o}(t)\right)=2\delta m_{s,o}(t) \\
\Sigma_{s,o}(t)+\Sigma^\dagger_{s,o}(t) &= -2\,\mathrm{Im}\left(-i\Sigma_{s,o}(t)\right)=\Gamma_{s,o}(t)
\end{aligned}
$$

- Ξ_{so} accounts for the production of singlets through the decay of octets, and Ξ_{os} and Ξ_{oo} account for the production of octets through the decays of singlets and octets respectively. There are two octet production mechanisms/octet chromoelectric dipole vertices in the pNRQCD Lagrangian.

Time scales

Environment correlation time: $\tau_E \sim \dfrac{1}{T}$

System intrinsic time scale: $\tau_S \sim \dfrac{1}{E}$

a_0=r

System relaxation time: $\tau_R \sim \dfrac{1}{\text{self-energy}} \sim \dfrac{1}{\alpha_s a_0^2 \Lambda^3}$

$a_0 =$ Bohr radius, $\Lambda = T, E$

- Because we have assumed $1/a_0 \gg \Lambda$, it follows $\tau_R \gg \tau_S, \tau_E$ which, after resummation, qualifies the system as Markovian.
  - Akamatsu PRD 91 (2015) 056002
- If $T \gg E$ then $\tau_S \gg \tau_E$ which qualifies the motion of the system as quantum Brownian.

Time scales

Environment correlation time: $\tau_E \sim \dfrac{1}{T}$

System intrinsic time scale: $\tau_S \sim \dfrac{1}{E}$

a_0=r

System relaxation time: $\tau_R \sim \dfrac{1}{\text{self-energy}} \sim \dfrac{1}{\alpha_s a_0^2 \Lambda^3}$ $\quad a_0 =$ Bohr radius, $\Lambda = T, E$

- Because we have assumed $1/a_0 \gg \Lambda$, it follows $\tau_R \gg \tau_S, \tau_E$ which, after resummation, qualifies the system as Markovian.
- If $T \gg E$ then $\tau_S \gg \tau_E$ which qualifies the motion of the system as quantum Brownian.

○ Akamatsu PRD 91 (2015) 056002

From the evolution equations to the Linblad equations

Under the Markovian

$$\tau_R \gg \tau_S, \tau_E \quad \text{or} \quad \frac{1}{a_0} \gg E, T$$

and quantum Brownian motion condition

$$\tau_S \gg \tau_E \quad \text{or} \quad T \gg E$$

at least at LO in E/T the evolution equations can be written in the Lindblad form.

nonequilibrium evolution of quarkonium: Linblad equations

If $E \ll T \sim m_D$ the Lindblad equation for a strongly coupled plasma reads

$$\rho = \begin{pmatrix} \rho_s & 0 \\ 0 & \rho_o \end{pmatrix}$$

$$\frac{d\rho}{dt} = -i[H, \rho] + \sum_i \left(C_i \rho C_i^\dagger - \frac{1}{2}\{C_i^\dagger C_i, \rho\} \right)$$

C collapse operators

$$H = \begin{pmatrix} h_s & 0 \\ 0 & h_o \end{pmatrix} + \frac{r^2}{2}\gamma(t) \begin{pmatrix} 1 & 0 \\ 0 & \frac{7}{16} \end{pmatrix},$$

$$C_i^0 = \sqrt{\frac{\kappa(t)}{8}}\, r^i \begin{pmatrix} 0 & 1 \\ \sqrt{8} & 0 \end{pmatrix}, \qquad C_i^1 = \sqrt{\frac{5\kappa(t)}{16}}\, r^i \begin{pmatrix} 0 & 0 \\ 0 & 1 \end{pmatrix}$$

nonequilibrium evolution of quarkonium: Linblad equations

If $E \ll T \sim m_D$ the Lindblad equation for a strongly coupled plasma reads

$$\rho = \begin{pmatrix} \rho_s & 0 \\ 0 & \rho_o \end{pmatrix}$$

$$\frac{d\rho}{dt} = -i[H,\rho] + \sum_i \left(C_i \rho C_i^\dagger - \frac{1}{2}\{C_i^\dagger C_i, \rho\}\right)$$

C collapse operators

$$H = \begin{pmatrix} h_s & 0 \\ 0 & h_o \end{pmatrix} + \frac{r^2}{2}\gamma(t)\begin{pmatrix} 1 & 0 \\ 0 & \frac{7}{16} \end{pmatrix},$$

$$C_i^0 = \sqrt{\frac{\kappa(t)}{8}}\, r^i \begin{pmatrix} 0 & 1 \\ \sqrt{8} & 0 \end{pmatrix}, \qquad C_i^1 = \sqrt{\frac{5\kappa(t)}{16}}\, r^i \begin{pmatrix} 0 & 0 \\ 0 & 1 \end{pmatrix}$$

the sQGP is characterised by two nonperturbative parameters (transport coefficients) kappa and gamma that must be calculated on the lattice

κ is the heavy-quark momentum diffusion coefficient:

$$\kappa = \frac{g^2}{18}\,\mathrm{Re}\int_{-\infty}^{+\infty} ds\, \langle \mathrm{T}\, E^{a,i}(s,\mathbf{0})\, \phi^{ab}(s,0)\, E^{b,i}(0,\mathbf{0})\rangle$$

$$\gamma = \frac{g^2}{18}\,\mathrm{Im}\int_{-\infty}^{+\infty} ds\, \langle \mathrm{T}\, E^{a,i}(s,\mathbf{0})\, \phi^{ab}(s,0)\, E^{b,i}(0,\mathbf{0})\rangle$$

nonequilibrium evolution of quarkonium: Linblad equations

If $E \ll T \sim m_D$ the Lindblad equation for a strongly coupled plasma reads

$$\rho = \begin{pmatrix} \rho_s & 0 \\ 0 & \rho_o \end{pmatrix}$$

$$\frac{d\rho}{dt} = -i[H,\rho] + \sum_i \left(C_i \rho C_i^\dagger - \frac{1}{2}\{C_i^\dagger C_i, \rho\}\right)$$

C collapse operators

$$H = \begin{pmatrix} h_s & 0 \\ 0 & h_o \end{pmatrix} + \frac{r^2}{2}\gamma(t)\begin{pmatrix} 1 & 0 \\ 0 & \frac{7}{16} \end{pmatrix},$$

$$C_i^0 = \sqrt{\frac{\kappa(t)}{8}}\, r^i \begin{pmatrix} 0 & 1 \\ \sqrt{8} & 0 \end{pmatrix}, \qquad C_i^1 = \sqrt{\frac{5\kappa(t)}{16}}\, r^i \begin{pmatrix} 0 & 0 \\ 0 & 1 \end{pmatrix}$$

the sQGP is characterised by two nonperturbative parameters (transport coefficients) kappa and gamma that must be calculated on the lattice

κ is the heavy-quark momentum diffusion coefficient:

$$\kappa = \frac{g^2}{18}\,\mathrm{Re}\int_{-\infty}^{+\infty} ds\, \langle \mathrm{T}\, E^{a,i}(s,\mathbf{0})\, \phi^{ab}(s,0)\, E^{b,i}(0,\mathbf{0})\rangle$$

$$\gamma = \frac{g^2}{18}\,\mathrm{Im}\int_{-\infty}^{+\infty} ds\, \langle \mathrm{T}\, E^{a,i}(s,\mathbf{0})\, \phi^{ab}(s,0)\, E^{b,i}(0,\mathbf{0})\rangle$$

the EFT allows to use lattice QCD equilibrium calculation to study the non equilibrium evolution! EFT is intermediate layer to non equilibrium

Our evolution equations depend
on two transport coefficients kappa and gamma that inside
pNRQCD acquire a field theoretical definition
as gauge invariant correlators of chromoelectric fields

Our evolution equations depend
on two transport coefficients kappa and gamma that inside
pNRQCD acquire a field theoretical definition
as gauge invariant correlators of chromoelectric fields

How to calculate these nonperturbative
transport coefficients?

use lattice QCD

The heavy quark diffusion coefficient

D in real space, related to κ in momentum space

Langevin dynamics of the heavy quark in the med

$$\frac{dp_i}{dt} = -\eta_D p_i + \xi_i(t)$$

$$\langle \xi(t)\xi(t') \rangle = \kappa\delta(t - t')$$

$$< x^2(t) >= 6Dt$$

$$\eta_D = \frac{\kappa}{2MT}$$

$$D = \frac{2T^2}{\kappa}$$

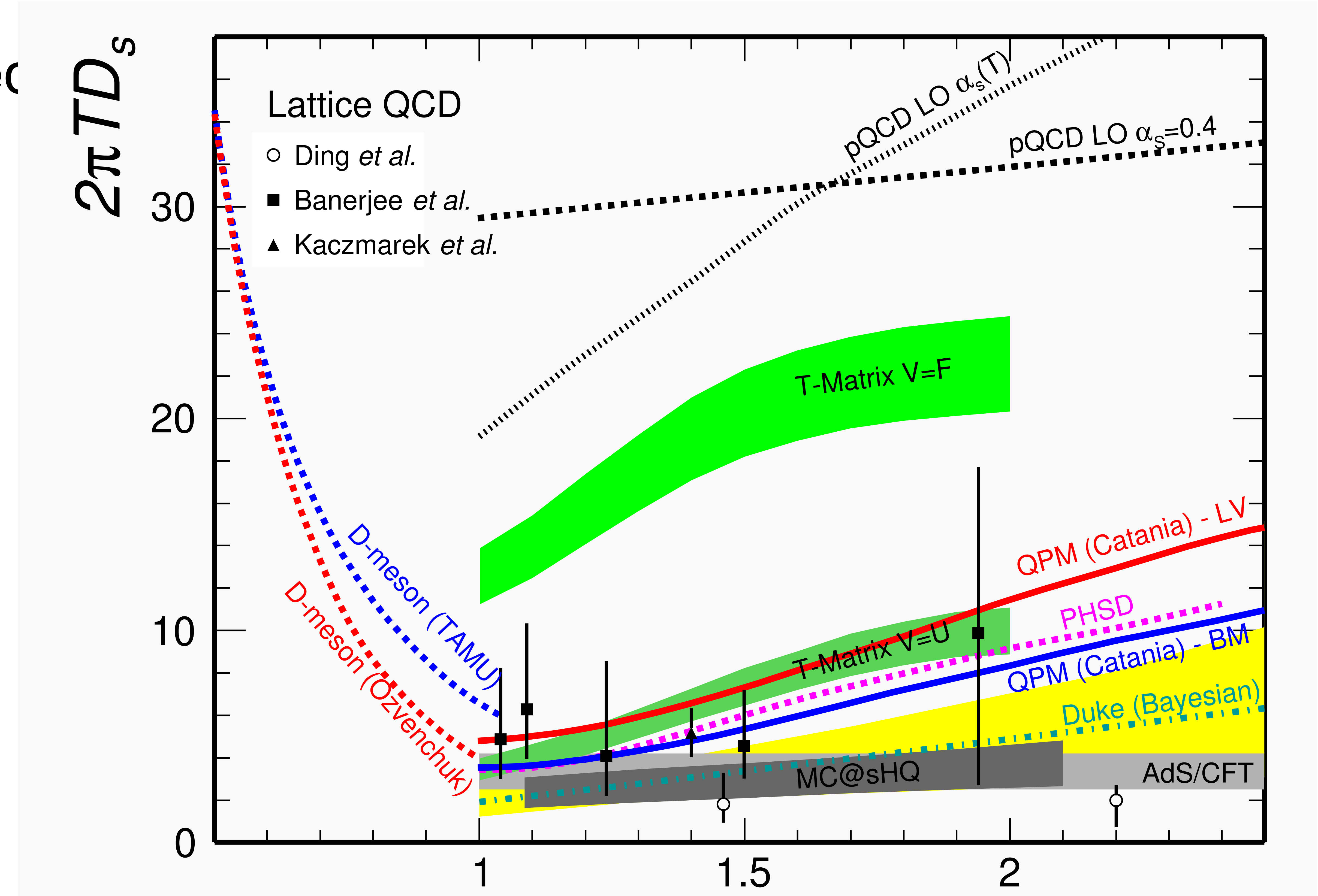

Figure from: X. Dong CIPANP (2018)

$\frac{T}{T_c}$

The heavy quark diffusion coefficient

D in real space, related to κ in momentum space

Langevin dynamics of the heavy quark in the mec

$$\frac{dp_i}{dt} = -\eta_D p_i + \xi_i(t)$$

$$\langle \xi(t)\xi(t') \rangle = \kappa\delta(t-t')$$

$$\eta_D = \frac{\kappa}{2MT}$$

$$< x^2(t) >= 6Dt \qquad D = \frac{2T^2}{\kappa}$$

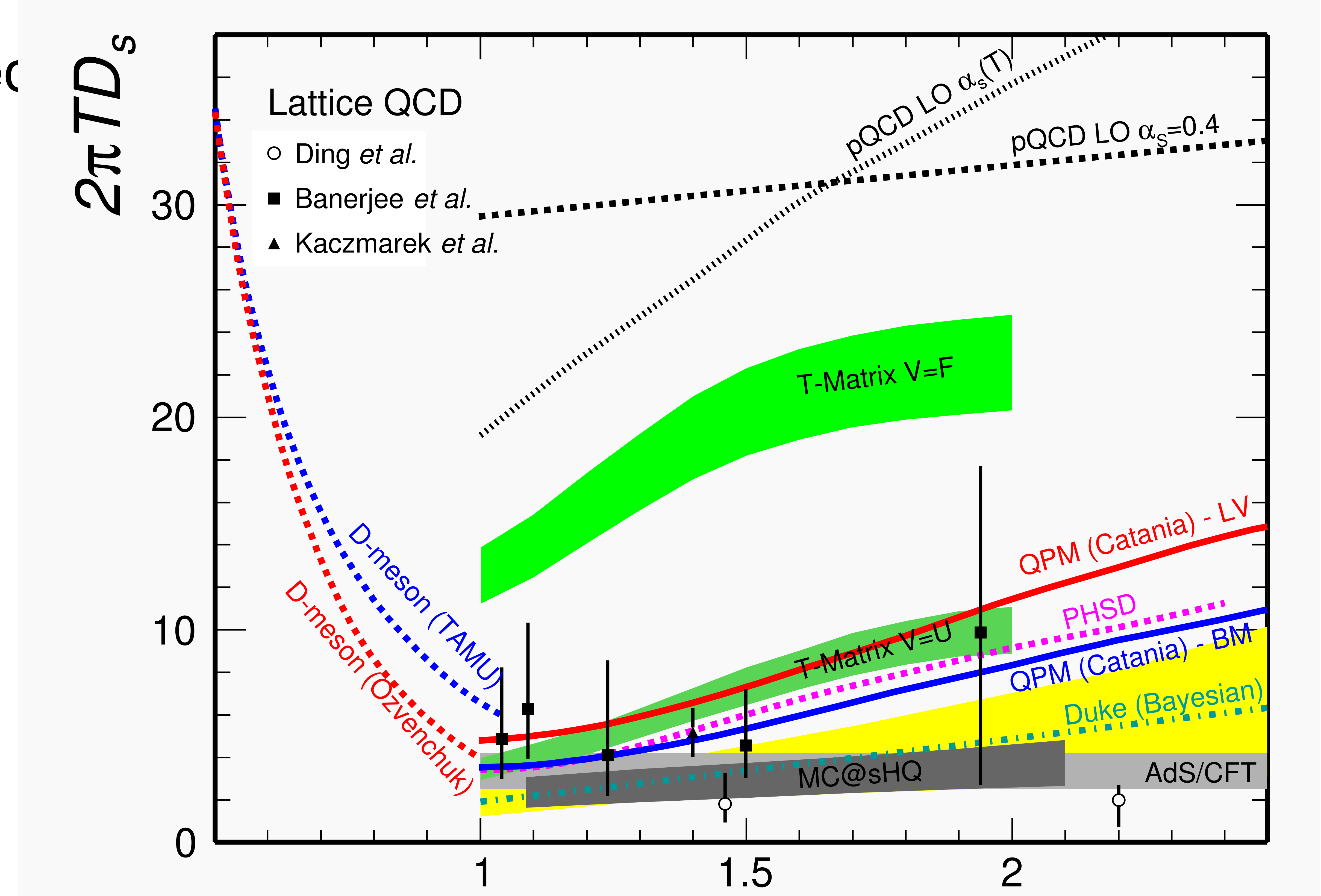

X. Dong CIPANP (2018)

in the limit in which the mass M of the heavy quark is the biggest scale one can integrate it out non relativistic effective field theory and from the current current correlator obtain

$$\kappa = \frac{g^2}{18}\,\mathrm{Re}\int_{-\infty}^{+\infty} ds\,\langle\,\mathrm{T}\,E^{a,i}(s,\mathbf{0})\,\phi^{ab}(s,0)\,E^{b,i}(0,\mathbf{0})\rangle$$

which is the same transport coefficient kappa that we found studying the non equilibrium evolution of quarkonium in the QGP!

1903.08063

this object was already studied on quenched lattice

Meyer NJP13 (2011),

Ding *et.al.*JPG38 (2011),

Banarjee *et.al.* PRD85 (2012),

Francis *et.al.* PRD92 (2015)

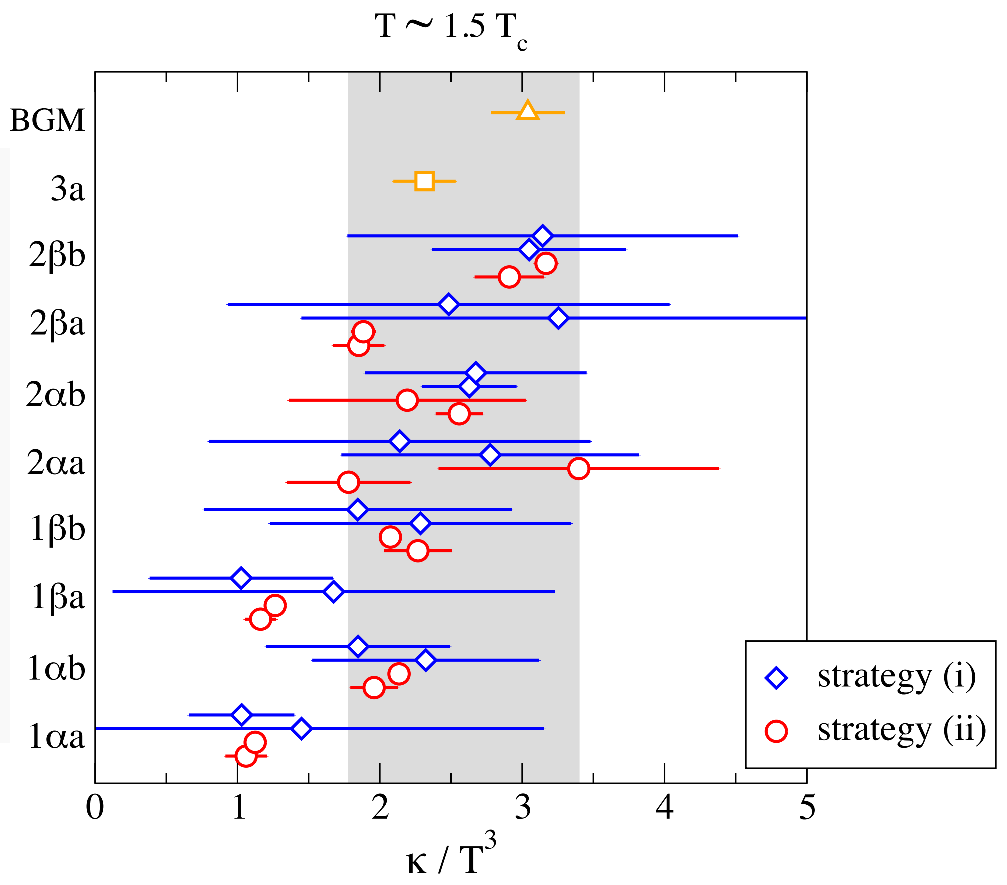

this object was already studied on quenched lattice

Meyer NJP13 (2011),

Ding *et.al.* JPG38 (2011),

Banarjee *et.al.* PRD85 (2012),

Francis *et.al.* PRD92 (2015)

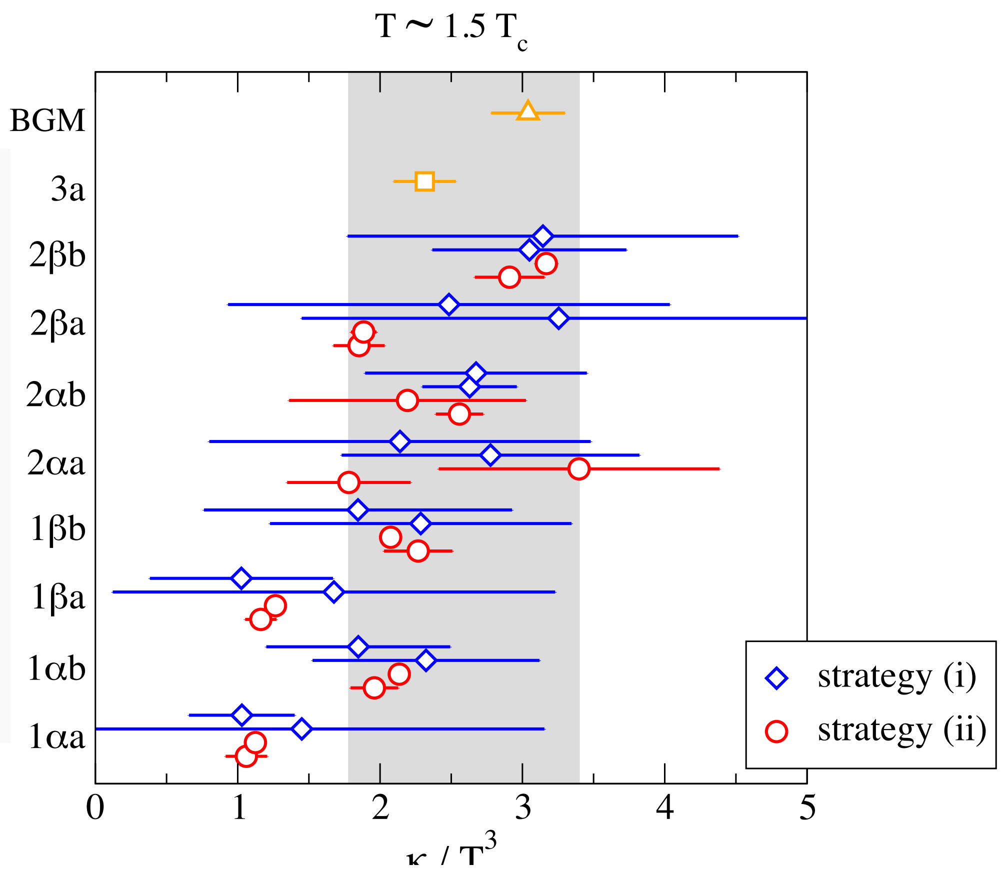

in TUMQCD we studied kappa on quenched latticed with the multilevel algorithm

in a window of T never attempted before

-> we get the T dependence of kappa

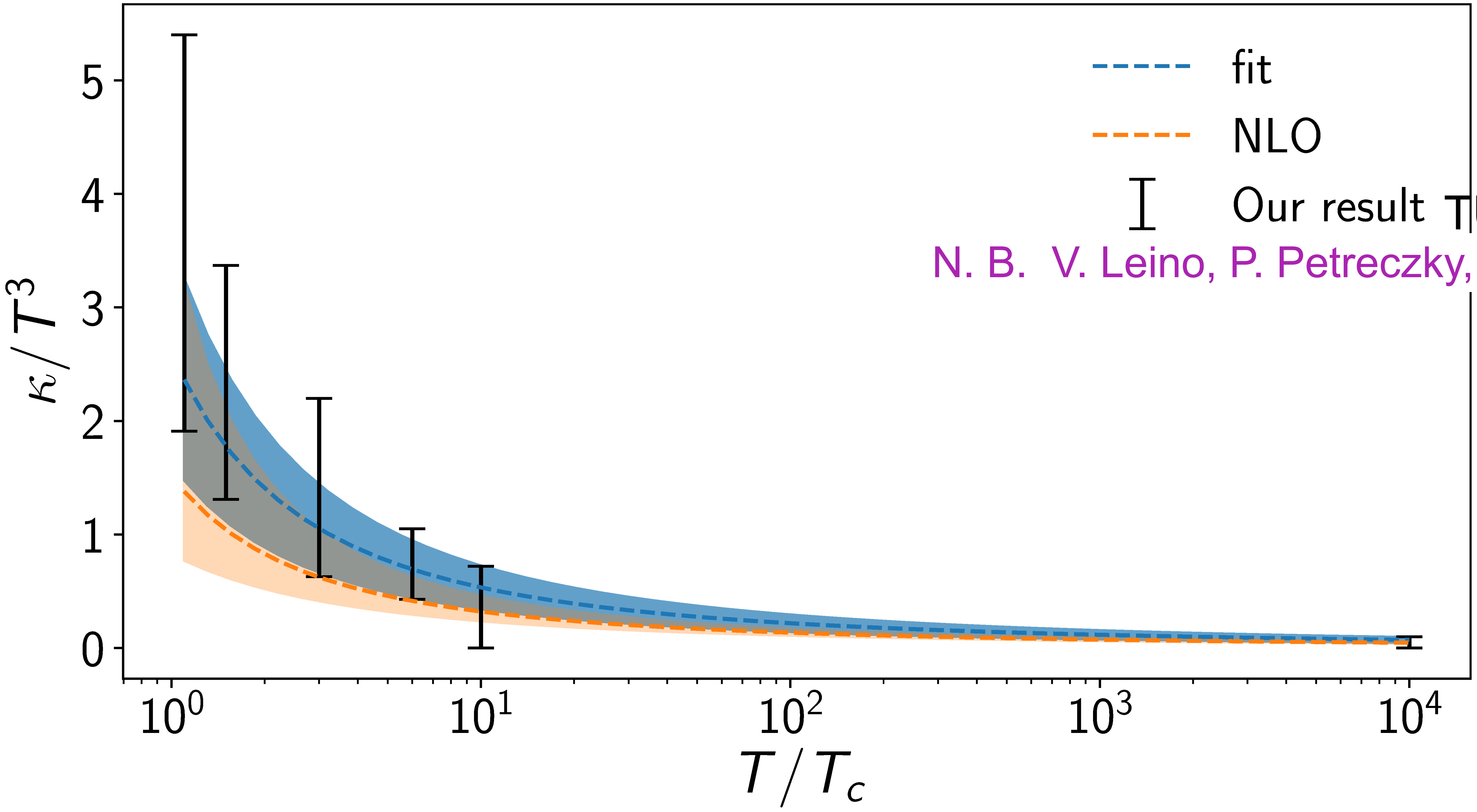

TUMQCD

N. B. V. Leino, P. Petreczky, A. Vairo 2020

$$1.91 < \frac{\kappa}{T^3} < 5.4 \text{ for } T = 1.1\, T_c\,,$$

$$1.31 < \frac{\kappa}{T^3} < 3.64 \text{ for } T = 1.5\, T_c\,,$$

$$0.63 < \frac{\kappa}{T^3} < 2.20 \text{ for } T = 3\, T_c\,,$$

$$0.43 < \frac{\kappa}{T^3} < 1.05 \text{ for } T = 6\, T_c\,,$$

$$0 < \frac{\kappa}{T^3} < 0.72 \text{ for } T = 10\, T_c\,,$$

$$0 < \frac{\kappa}{T^3} < 0.10 \text{ for } T = 10^4\, T_c\,,$$

within the errors the lattice results are compatible with the next-to-leading order perturbative results this object was already studied on quenched lattice

Meyer NJP13 (2011),

Ding *et.al.*JPG38 (2011),

Banarjee *et.al.* PRD85 (2012),

Francis *et.al.* PRD92 (2015)

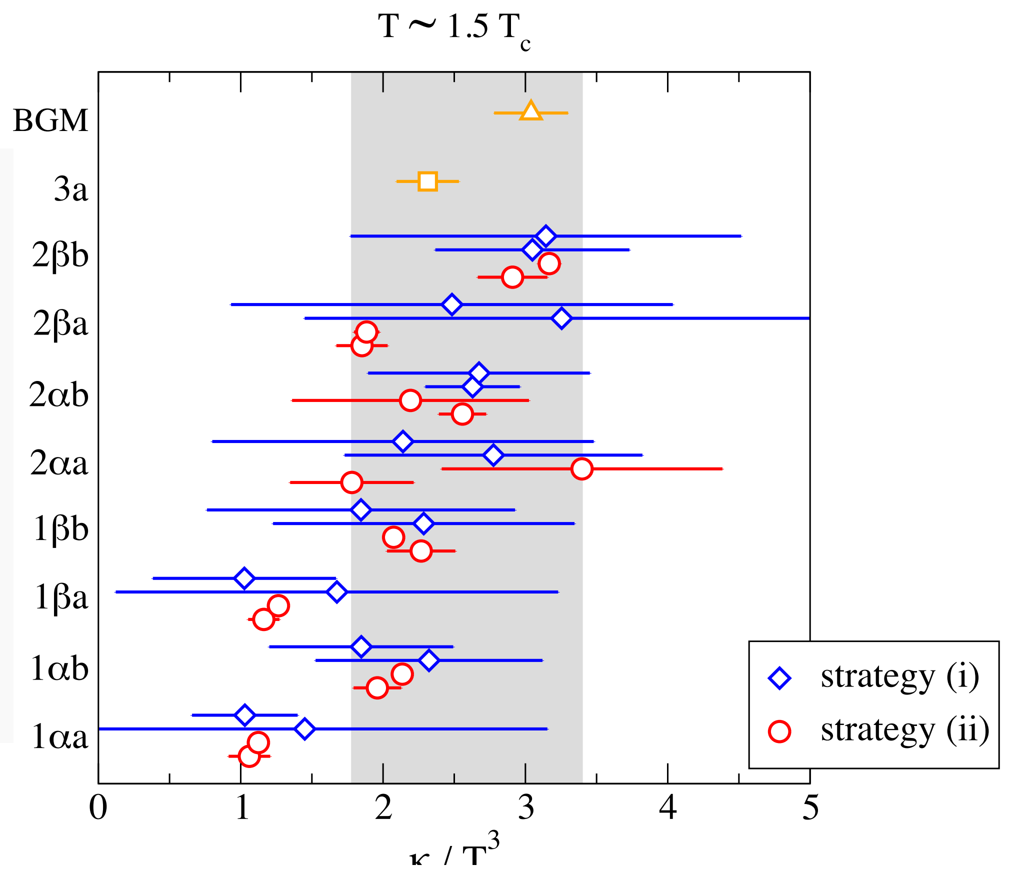

in TUMQCD we studied kappa on quenched latticed with the multilevel algorithm

in a window of T never attempted before

-> we get the T dependence of kappa

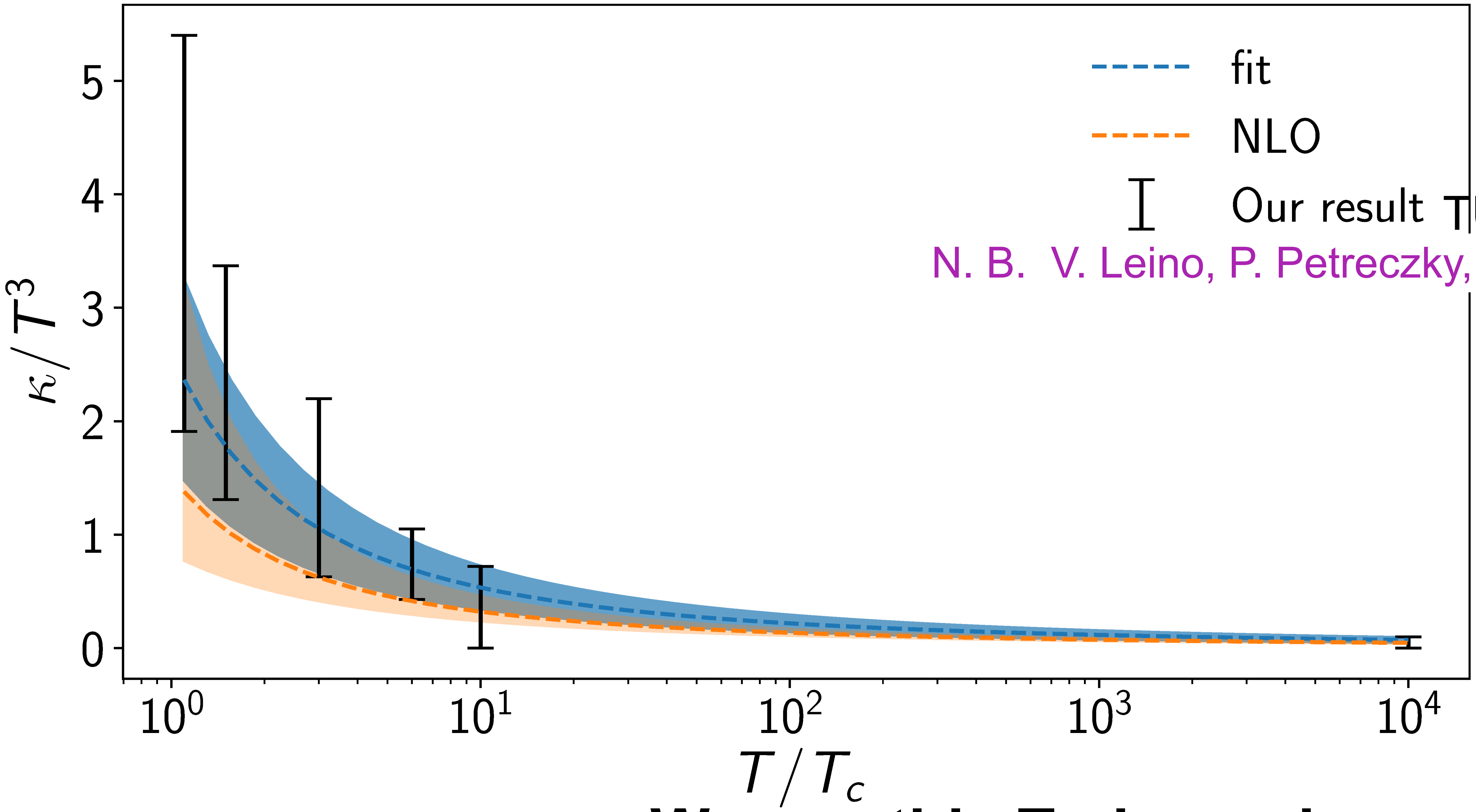

TUMQCD

N. B. V. Leino, P. Petreczky, A. Vairo 2020

$$1.91 < \frac{\kappa}{T^3} < 5.4 \text{ for } T = 1.1\, T_c\,,$$

$$1.31 < \frac{\kappa}{T^3} < 3.64 \text{ for } T = 1.5\, T_c\,,$$

$$0.63 < \frac{\kappa}{T^3} < 2.20 \text{ for } T = 3\, T_c\,,$$

$$0.43 < \frac{\kappa}{T^3} < 1.05 \text{ for } T = 6\, T_c\,,$$

$$0 < \frac{\kappa}{T^3} < 0.72 \text{ for } T = 10\, T_c\,,$$

$$0 < \frac{\kappa}{T^3} < 0.10 \text{ for } T = 10^4\, T_c\,,$$

We use this T dependence of kappa in our Linblad equation

within the errors the lattice results are compatible with the next-to-leading order perturbative results

Use the EFT to relate kappa (and gamma) to observables: quarkonium thermal mass shift and thermal widths

N.B., M. Escobedo, A. Vairo, P. vander Griend Phys.Rev. D100 (2019) no.5, 054025

kappa is related to the thermal decay width of quarkonium

in the hierarchy $\frac{1}{r} \gg T \gg E$ pNRQCD predicts for 1S states

$$\boxed{\Gamma(1S) = -2\langle \mathrm{Im}\,(-i\Sigma_s)\rangle} = 3 < r^2 > \quad \kappa$$

Use the EFT to relate kappa (and gamma) to observables: quarkonium thermal mass shift and thermal widths

N.B., M. Escobedo, A. Vairo, P. vander Griend Phys.Rev. D100 (2019) no.5, 054025

kappa is related to the thermal decay width of quarkonium

in the hierarchy $\frac{1}{r} \gg T \gg E$ pNRQCD predicts for 1S states

$$\boxed{\Gamma(1S) = -2\langle \mathrm{Im}\,(-i\Sigma_s)\rangle} = 3 < r^2 > \kappa$$

gamma is related to the thermal mass shift of quarkonium pNRQCD predicts for 1S states

$$\boxed{\delta M(1S) = \langle \mathrm{Re}\,(-i\Sigma_s)\rangle} = \frac{3}{2} < r^2 > \gamma$$

Use the EFT to relate kappa (and gamma) to observables: quarkonium thermal mass shift and thermal widths

N.B., M. Escobedo, A. Vairo, P. vander Griend Phys.Rev. D100 (2019) no.5, 054025

kappa is related to the thermal decay width of quarkonium

in the hierarchy $\frac{1}{r} \gg T \gg E$ pNRQCD predicts for 1S states

$$\boxed{\Gamma(1S) = -2\langle \mathrm{Im}\,(-i\Sigma_s)\rangle} = 3 < r^2 > \kappa$$

gamma is related to the thermal mass shift of quarkonium pNRQCD predicts for 1S states

$$\boxed{\delta M(1S) = \langle \mathrm{Re}\,(-i\Sigma_s)\rangle} = \frac{3}{2} < r^2 > \gamma$$

Therefore we can use unquenched lattice data on quarkonium thermal mass shift and widths to get unquenched determination of these transport coefficients

Use lattice data from Aarts, Allton, Kim, Lombardo, Oktay, Ryan, Sinclair and Skullerud (2011) and Kim, Petreczky and Rothkopf (2018). Unquenched.

and the new data from R. Larsen, S. Meinel, S. Mukherjee, P. Petreczy 2019, 2020

Unquenched determinations of kappa and gamma

N.B., M. Escobedo, A. Vairo, P. vander Griend
Phys.Rev. D100 (2019) no.5, 054025

Extraction of kappa from unquenched lattice data for the thermal width of the Y(1S) (black lines) in comparison to a quenched lattice determination (brown) , determinations from the D meson v2 from Alice and Star data (green), model compilation from 1903.07709) (red) and the perturbative calculation (truncated g^5) (blue)

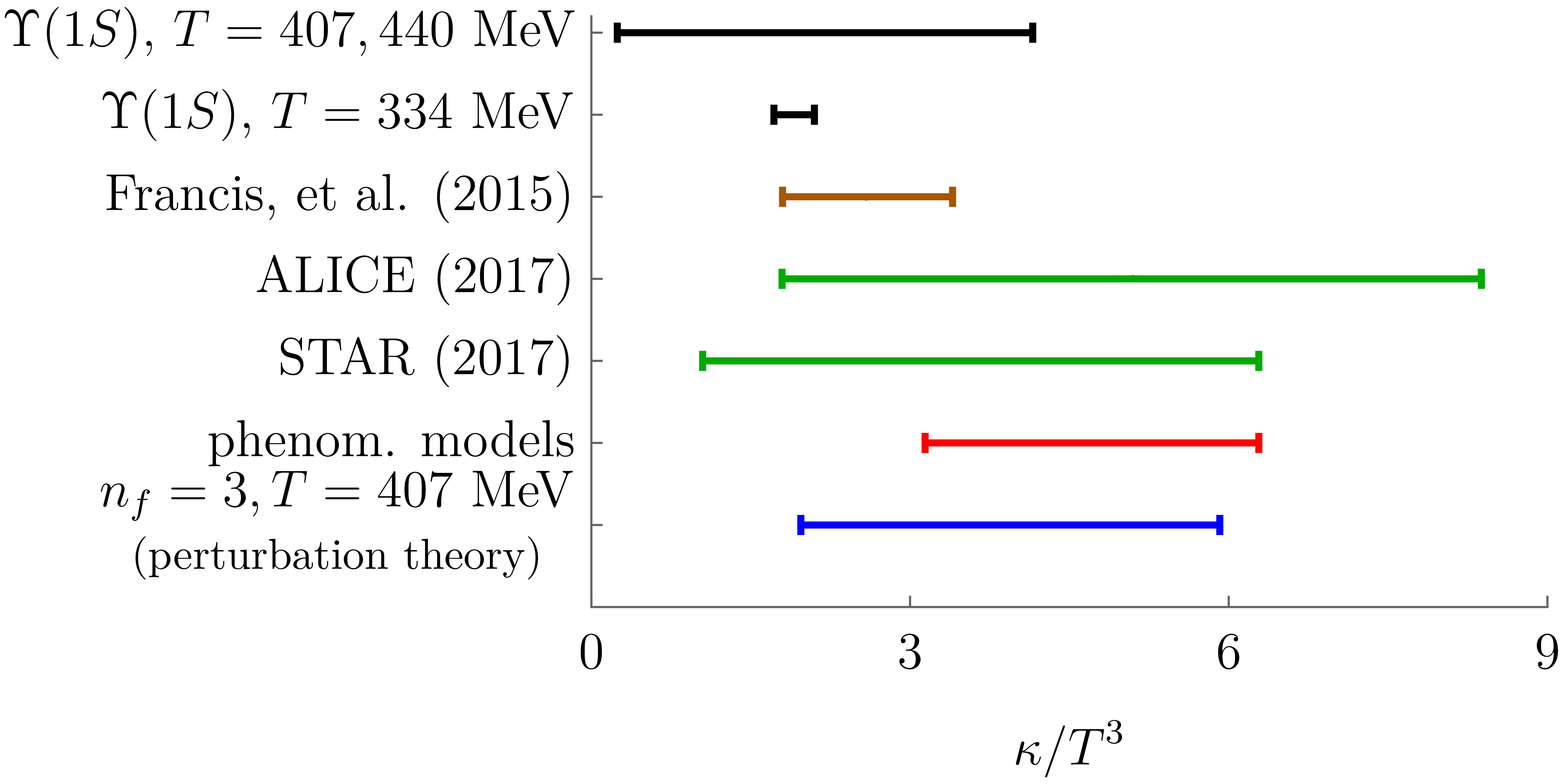

Unquenched determinations of kappa and gamma

N.B., M. Escobedo, A. Vairo, P. vander Griend
Phys.Rev. D100 (2019) no.5, 054025

Extraction of kappa from unquenched lattice data for the thermal width of the Y(1S) (black lines) in comparison to a quenched lattice determination (brown) , determinations from the D meson v2 from Alice and Star data (green), model compilation from 1903.07709) (red) and the perturbative calculation (truncated g^5) (blue)

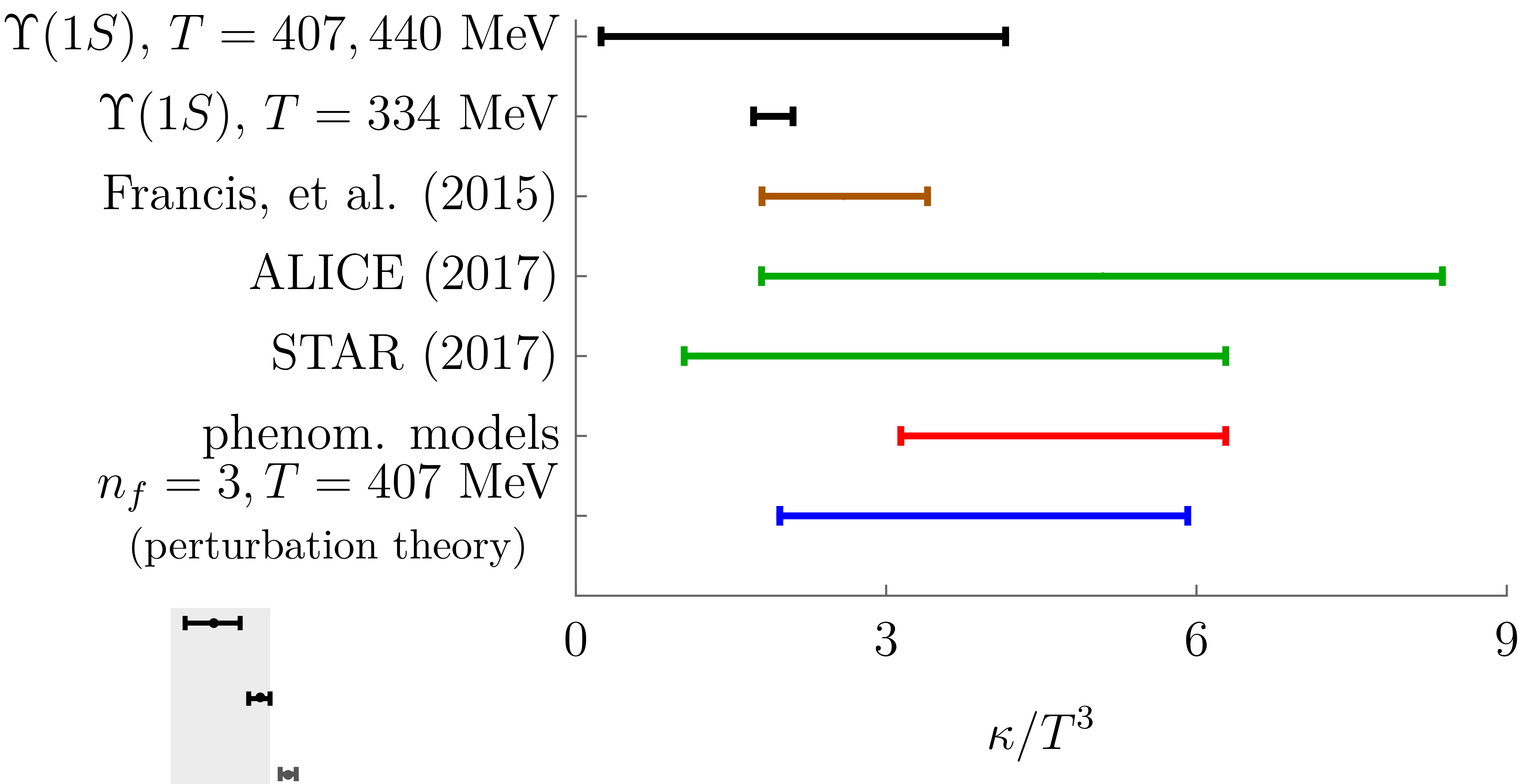

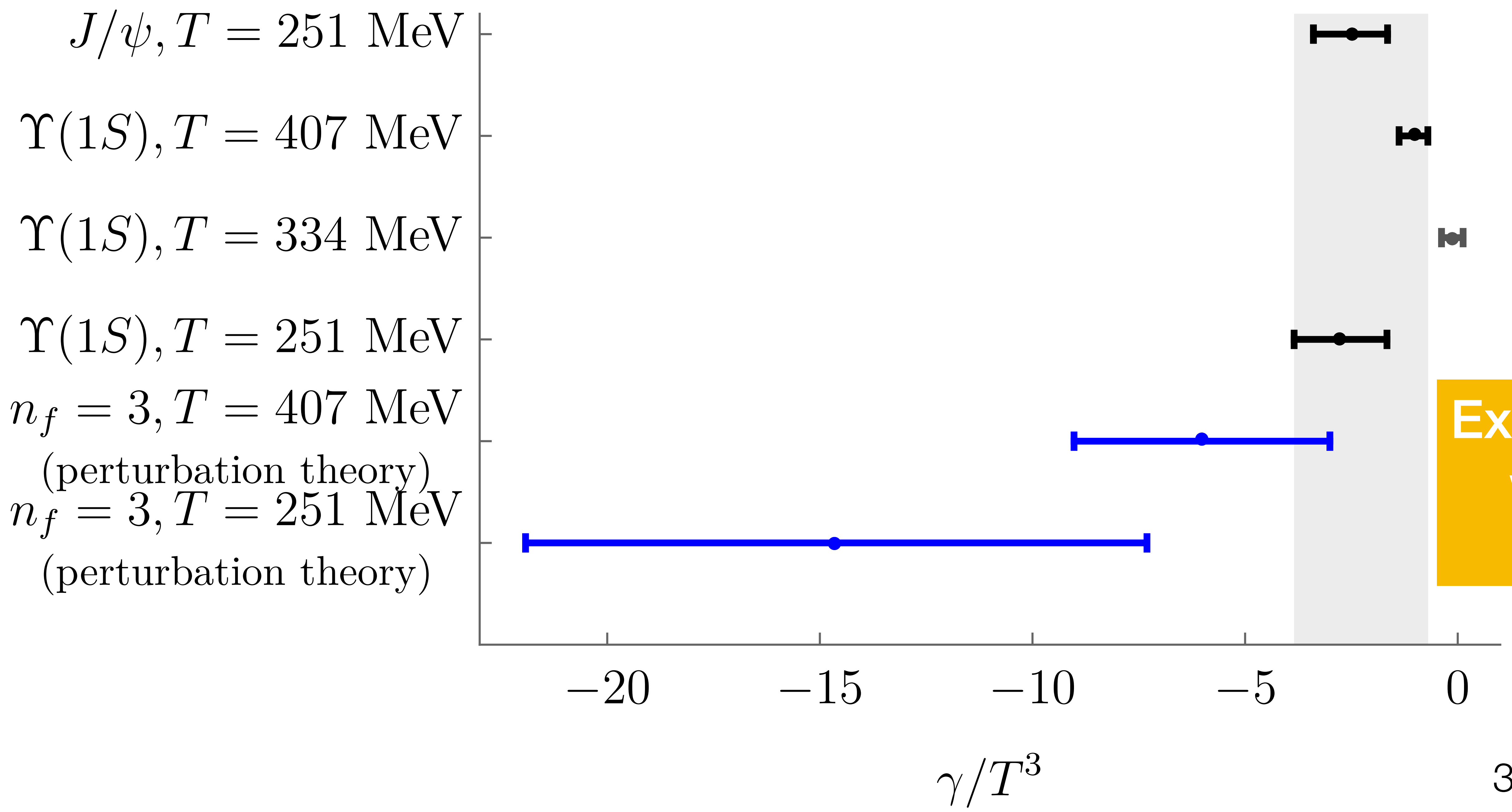

Extraction of gamma from unquenched lattice data for the thermal width of the Y(1S) and J/psi (black lines)n comparison to NLO order perturbation theory at two different T

Solving the Linblad equation

Initial conditions

- The production of singlets is $\alpha_{\rm s}$ suppressed compared to that of octets.
  - Cho Leibovich PRD 53 (1996) 6203

$$\rho_s = N|\mathbf{0}\rangle\langle\mathbf{0}|, \qquad \rho_o = \frac{1}{\alpha_s}\rho_s$$

N is fixed by $\mathrm{Tr}\{\rho_s\} + \mathrm{Tr}\{\rho_o\} = 1$

evolve in QGP from t_0 =0.6 fm up T= 250 MeV

Solving the Linblad equation

a pretty challenging tasks

Initial conditions

- The production of singlets is α_s suppressed compared to that of octets.
  - Cho Leibovich PRD 53 (1996) 6203

$$\rho_s = N|\mathbf{0}\rangle\langle\mathbf{0}|, \qquad \rho_o = \frac{1}{\alpha_s}\rho_s$$

N is fixed by $\mathrm{Tr}\{\rho_s\} + \mathrm{Tr}\{\rho_o\} = 1$

evolve in QGP from t_0 =0.6 fm up T= 250 MeV

initially we used

$$T = T_0 \left(\frac{t_0}{t}\right)^{v_s^2}, \quad t_0 = 0.6\ \mathrm{fm}, \quad v_s^2 = \frac{1}{3} \text{ (sound velocity)}$$

expand the density matrix in spherical harmonics, keep only l=0 and 1 use QuTiP

Brambilla Escobedo Soto Vairo PRD 96 (2017) 034021

Solving the Linblad equation   a pretty challenging tasks

Initial conditions

- The production of singlets is α_s suppressed compared to that of octets.
  - Cho Leibovich PRD 53 (1996) 6203

$$\rho_s = N|\mathbf{0}\rangle\langle\mathbf{0}|, \qquad \rho_o = \frac{1}{\alpha_s}\rho_s$$

N is fixed by $\mathrm{Tr}\{\rho_s\} + \mathrm{Tr}\{\rho_o\} = 1$

evolve in QGP from t_0 =0.6 fm up T= 250 MeV

initially we used

$$T = T_0 \left(\frac{t_0}{t}\right)^{v_s^2}, \quad t_0 = 0.6 \text{ fm}, \quad v_s^2 = \frac{1}{3}$$ (sound velocity)

expand the density matrix in spherical harmonics, keep only l=0 and 1 use QuTiP

Brambilla Escobedo Soto Vairo PRD 96 (2017) 034021

Recently **thanks to the collaboration with Mike Strickland** we developed a much more efficient (embarassingly parallel) program based on the quantum trajectory algorithm (Qtraj) and we coupled this to the hydrodynamical evolution of the QGP using a 3+1D dissipative relativistic hydrodynamics code that makes use of the quasiparticle anisotropic hydrodynamics (aHydroQP) framework. The code uses a realistic equation of state fit to lattice QCD measurements and is tuned to soft hadronic data collected in 5.02 TeV collisions using smooth optical Glauber initial conditions.

N.B. Escobedo , Strickland, Vairo, Vander Griend, Weber, 2012.01240

nonequilibrium evolution of quarkonium in medium: nuclear modification factor R_AA

We compute the nuclear modification factor R_{AA}:

$$R_{AA}(nS) = \frac{\langle n, \mathbf{q} | \rho_s(t_F; t_F) | n, \mathbf{q} \rangle}{\langle n, \mathbf{q} | \rho_s(0; 0) | n, \mathbf{q} \rangle}$$

calculation with no free parameters, results depends on kappa function of T (calculated on the lattice) and gamma (extracted from the lattice)

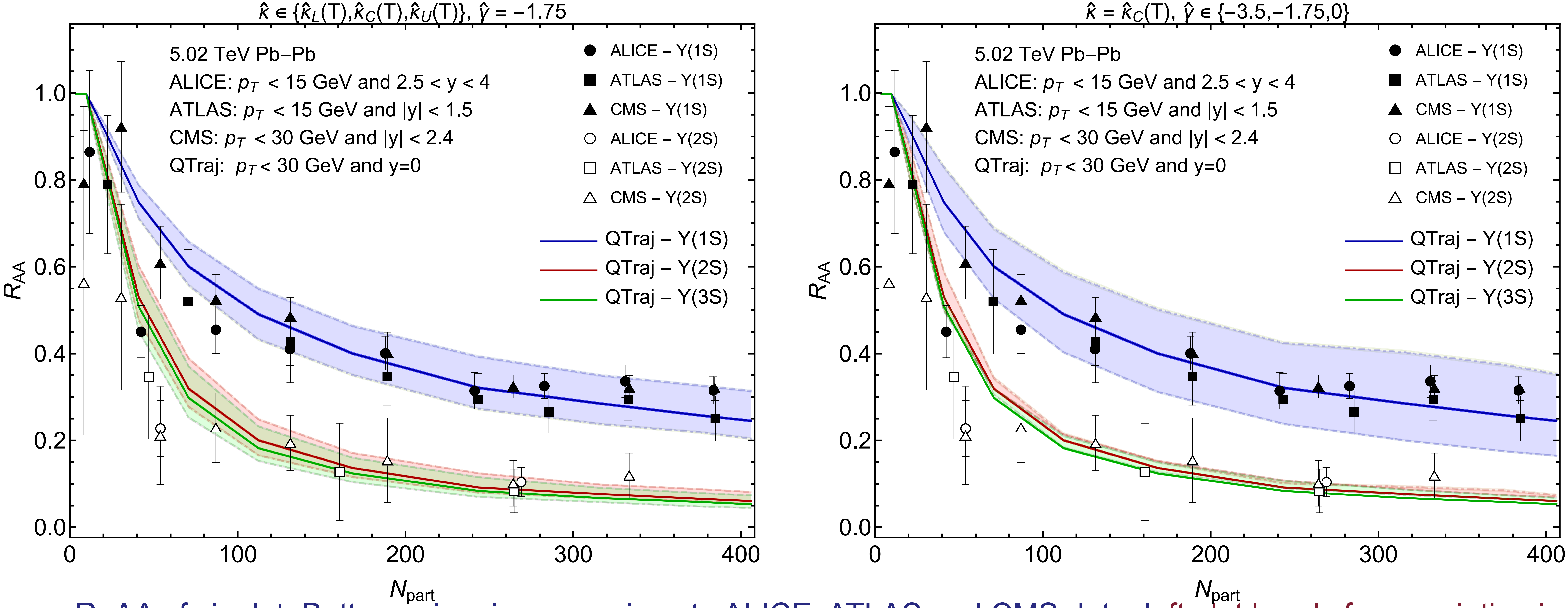

R_AA of singlet Bottomonium in comparison to ALICE, ATLAS and CMS data, left plot bands from variation in kappa, right plot variation in gamma —> we can use R_AA to learn about the QGP!

N.B. Escobedo , Strickland, Vairo, Vander Griend, Weber, 2012.01240

Differential quantities

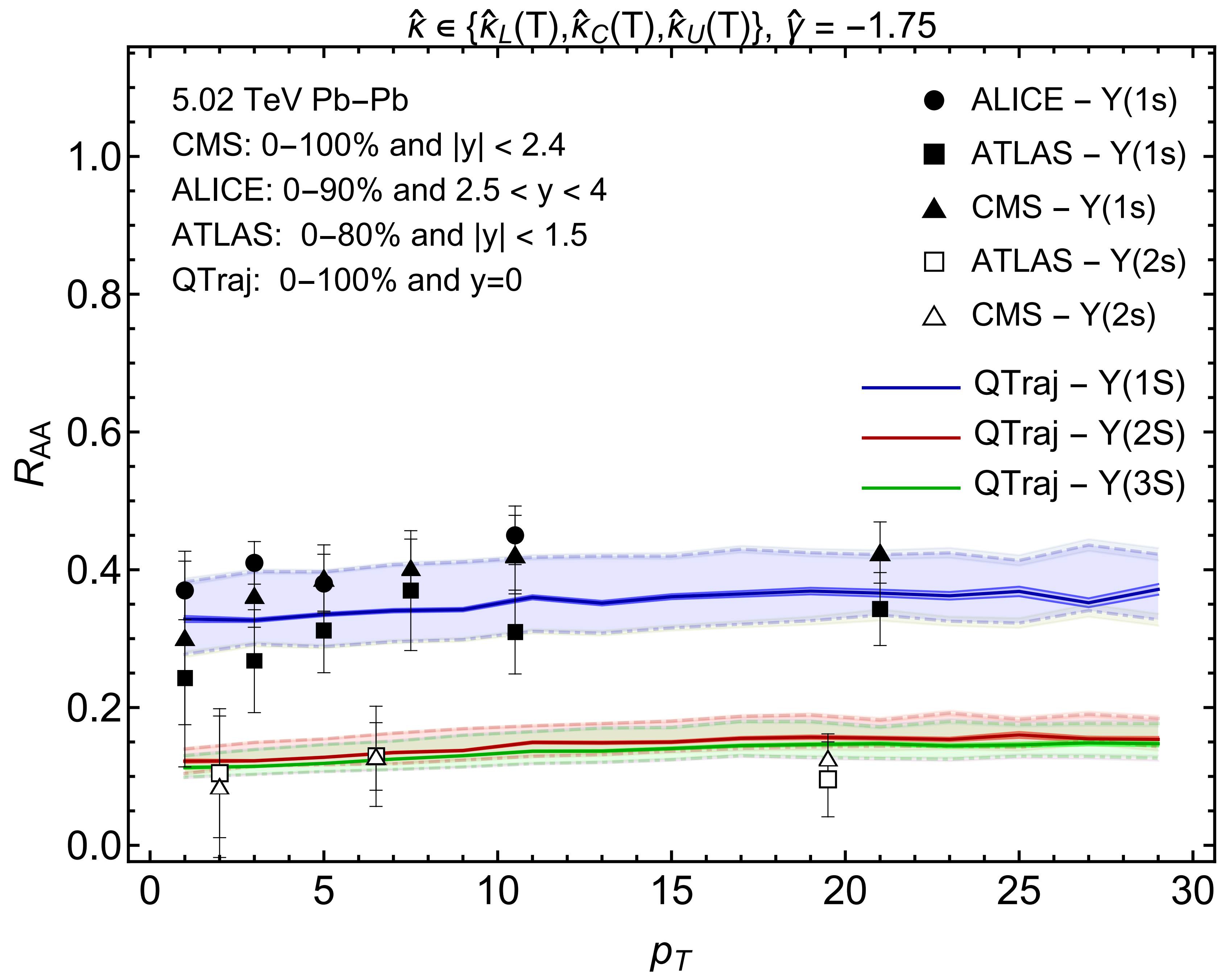

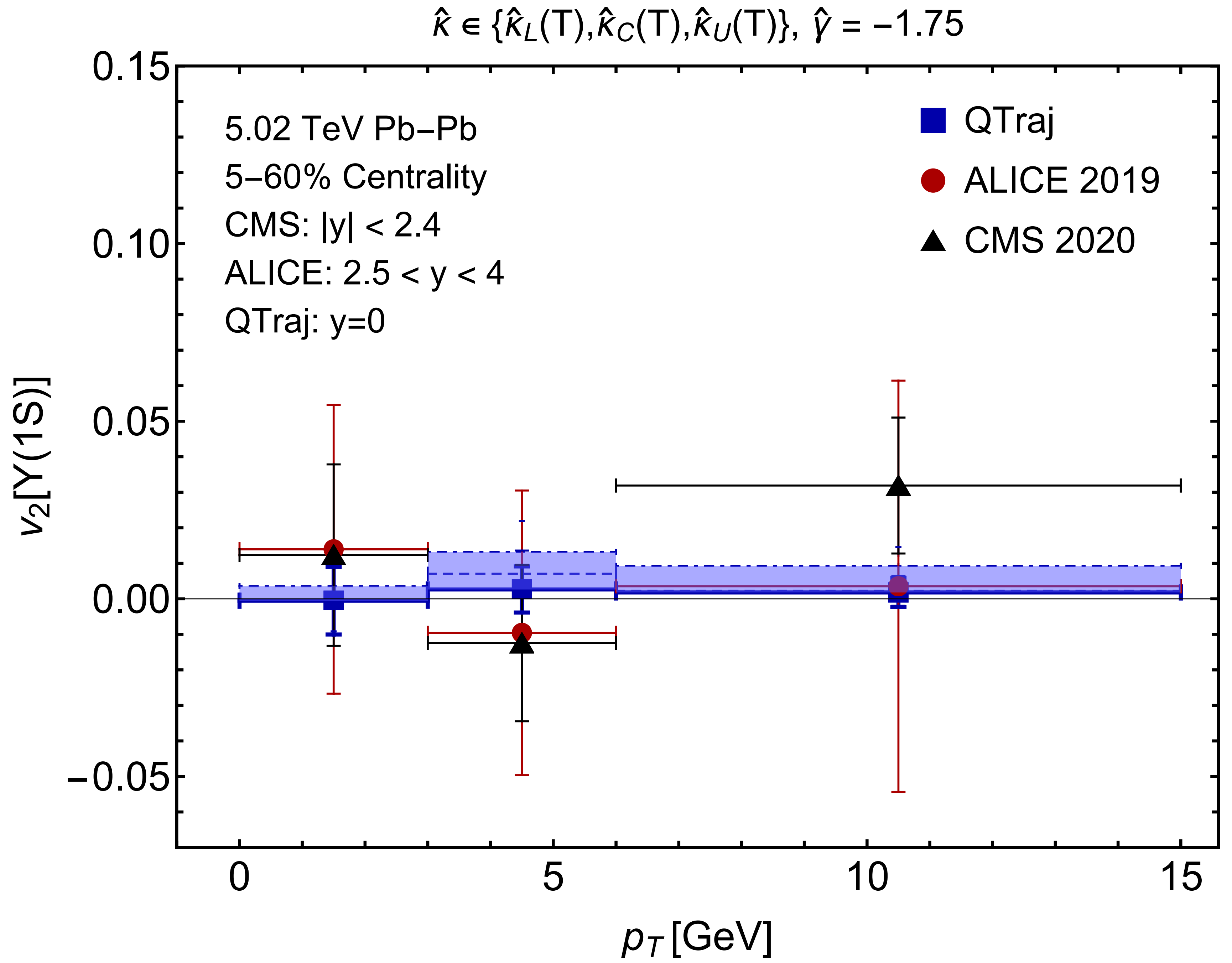

Full diagnostic of the medium in terms of objects with a proper field theoretical definition, evaluated on the lattice

N.B. Escobedo , Strickland, Vairo, Vander Griend, Weber, 2107.06222

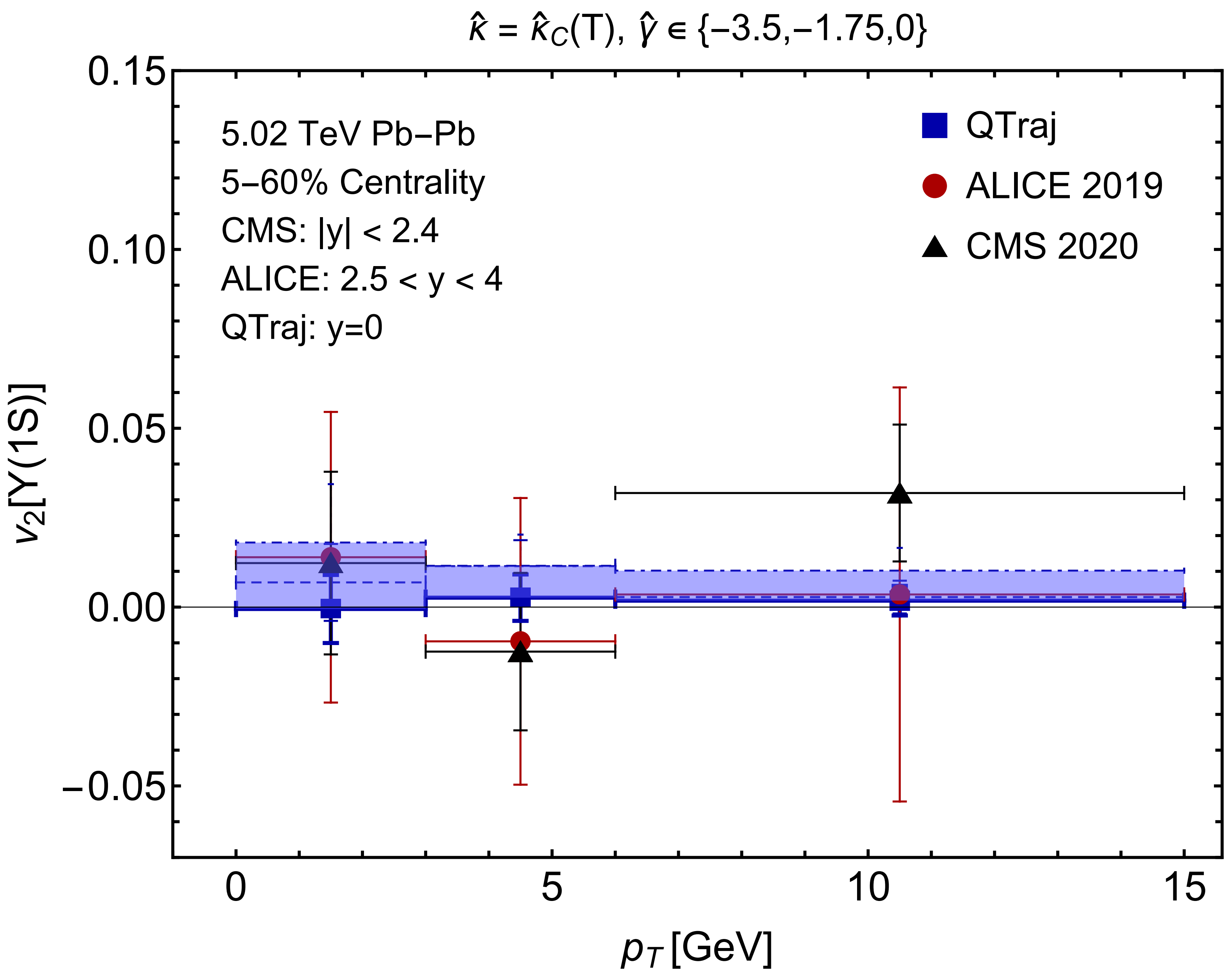

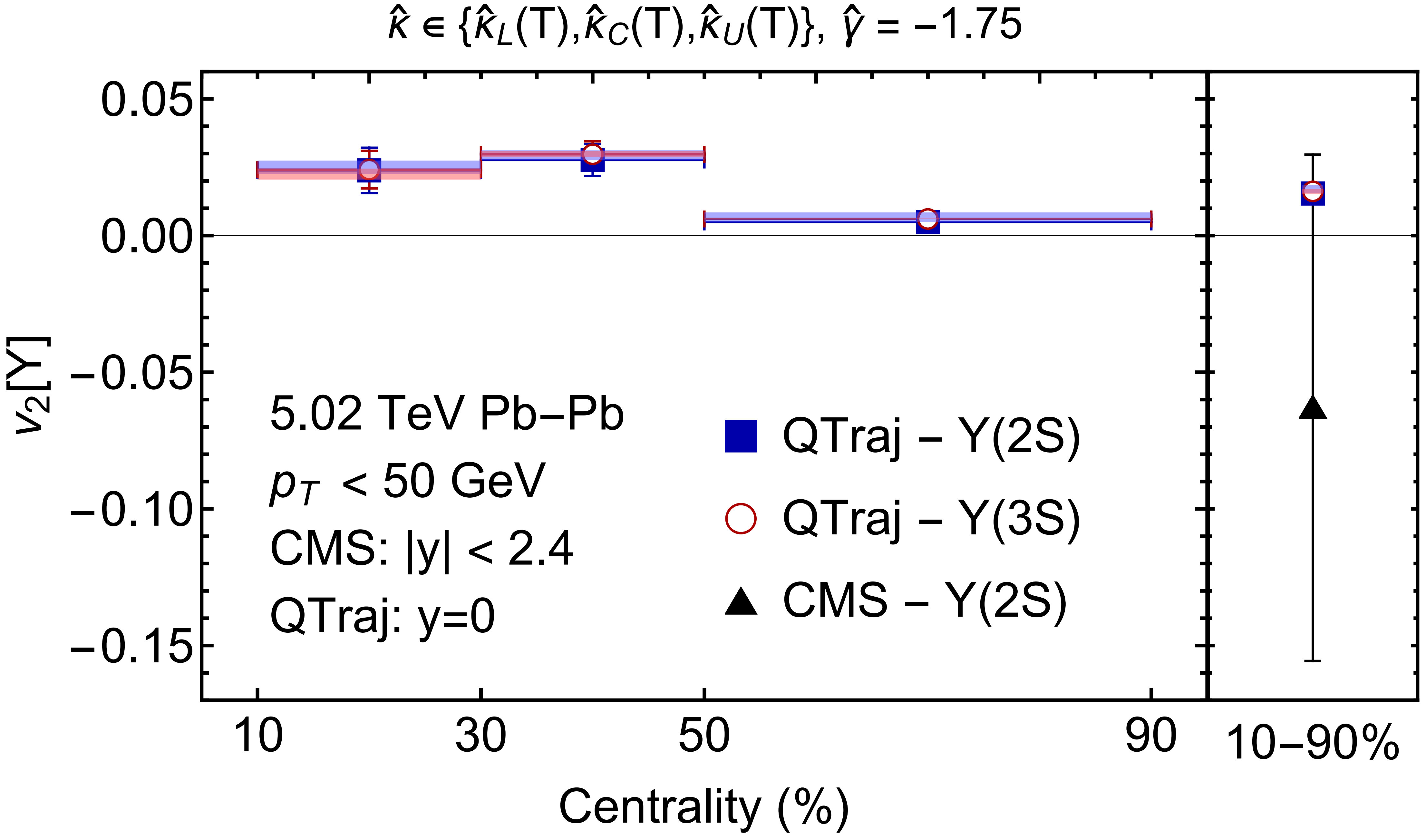

- This calculation with no free parameter can reproduce *inside errors* all the experimental data on bottomonia 1S 2S 3S:

- The band in our prediction depends on the indetermination on the transport coefficients

- Recombination is there but it is small for Y(1S) bottomonium

- The evolution equations we obtained do not make any special assumption on the medium

- This calculation with no free parameter can reproduce *inside errors* all the experimental data on bottomonia 1S 2S 3S:
  - R_AA as a function of N_part and as a function of p_T
  - Ratios of R_AA, v_2
- The band in our prediction depends on the indetermination on the transport coefficients
- Recombination is there but it is small for Y(1S) bottomonium
- The evolution equations we obtained do not make any special assumption on the medium

■ This calculation with no free parameter can reproduce *inside errors* all the experimental data on bottomonia 1S 2S 3S:

- R_AA as a function of N_part and as a function of p_T
- Ratios of R_AA, v_2

■ The band in our prediction depends on the indetermination on the transport coefficients

- Increasing kappa decreases survival for all states, while the impact of gamma varies from one state to the other
- More precise data could select the values of these coefficients and act as a direct diagnostic of the QGP

■ Recombination is there but it is small for Y(1S) bottomonium

■ The evolution equations we obtained do not make any special assumption on the medium

■ This calculation with no free parameter can reproduce *inside errors* all the experimental data on bottomonia 1S 2S 3S:

- R_AA as a function of N_part and as a function of p_T
- Ratios of R_AA, v_2

■ The band in our prediction depends on the indetermination on the transport coefficients

- Increasing kappa decreases survival for all states, while the impact of gamma varies from one state to the other
- More precise data could select the values of these coefficients and act as a direct diagnostic of the QGP

■ Recombination is there but it is small for Υ(1S) bottomonium

- For Υ(2S) and Υ(3S) recombination is more relevant and it is interfering with dissociation
- We expect recombination to be much more important for charmonium

■ The evolution equations we obtained do not make any special assumption on the medium

■ This calculation with no free parameter can reproduce *inside errors* all the experimental data on bottomonia 1S 2S 3S:

- R_AA as a function of N_part and as a function of p_T
- Ratios of R_AA, v_2

■ The band in our prediction depends on the indetermination on the transport coefficients

- Increasing kappa decreases survival for all states, while the impact of gamma varies from one state to the other
- More precise data could select the values of these coefficients and act as a direct diagnostic of the QGP

■ Recombination is there but it is small for Y(1S) bottomonium

- For Y(2S) and Y(3S) recombination is more relevant and it is interfering with dissociation
- We expect recombination to be much more important for charmonium

■ The evolution equations we obtained do not make any special assumption on the medium

They could be used far from equilibrium or for a medium with a scale different from T-> use different methods to evaluate kappa and gamma (kinetic theory, classical simulations)

We focused on heavy quarks but there are other hard probes to which EFTs and open quantum system approach could be applied

example: jet quenching and qhat

A systematic treatment of a complex phenomenon like jet quenching is possible in an EFT framework owning to the hierarchy of scales that characterize the system. These are the typical SCET scales, Q, $Q\lambda$, $Q\lambda^2$, with $\lambda = T/Q$, which characterize the propagation of a very energetic parton in the medium and the thermal scales that characterize the medium itself, T, m_D, magnetic mass.

$$\hat{q} = \frac{\langle k_\perp^2 \rangle}{L} = \frac{1}{L} \int \frac{d^2 k_\perp}{(2\pi)^2}\, k_\perp^2 \, P(k_\perp)$$

$P(k_\perp)$ is the probability that after propagating through the medium for a distance L the hard parton acquires transverse momentum $k_\perp$,

$\hat{q}$ is the jet quenching parameter, i.e. the mean square transverse momentum picked up by the hard parton per unit distance traveled,

EFTs take advantage in a systematic way of the many scales involved in the problems and can be used together with open quantum systems to describe the jet evolution

see e.g. 'EFTs for jet substructure in heavy ions collisions' V. Vaydia eprint 2010.00028

CONCLUSIONS

We have shown how the heavy quark-antiquark pair out-of-equilibrium evolution can be treated in the framework of pNRQCD. With respect to previous determinations:

- the medium may be a strongly-coupled plasma (not necessarily a quark-gluon plasma) whose characteristics are determined by lattice calculations;
- the total number of heavy quarks, i.e., $\mathrm{Tr}\{\rho_s\} + \mathrm{Tr}\{\rho_o\}$, is preserved by the evolution equations;
- the non-abelian nature of QCD is fully accounted for;
- the treatment does not rely on classical approximations.

The evolution equations follow from assuming the inverse size of the quark-antiquark system to be larger than any other scale of the medium and from being accurate at first non-trivial order in the multipole expansion and at first order in the heavy-quark density.

Under some conditions (large time, quasistatic evolution, quantum Brownian motion) the evolution equations are of the Lindblad form. Their numerical solution provides $R_{AA}[\Upsilon(nS)]$ and differential observables in good agreement with LHC data.

CONCLUSIONS

- Quarkonium suppression may be systematically studied with the use of **effective field theories** and **lattice QCD**
- **In equilibrium** properties like **dissociation width, cross section, mass shift...** have been computed as expansions in the small parameters of the system.
- **Out of equilibrium** properties, like octet recombination, can be studied by treating quarkonium as an open quantum system. Lattice input is crucial.

We have shown how the heavy quark-antiquark pair out-of-equilibrium evolution can be treated in the framework of pNRQCD. With respect to previous determinations:

- the medium may be a strongly-coupled plasma (not necessarily a quark-gluon plasma) whose characteristics are determined by lattice calculations;
- the total number of heavy quarks, i.e., $\mathrm{Tr}\{\rho_s\} + \mathrm{Tr}\{\rho_o\}$, is preserved by the evolution equations;
- the non-abelian nature of QCD is fully accounted for;
- the treatment does not rely on classical approximations.

The evolution equations follow from assuming the inverse size of the quark-antiquark system to be larger than any other scale of the medium and from being accurate at first non-trivial order in the multipole expansion and at first order in the heavy-quark density.

Under some conditions (large time, quasistatic evolution, quantum Brownian motion) the evolution equations are of the Lindblad form. Their numerical solution provides $R_{AA}[\Upsilon(nS)]$ and differential observables in good agreement with LHC data.

Outlook

- We need precise and unquenched determinations of the kappa and gamma transport coefficients
- Recombination effects are small for bottomonium for not for charmonium: we should go beyond the linear density approximation in that case
- We should investigate the effect of quarkonium moving with respect to the QGP and the anisotropy
- We should investigate the full master equations farther out of equilibrium: all the calculations holds if T is substituted by a generic scale
- We should investigate the full master equations farther Initial conditions may be tuned to account for pre equilibrium states like plasma

Outlook

- We need precise and unquenched determinations of the kappa and gamma transport coefficients
- Recombination effects are small for bottomonium for not for charmonium: we should go beyond the linear density approximation in that case
- We should investigate the effect of quarkonium moving with respect to the QGP and the anisotropy
- We should investigate the full master equations farther out of equilibrium: all the calculations holds if T is substituted by a generic scale
- We should investigate the full master equations farther Initial conditions may be tuned to account for pre equilibrium states like plasma

Inside EFT and OQS and with the help of the lattice
quarkonium holds the promise to be a golden probe of QGP!

$v_2[\Upsilon(1S)]$ vs. Centrality

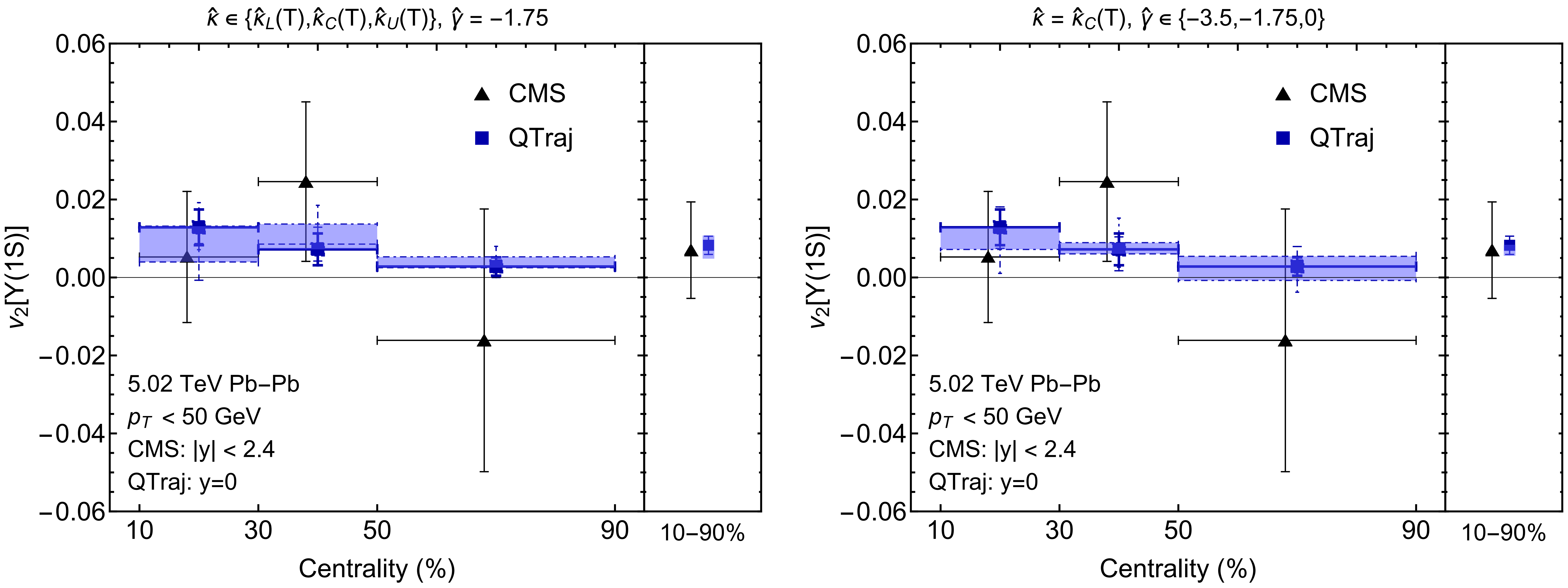

Figure: The elliptic flow v_2 of the $\Upsilon(1S)$ as a function of centrality compared to experimental measurements. The bands in the left plot represent variation of $\hat{\kappa}$ at fixed $\hat{\gamma} = -1.75$; the bands in the right plot represent variation of $\hat{\gamma}$ at fixed $\hat{\kappa} = \hat{\kappa}_C$.

$v_2[\Upsilon(1S)]$ vs. p_T

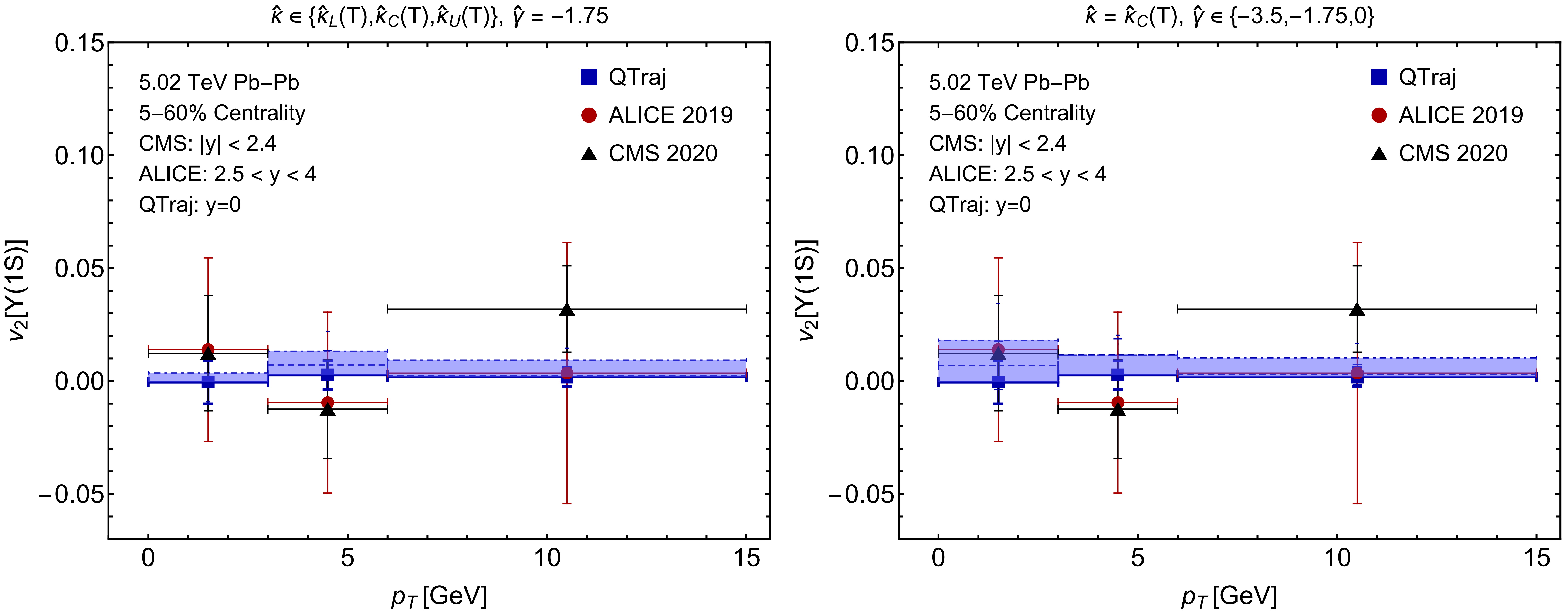

Figure: The elliptic flow v_2 of the $\Upsilon(1S)$ as a function of p_T compared to experimental measurements. The bands in the left plot represent variation of $\hat{\kappa}$ at fixed $\hat{\gamma} = -1.75$; the bands in the right plot represent variation of $\hat{\gamma}$ at fixed $\hat{\kappa} = \hat{\kappa}_C$.

Double Ratio 2S vs. p_T

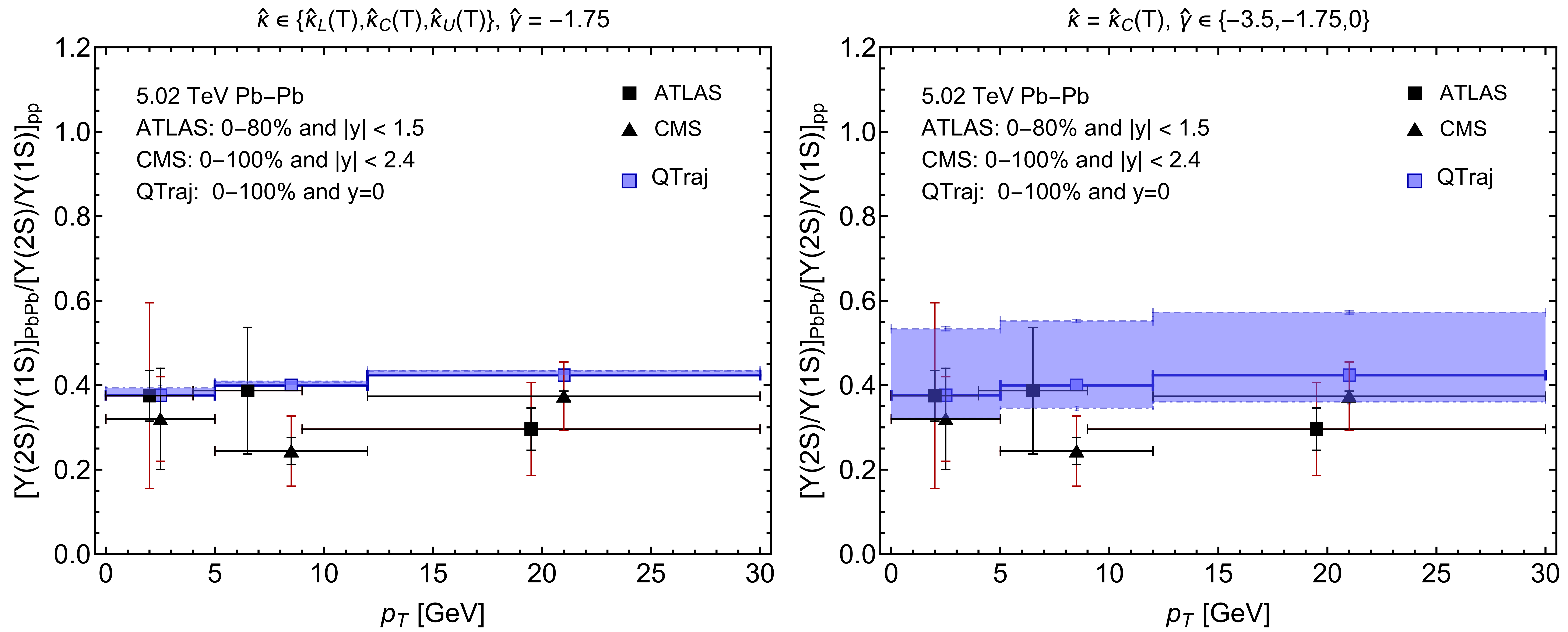

Figure: The double ratio of the nuclear modification factor $R_{AA}[\Upsilon(2S)]$ to $R_{AA}[\Upsilon(1S)]$ as a function of p_T compared to experimental measurements. The bands in the left plot represent variation of $\hat{\kappa}$ at fixed $\hat{\gamma} = -1.75$; the bands in the right plot represent variation of $\hat{\gamma}$ at fixed $\hat{\kappa} = \hat{\kappa}_C$. The black and red bars in the experimental data represent statistical and systematic uncertainties, respectively.

Double Ratio 2S vs. Centrality

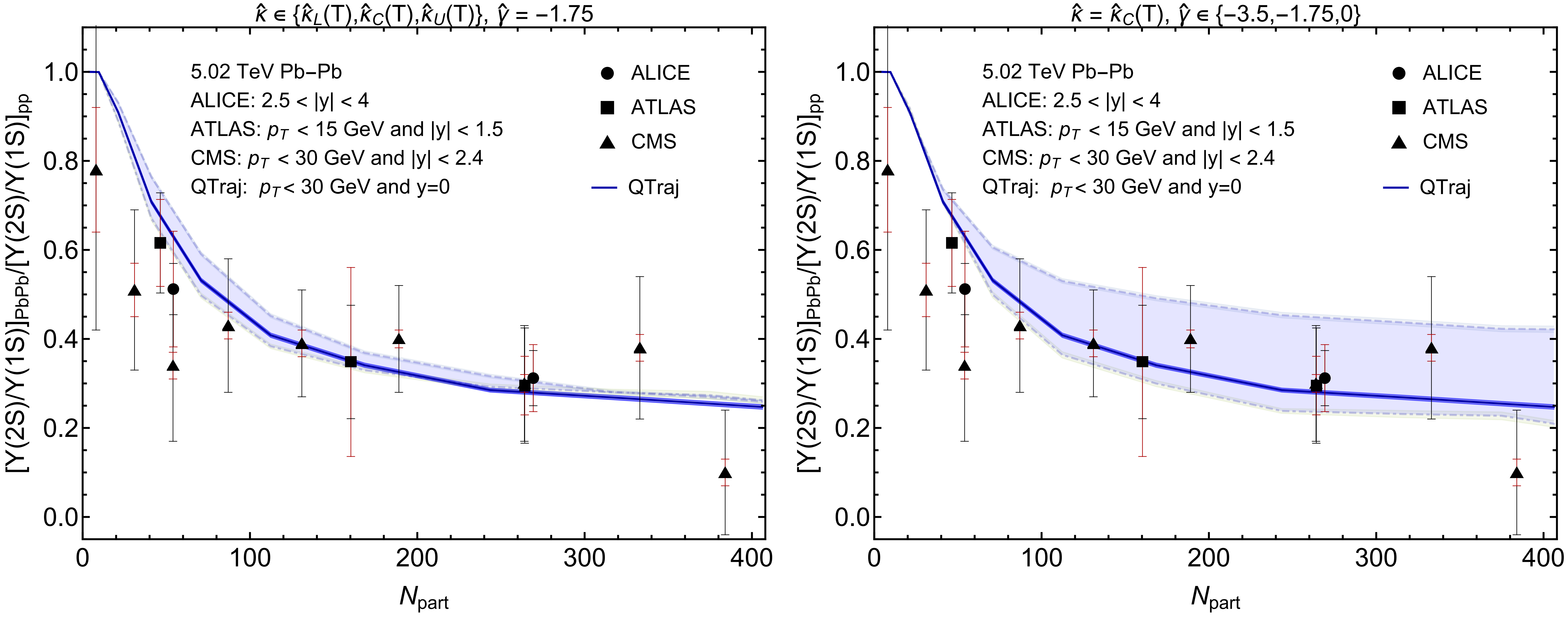

Figure: Ratio of $R_{AA}(2S)$ to $R_{AA}(1S)$ computed in QTraj compared to experimental results.

Double Ratio 3S vs. Centrality

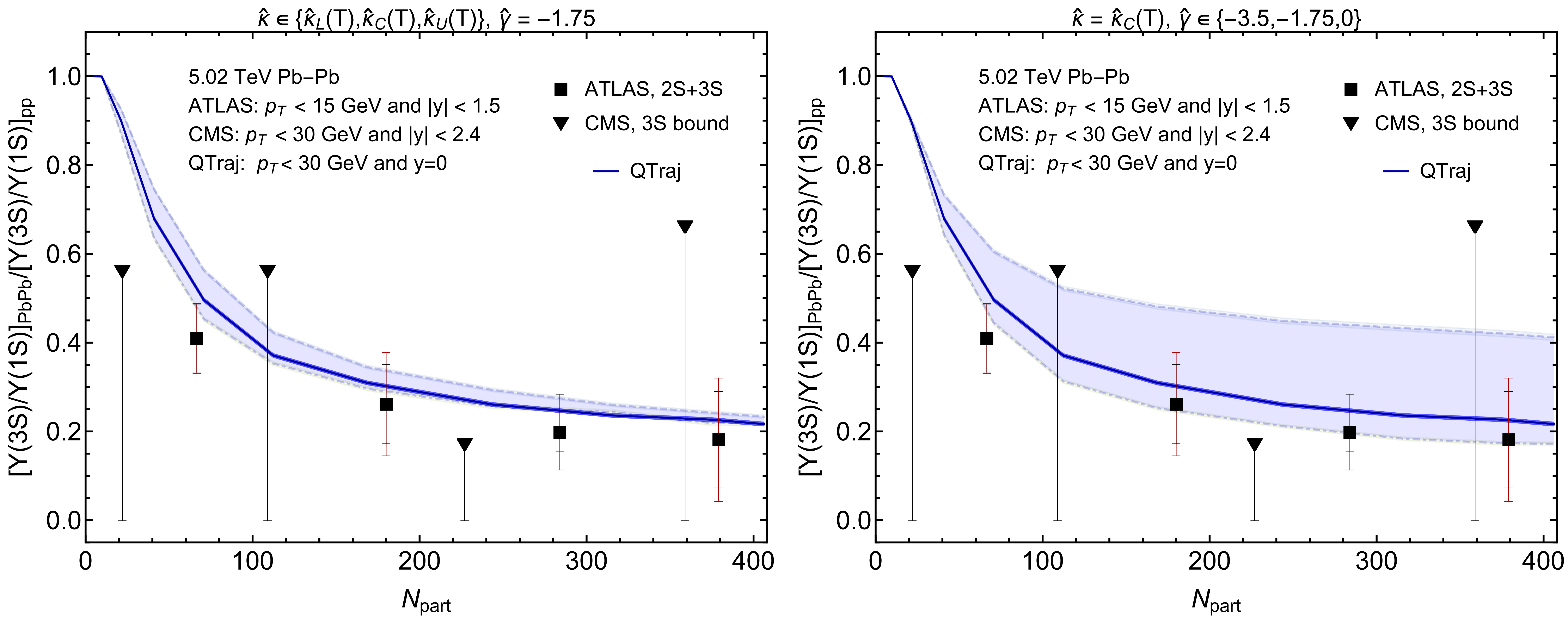

Figure: Ratio of $R_{AA}(2S)$ to $R_{AA}(1S)$ computed in QTraj compared to experimental results.

$v_2[\Upsilon(2,3S)]$ vs. Centrality

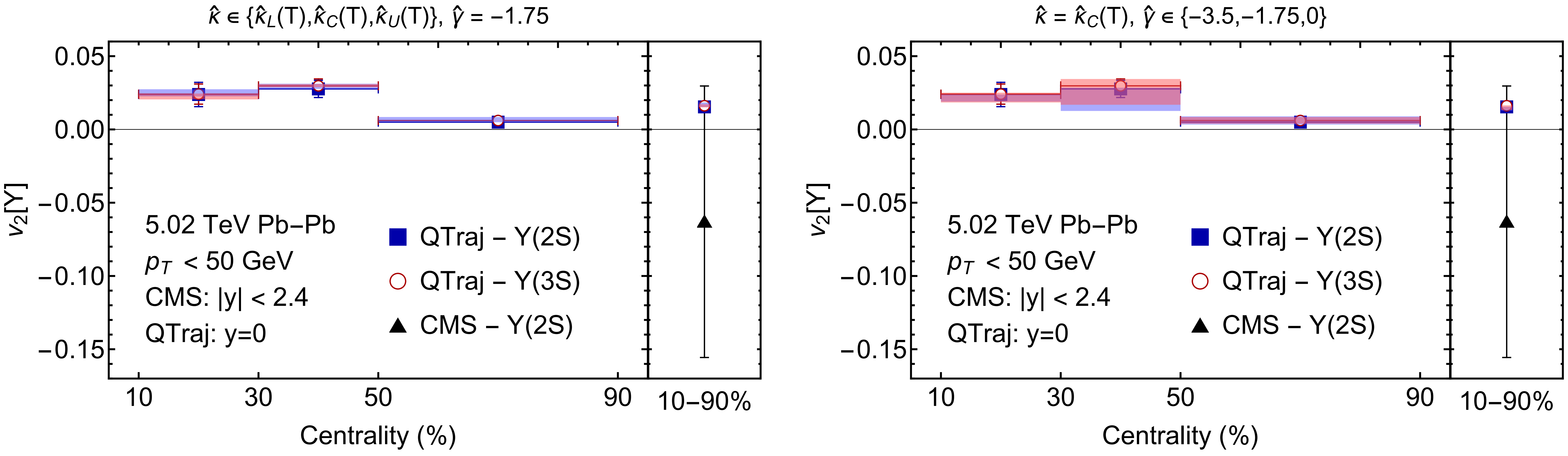

Figure: The elliptic flow v_2 of the $\Upsilon(2S)$ and $\Upsilon(3S)$ as a function of centrality compared to experimental measurements. The bands in the left plot represent variation of $\hat{\kappa}$ at fixed $\hat{\gamma} = -1.75$; the bands in the right plot represent variation of $\hat{\gamma}$ at fixed $\hat{\kappa} = \hat{\kappa}_C$.